

Università degli Studi di Padova

Dipartimento di Ingegneria Industriale
Corso di Laurea Magistrale in Ingegneria Meccanica

Tesi di Laurea Magistrale

Development and experimental validation of a mathematical model of an absorption chiller

Relatore:

Prof. Ing. Davide Del Col (DII-Università di Padova)

Correlatori:

Prof. Ing. Andrea Luke (TTK Universität Kassel)

Ing. Michael Olbricht (TTK Universität Kassel)

Laureando:

Enrico Cecchinato

matricola 1061178

Anno Accademico 2014 - 2015

Abstract

This master thesis has been carried out at the Institut für Thermische Energietechnik of the University of Kassel, Germany.

The development of a mathematical model, which can simulate the performance of a $H_2O - LiBr$ laboratory absorption chiller, represented the main purpose of the thesis work. In particular, it has focused on the COP and cooling capacity results. A condenser, an evaporator, an absorber, a generator and a solution heat exchanger make up the absorption cycle of the laboratory facility.

In order to achieve the final purpose, both an experimental session conducted in the laboratory and a modelling one, have been performed. The first one concerned the study of the performance and behavior of the facility and the second one represented the development of the mathematical model.

In particular, the experimental working session was divided in:

- Study of the facility dynamic behavior, focusing on the time that the cycle parameters took to reach steady state conditions, after the variation of the hot water temperature at the generator inlet. That working session has been meaningful to recognize the facility parameters which needed more time to get stable and therefore fit to be inserted into the model.
- Measuring and data reduction to get both the solution film convective heat transfer coefficient (external side of the absorber pipes) and the overall absorber heat transfer coefficient. The *Engineering Equation Solver – EES* software has been used for the data reduction procedure. The resulting values of the overall heat transfer coefficient have been inserted as input data into the mathematical model.

The modelling session has been performed through the software *EES* as well and has concerned the development of the mathematical model. It is represented by many systems of equations (167), which describe the thermodynamics characteristics of each apparatus of the laboratory facility. In particular, those relations involve heat transfer equations for each system component, as well as the ones relative to the first thermodynamics law applications, written both for the secondary fluid side and the refrigerant side, for every heat exchanger.

Moreover, mass balances have been implemented to the absorber and generator.

The model input data are represented by the secondary fluid inlet temperatures and their volumetric flow rates, as well as the overall heat transfer coefficients and

exchanger areas of the five machine heat exchangers. Steady state working conditions have been hypothesized for the model.

The work final results are represented by the comparisons between experimental data and the simulation results, focusing on the COP and cooling capacity. They are dealt with in chapter 5, in function of the hot water generator temperature and for different cold water temperatures at the evaporator inlet. Those experimental data have been collected prior to this thesis work, for the same working conditions of the simulations.

It has been noticed that the model can simulate both the COP and cooling capacity trends, in every working condition. Moreover, it has turned out to be a reliable instrument to predict the real cooling capacity values.

The results also show that the model can operate in a wide range of values of the hot source temperature and of the temperature of the cold water at the evaporator inlet.

Sommario

La presente tesi magistrale è stata svolta presso l'Institut für Thermische Energietechnik dell'Università di Kassel, Germania.

L'obiettivo principale del lavoro è stato quello di sviluppare un modello matematico, in grado di simulare in modo attendibile le performance di una macchina ad assorbimento $H_2O - LiBr$ da laboratorio, dando particolare importanza ai valori del COP e della capacità frigorifera ottenuti. La macchina ad assorbimento oltre al condensatore, evaporatore, generatore ed assorbitore, possiede anche uno scambiatore rigenerativo.

Per il raggiungimento dello scopo finale, si sono rese necessarie sia una sessione di lavoro sperimentale in laboratorio che una di simulazione al computer, con la prima che ha visto lo studio del comportamento e delle prestazioni della macchina e la seconda lo sviluppo del modello.

In particolare, la sessione sperimentale ha previsto 2 fasi:

- Studio del comportamento dinamico della macchina, focalizzandosi sul tempo che i parametri termodinamici del ciclo impiegano per raggiungere condizioni stazionarie, dopo la variazione della temperatura dell'acqua calda al generatore. Tale sotto-sessione è stata utile per capire quali fossero i parametri che richiedessero più tempo per raggiungere la stabilità e quindi essere idonei per il loro inserimento nel modello, vista l'ipotesi di condizioni stazionarie di quest'ultimo.
- Misurazioni e riduzione dei dati per l'ottenimento dei valori del coefficiente di scambio termico convettivo lato soluzione, all'esterno dei tubi, e del coefficiente globale di scambio dell'assorbitore. Per la riduzione dei dati, si è fatto uso del software *Engineering Equation Solver - EES*. I valori del coefficiente globale di scambio termico ottenuti, sono stati inseriti come dati di input nel modello matematico.

La sessione di simulazione al computer, eseguita tramite il software *EES*, ha visto la scrittura del modello matematico, il quale è rappresentato da un sistema composto da un totale di 167 di equazioni, che descrivono le caratteristiche termodinamiche di ogni componente della macchina in laboratorio. Tali relazioni comprendono, in particolare, equazioni di trasmissione globale del calore per ogni apparato e quelle relative all'applicazione del primo principio della termodinamica, sia per il lato refrigerante che per quello del fluido secondario, per ogni scambiatore.

Al generatore ed assorbitore, inoltre, sono state applicate equazioni di bilancio di massa.

I dati di input sono rappresentati dalle temperature e portate volumetriche dei fluidi secondari, in ingresso alla macchina, e dalle aree e coefficienti globali di scambio di tutti e cinque gli scambiatori. Il modello, come è stato accennato, ipotizza condizioni di lavoro stazionarie.

I risultati finali della presente tesi sono rappresentati dai confronti tra valori sperimentali e quelli forniti dal modello, in particolare del COP e della capacità frigorifera, al variare della temperatura dell'acqua calda al generatore e per varie temperature dell'acqua fredda in ingresso all'evaporatore. Tali dati sperimentali sono stati raccolti in un momento precedente allo svolgimento del presente lavoro di tesi, per le stesse condizioni di lavoro ipotizzate poi nelle simulazioni.

Si è potuto notare che il modello matematico è in grado di simulare, in ogni condizione di lavoro, i trend sperimentali sia del COP che della capacità frigorifera, dimostrandosi anche uno strumento particolarmente affidabile nel calcolo del reale valore di quest'ultima. Si è potuto vedere, inoltre, che il modello è in grado di operare in un ampio intervallo di valori delle temperature dell'acqua di alimentazione sia del generatore che dell'evaporatore.

Index

List of symbols	III
List of subscripts	IV
List of abbreviations	V
1. INTRODUCTION	1
2. FUNDAMENTALS	3
2.1 Absorption cooling technology	3
3. EXPERIMENTAL INVESTIGATION	9
3.1 Facility description	9
3.1.1 <i>The absorption chiller</i>	9
3.1.2 <i>The secondary fluid loops</i>	12
3.1.3 <i>The control and measurement systems</i>	18
3.2 Experimental setup	24
3.2.1 <i>Heat source preparation</i>	24
3.2.2 <i>Experiment preparation</i>	25
3.2.3 <i>Switching off of the plant</i>	28
3.3 Experimental procedure	29
3.3.1 <i>COP curve</i>	30
3.3.2 <i>Dynamic behavior</i>	33
3.3.3 <i>Absorber heat transfer</i>	35
4. MATHEMATICAL MODEL	47
4.1 Model introduction	47
4.2 Input data	49
4.3 Model description	52
4.3.1 <i>Guess values</i>	63
5. RESULTS	65
5.1 Experimental investigation	65
5.1.1 <i>Dynamic behavior</i>	65
5.1.2 <i>Absorber heat and mass transfer</i>	77
5.2 Simulation	82
6. CONCLUSIONS	91

7.	APPENDIX	93
7.1	Attachment A: Vessel technical data	93
7.2	Attachment B: Shell and tube heat exchanger geometry	94
7.3	Attachment C: Recorded facility data	96
7.4	Attachment C: COP and cooling capacity results	97
7.5	Attachment D: EES – script, absorber coefficients calculations	100
7.6	Attachment E: EES input data – heat transfer coefficients calculations.....	104
7.7	Attachment F: EES script – absorption chiller performance	105
8.	REFERENCES	117

List of symbols

A	Heat exchanger area	m^2
c_p	Specific heat at constant pressure	$\text{J}/(\text{kg} \cdot \text{K})$
d	Diameter	m
h	Specific enthalpy	J/kg
K	Overall heat transfer coefficient	$\text{W}/(\text{m}^2 \cdot \text{K})$
L	Heat of mixing for 1kg of refrigerant	J/kg
l	Pipe length	m
\dot{M}	Mass flow rate	kg/s
n_{RR}	Column number of the heat exchanger	
Nu	Nusselt number	
P	Pressure	Pa or mbar
Pr	Prandtl number	
\dot{Q}	Heat flux	W
Re	Reynolds number	
r	Latent heat	J/kg
Sc	Sub cooling	W
Sh	Superheating	W
T	Temperature	$^{\circ}\text{C}$ or K
\dot{V}	Volume flow rate	m^3/s
u	Water mean velocity	m/s
w	Solution concentration at 20°C	
x	Solution concentration or quality	
α	Convection heat transfer coefficient	$\text{W}/(\text{m}^2 \cdot \text{K})$
Γ_{ls}	Solution mass flow rate for pipe length	$\text{kg}/(\text{m} \cdot \text{s})$
$\delta_{T,Lm}$	Logarithmic mean temperature difference	$^{\circ}\text{C}$ or K
δ	Small temperature difference	$^{\circ}\text{C}$ or K
ε	Efficiency	
η	Dynamics viscosity	$\text{Pa} \cdot \text{s}$
λ	Thermal conductivity	$\text{W}/(\text{m} \cdot \text{K})$
ρ	Density	kg/m^3

List of subscripts

<i>ab</i>	Absorber
<i>al</i>	Poor solution
<i>aus</i>	Outlet
<i>av</i>	Average
<i>cold</i>	Cold water
<i>cool</i>	Cooling water
<i>e</i>	External
<i>ein</i>	Inlet
<i>g</i>	Generator
<i>gg</i>	Equilibrium
<i>hot</i>	Hot water
<i>i</i>	Internal
<i>id</i>	ideal
<i>k</i>	Condenser or cooling water
<i>kond</i>	Condensation or condenser
<i>kw</i>	Cooling water
<i>ls</i>	Solution
<i>probe</i>	Sample
<i>ref</i>	Refrigerant
<i>rl</i>	Rich solution
<i>sat</i>	Saturation
<i>shx</i>	Solution heat exchanger
<i>v</i>	Evaporator
<i>vap</i>	Vaporization
<i>var</i>	Varying
<i>w</i>	Water

List of abbreviations

<i>COP</i>	Coefficient of performance
<i>Cu</i>	Copper
<i>EES</i>	Engineering Equation Solver (Software)
<i>FU</i>	Pump controller
<i>H</i>	Heater
<i>LiBr</i>	Lithium Bromide
<i>MDI</i>	Magnetic inductive flow sensor
<i>P</i>	Secondary fluid pump
<i>Pi</i>	Pressure sensor
<i>PT</i>	platinum resistance thermometers
<i>R</i>	Mixing valve controller
<i>TC</i>	Thermocouples
<i>UWP</i>	Facility pump
<i>V</i>	Facility valve

1. INTRODUCTION

The absorption machine is one of the most interesting system for producing cold, used since the late 19th century (Carrè, 1857). Despite it has been known for quite a long time, this technology started to get more attention in the two past decades, because of environmental interests [1]. In fact, the increase of global warming and the focusing on the harmful effects of the chlorofluorocarbon made these machines more attractive [2], although they have a lower efficiency than the vapor compression systems and they continue to be bulky and expensive for buildings applications [3]. The absorption systems are able to utilize natural refrigerants (ammonia, water...) and they can use wasted heat to work. If the chiller is allowed to operate with low input temperatures, it can be suitable for trigeneration processes as well [1]. For these reasons, this refrigeration technology represents a reliable way to reduce greenhouses gasses [4-6].

Moreover, they can reduce the global electricity consumption [3], for example by filling the electric energy peaks during the summer.

The present report, in particular, concerns the study of a $H_2O - LiBr$ facility, built between 2011 and 2013, at the University of Kassel. Such a device works with fluids which present important advantages [7]:

- High enthalpy of vaporization;
- No toxicity;
- No flammability;
- Environmental friendly (no ozone depletion, no acidification, no photo – oxidation);
- Inert and chemically stable;
- High specific heat capacity;
- Odorless;
- Cheaply traceable in high purity.

The effectiveness of this kind of machine is influenced by many parameters, therefore simulations through the computer could be very useful to analyzed the various aspects of this kind of facilities.

The present master thesis focuses, primarily, on the development of a mathematical model, which simulates the performance of the system under consideration. In fact, after the first performance tests and their report [7], the

necessity to have a virtual model, which could simulate the real facility, arose. In particular, the need to estimate the machine performance, without carrying out the experiments, occurred. The model was used to calculate the system characteristics for a variety of operating conditions.

For the thesis work, some experimental investigations have been carried out as well, in order to reduce the uncertainty of the above mentioned model. First of all the absorber overall heat transfer coefficient have been calculated, to make the model input data closer to the reality. At a later stage, the facility dynamic behavior has been analyzed too, for the purpose of identifying the working limits of the mathematical model.

2. FUNDAMENTALS

2.1 Absorption cooling technology

An absorption refrigerator is a thermal machine that provides the refrigerating effect by using heat input, rather than electrical input as in the more common vapor compression cycle.

An absorption basic system consists of the following components [8]:

Condenser

Inside that heat exchanger the refrigerant steam is condensed to liquid, releasing heat to the secondary fluid.

Evaporator

Inside that heat exchanger the liquid refrigerant evaporates, removing heat from the secondary fluid. This cooling process represents the output effect of the facility.

Expansion device

This device has the purpose to reduce the pressure of the refrigerant, from condenser one to evaporator one.

In addition, a little amount of liquid is turned into steam: the quality at the inlet of the evaporator is more than 0.

Absorber

In this apparatus the refrigerant vapor, formed in the evaporator, is absorbed and the liquid solution is formed. In particular the weak solution, coming from the generator, is combined with the refrigerant, forming the so-called *rich solution*. It flows from the outlet of the absorber up to the generator, passing through the solution heat exchanger.

This process releases heat and for this reason a cooling secondary fluid has to flow inside the heat exchanger. The cooling down process helps the mixing between weak solution and refrigerant as well.

The heat that the secondary fluid has to export from the absorber is the sum of two effects: the condensation of the steam produced in the evaporator plus the heat of solution relative to the working media. Mostly the fluid which cools the absorber down is the same of the condenser, where it flows at a later stage.

Generator

In the generator the refrigerant evaporates, therefore is separated from the solution by heat input.

In the most common case the refrigerant is boiled off, so it can be separated from the solution (distillation process) and can flow inside the condenser.

The residual solution, which owns just a little amount of refrigerant, flows back to the absorber and is called *poor solution*.

The heat that supplies the generator is the driving energy of the system.

Pump

This component pumps the rich solution from the absorber up to the generator, bringing the fluid from the evaporator to condenser pressure.

Regulating valve

This device brings the poor solution from the high pressure of the generator to the lower one of the absorber.

Solution heat exchanger

This heat exchanger removes a certain amount of heat from the poor solution to preheat the rich solution, in order to improve the cycle efficiency decreasing the heat demand of the generator.

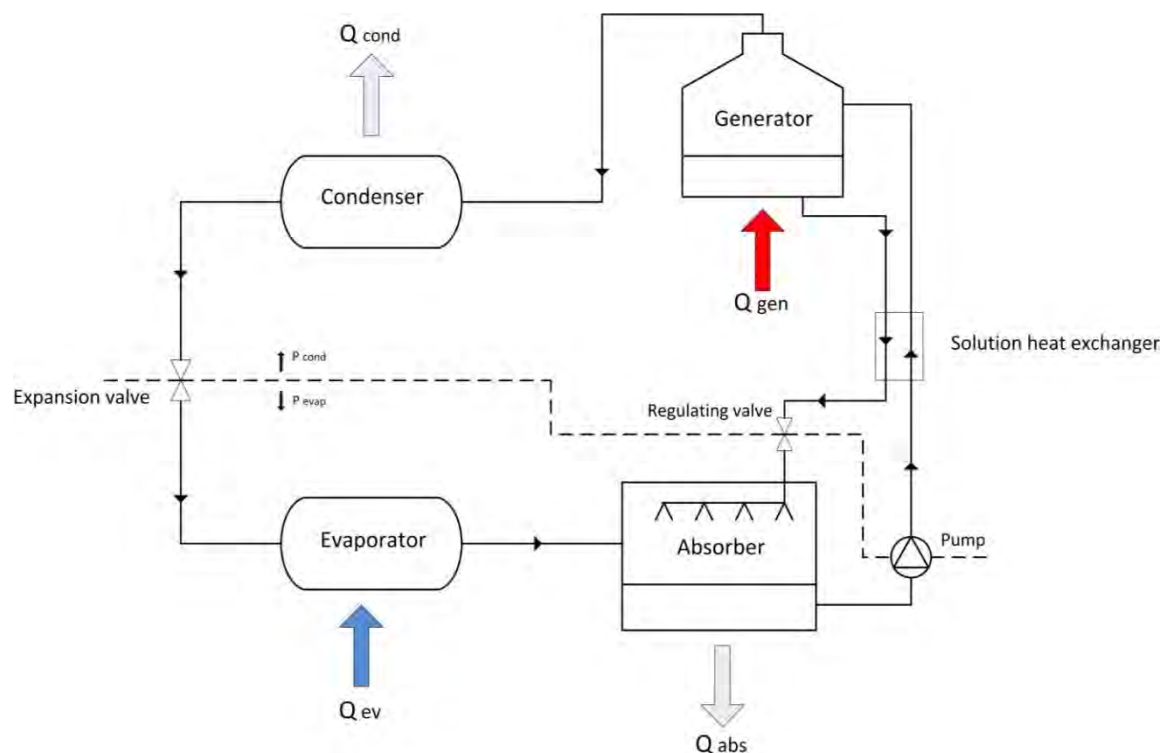


Figure 2.1. Simple scheme of an absorption refrigerator.

It is important to notice that the power energy demand of the pump represents just a little amount of the energy that would require a compressor, since the first compression is made on a liquid fluid.

The absorption cycle needs a pair of working media: the refrigerant and the absorption one. Both of them flow in two closed loops.

The refrigerant which has been separated from the solution in the generator flows into the condenser, where it turns into liquid and later through the expansion device, that makes the pressure equal to the evaporator one.

Afterwards the liquid becomes steam in the evaporator, producing the cooling effect on the secondary fluid and flows into the absorber, where it can rejoin the solution (poor) coming from the solution heat exchanger.

The rich solution at the outlet of the generator completes the cycle, flowing into the solution heat exchanger and after in the generator.

The most common working media are ammonia and water [8], with the first one representing the refrigerant and the second one the absorption fluid.

The ammonia and its combination with the water have important thermophysical properties, especially heat transfer characteristics. This is the main reason of the wide use of this pair.

However, one disadvantage is that the vapor from the generator includes a certain amount of water steam; so a rectifier has to be installed at the outlet of the generator, in order to improve the separation of the working media.

Moreover, ammonia is toxic and with the air forms a flammable mixture. For that reason the pair ammonia-water is not suitable for civil applications.

The working media for these kind of applications, for example air conditioning, are the pair *Water – Lithium Bromide* ($H_2O - LiBr$).

In this case the water is the refrigerant and the lithium bromide, which is a hygroscopic salt, the absorption fluid.

The first typical advantage for this kind of facility is the excellent separation between refrigerant and LiBr in the generator (LiBr is a salt). For this reason the rectifier is not required, as in the *ammonia – water* systems. Moreover, because of the low working pressures, the pump work is negligible in the energy overall system balance [9]. However, the low pressures make the water steam very huge.

Another one drawback of the low working pressures is that the system components have to be hermetically built, in order to avoid the leakages.

In addition the evaporation pressure, with this kind of systems, cannot be lower than 0 °C, to prevent the freezing of the refrigerant.

An important problem which can occur using this working pair is the crystallization: salt crystals may form in the solution and the cycle may be stopped.

This problem happens at low refrigerant concentrations in the solution and a respective low temperature.

For these reasons the critical point of the system is the solution heat exchanger, in the side where the poor solution flows and is cooled down.

That is why the crystallization must be prevented in the real system.

The Figure 2.2. shows the saturation curves of the solution $\text{H}_2\text{O} - \text{LiBr}$ for different concentrations and especially the area where the crystallization can happen.

It is important to mention that with these working fluids problems of corrosion can happen, especially in the generator, where copper and steel pipes are usually used to heat up the solution [8].

Other advantages and drawbacks, in particular related to environmental concerns, are listed in the *Introduction*.

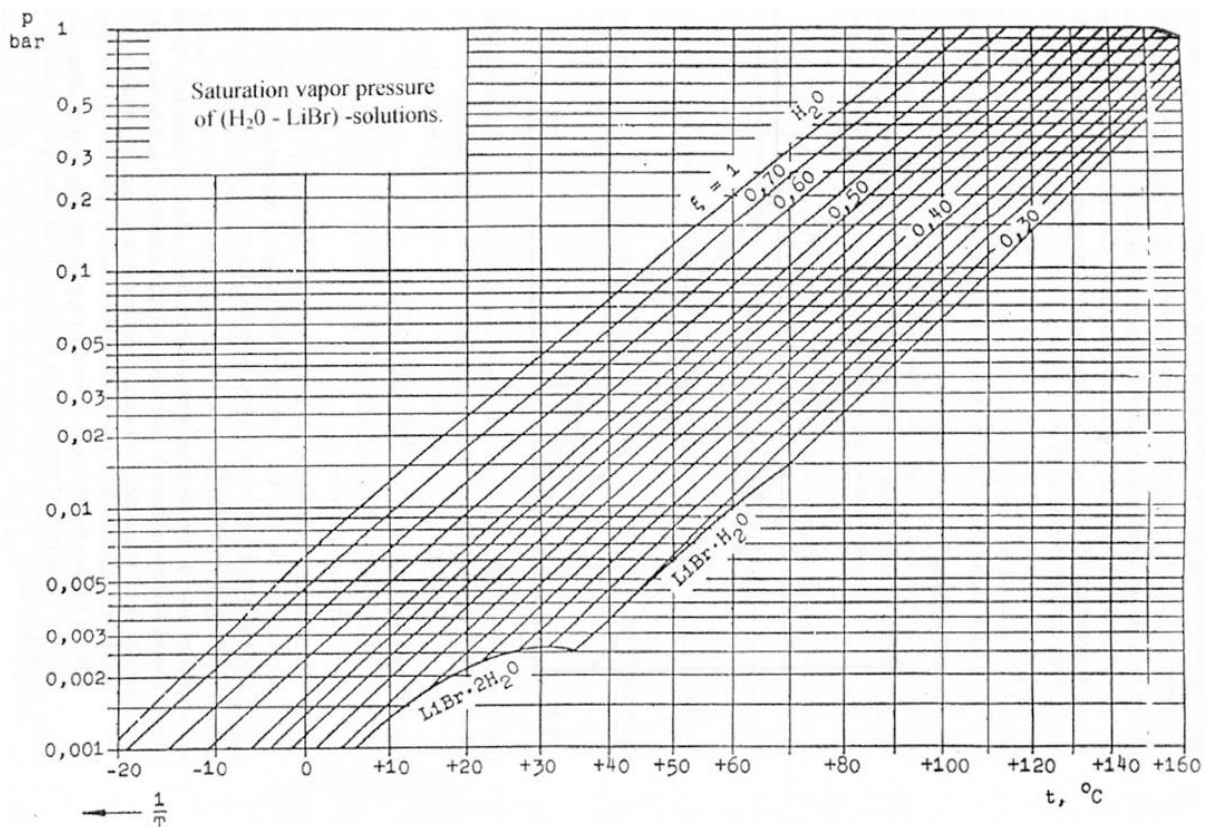


Figure 2.2. Saturation curves of the solution $\text{H}_2\text{O} - \text{LiBr}$, for different concentrations [8].

From the above diagram is possible to find the theoretical concentrations of the solutions that flow in the cycle.

The cooling and the cold temperatures at the inlet of the heat exchangers (respectively absorber and evaporator) fix the two pressure levels on the pure refrigerant curve and since $T_{ab} = T_k$, the rich solution concentration is found as well. Afterwards from the value of the hot water temperature the value of the poor solution concentration is determined too $P_g = P_k$.

The theoretical diagram obtained is the one below, in the Figure 1.3.

The absorber and the generator in the reality are not able to bring all the solution to saturation conditions and because of that the difference between the two concentrations is smaller than in the ideal calculations.

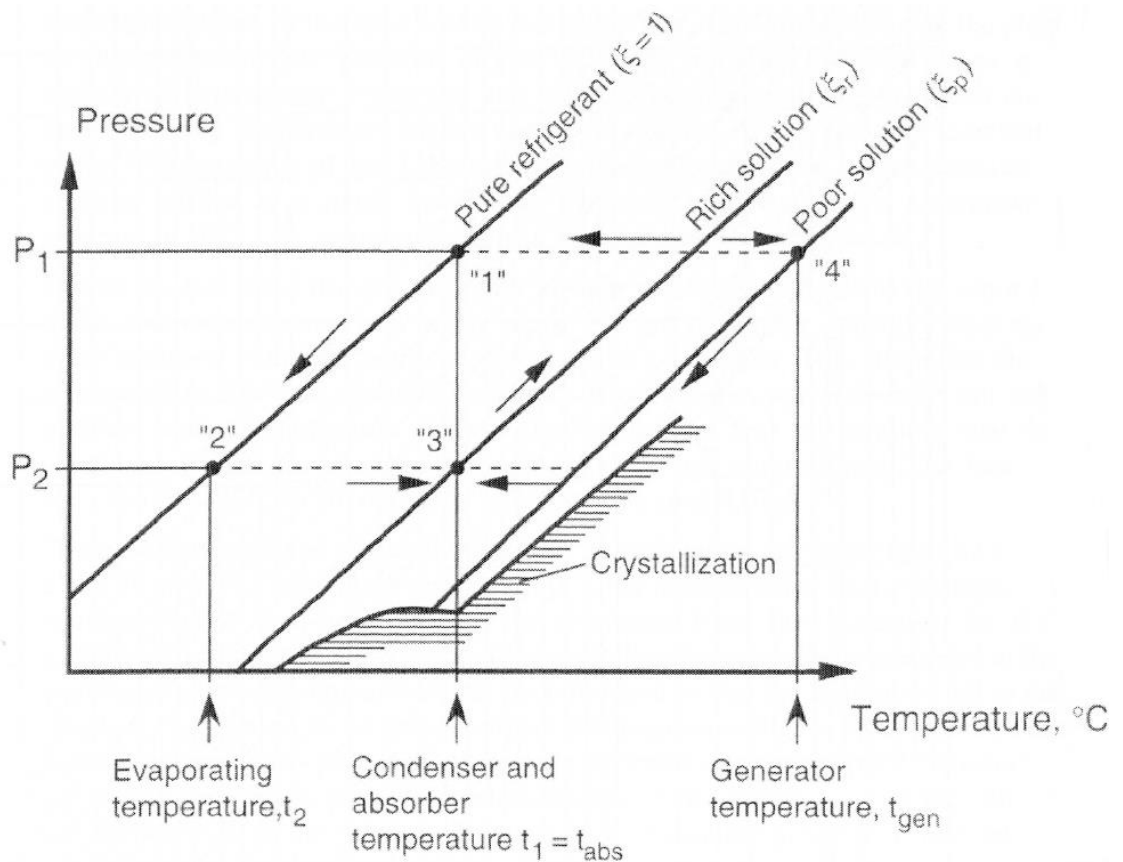


Figure 2.3. The absorption cycle represented in the saturation vapor diagram, ideal Case [8].

Supposing stationary conditions, the Coefficient of Performance of the cycle is the following [8]:

$$COP = \frac{\dot{Q}_v}{\dot{Q}_g} = \frac{(1 - x_{inlet}) \cdot r_v}{r_g + L} \quad 2.1$$

assuming:

- x_{inlet} = quality at evaporator inlet;
- r_v = latent heat of vaporization at evaporator conditions;
- r_g = latent heat of vaporization at generator conditions;
- L = heat of mixing for 1kg of refrigerant;
- \dot{Q}_v = cooling capacity at the evaporator;
- \dot{Q}_g = heat supplied at the generator.

Since the vaporization heat has not an important variation between the evaporator and generator conditions, from the above formula it can be seen that the COP for this kind of cycle cannot be more than 1.

However, there is difference between the COP of a real system and the theoretical one, which can be found just substituting the thermodynamics value in the formula. One of the main causes, which decrease the real COP, are the losses between the environment and the machine.

Another one drawback, which happens only in the $NH_3 - H_2O$ cycle, is the wasted heat to evaporate the water vapor in the generator. Because of that, the COP of this kind of system is lower than the $H_2O - LiBr$ system COP.

3. EXPERIMENTAL INVESTIGATIONS

3.1 Facility description

3.1.1 The absorption chiller

The absorption chiller investigated and used for the measurements is represented in the Figure 3.1.

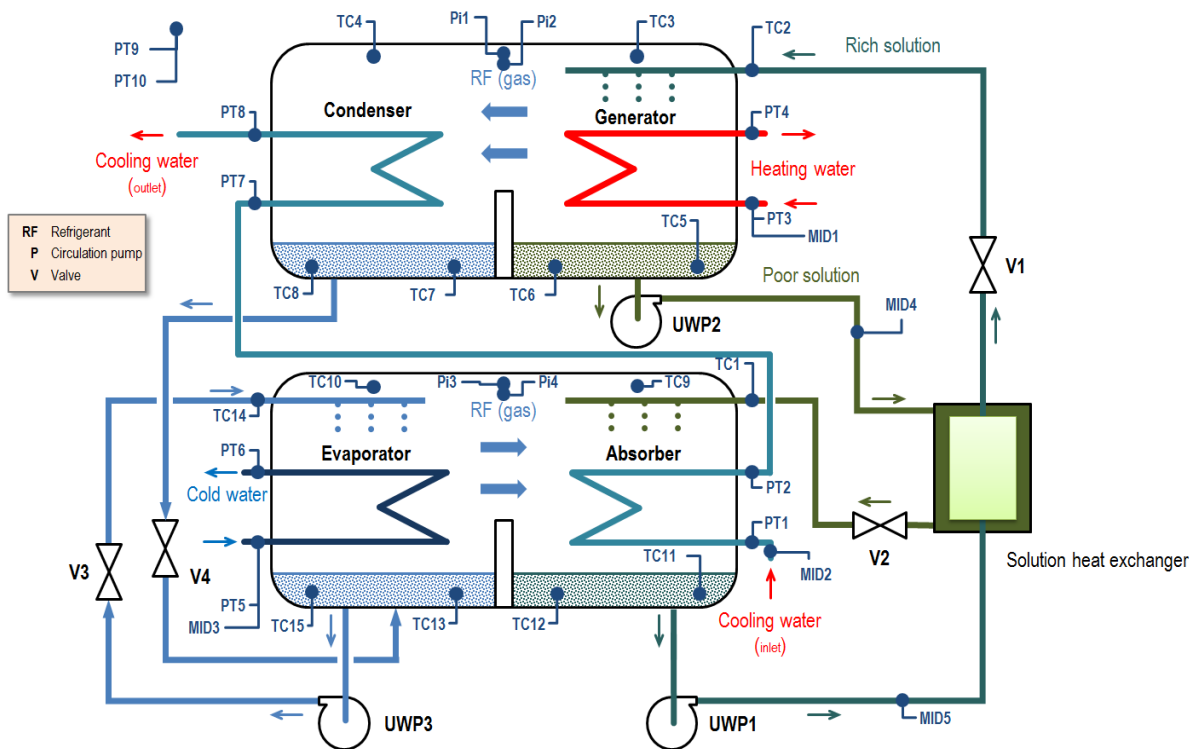


Figure 3.1. Framework of the absorption chiller.

In this facility the heat exchangers are situated inside two different steel vessels: the upper one works at high pressure and the lower one at low pressure.

The generator and the condenser are placed inside the high pressure vessel and the evaporator and the absorber in the low pressure one.

The technical data of the vessels are posted in the Attachment A [7].

It is an $H_2O - LiBr$ cycle with 4 shell and tube heat exchangers:

- Generator,
- Condenser,
- Evaporator,
- Absorber,

and one plate heat exchanger:

- Solution heat exchanger.

The shell and tube heat exchanger geometries are posted in the Attachment B.

The shell and tube heat exchanger pipes are made of pure copper and are wetted outside by the refrigerant, which on them forms a falling film. Inside these pipes the secondary fluid flow.

They are actually cross counter flow heat exchangers, but it is allowed to consider them as perfect counter flow heat ones, because in every pipe line is present solution with the same concentration and temperature [10].

The rich solution at the outlet of the absorber is pumped by the UWP1 pump through the solution heat exchanger up to the generator, and the poor solution at the outlet of the generator is pumped up to the absorber by the UWP2 pump, flowing similarly through the solution heat exchanger.

The UWP1 pump could be sustain a maximum pressure difference of 1,2 *bar* and UWP2 and UWP3 pumps about 0,8 *bar*.

The solution heat exchanger plates are made of steel, in particular AISI 316, brazed with copper.

The flow meter sensors MID5 and MID4 check the volume flow rates respectively of the rich and the poor solution, which can be varied by the 2 manual valves V1 and V2. The above mentioned sensors show the volume flow rate through 2 digital displays.

Both the poor and rich solution are sprayed on the pipes of the heat exchangers, respectively absorber and generator.

The recirculating loop, where the UWP3 pump is situated, brings the liquid refrigerant come from the condenser up to the pipes of the evaporator. This volume flow rate is regulated by the V3 manual valve.

Finally the V4 valve represents the expansion valve of the absorption refrigerator.

The boundary conditions of the cycle are fixed by the computer, through the LabVIEW program, and the electric control panel (Figure 3.6). Just the V1, V2, V3 and V4 valve are completely regulated by manual control.

The heat exchangers which work at high pressure, are put together in the same vessel and equally, the absorber and evaporator are positioned in the low pressure one.

In this way the pressure drops are decreased, especially when the refrigerant vapor flows between the evaporator and the absorber.

The vessels are covered by insulation, except for the condenser section, to facilitate the heat dissipation towards the environment.

The insulation is based on synthetic rubber and it is a very flexible material, in order to adapt it easily to the container shape.

The isolation is applied to the refrigerant and solution pipes as well: on the Table 3.1. are shown the insulations.

	Vessel wall	Pipes (28 mm)	Pipes (18 mm)
Product name	Microban AF-10 mm	AF2-028	AF2-018
Insulation thickness	10 mm	13 mm	11,5 mm
Thermal conductivity	$\lambda (0^{\circ}C) \leq 0,033 \frac{W}{m \cdot K}$	$\lambda (0^{\circ}C) \leq 0,033 \frac{W}{m \cdot K}$	$\lambda (0^{\circ}C) \leq 0,033 \frac{W}{m \cdot K}$

Table 3.1. Insulating from Armaflex manufacturer [7].

The solution heat exchanger is covered by polyurethane, kept around the apparatus by two retaining clips.

The two facility vessels are shown in the Figure 3.2.



Figure 3.2. A view of the absorption chiller. The two vessels are equipped with portholes to regulate the levels of the liquid inside.

3.1.2 The secondary fluid loops

The working secondary fluids, for the heating, cooling and cold loop are water without additives. They flow in three independent circuits.

The sensors system allows to measure, every 20 seconds, the temperatures and the volume flow rates of the secondary fluids, at the inlet and outlet of each heat exchanger.

That is why the applications of the first thermodynamic law to the secondary fluids represent an easy way to calculate the heat flux that is exchanged by each apparatus:

$$\dot{Q} = \dot{V} \cdot \rho \cdot c_p (T_{aus} - T_{ein}) \quad 3.1$$

The values of both the density and the specific heat can be calculated through the internal library of the *Engineering Equation Solver* – EES software, for average temperature value (between T_{aus} and T_{ein}).

The next sections describe the secondary loops. In the relative pictures all the sensors are not shown, but just those ensure the inlet conditions of the machine. The sensor overview is presented in the paragraph 3.1.3.

Heating loop

The heating loop simulates the driving energy of the facility, which in the industrial applications can be wasted heat from other manufacturing processes.

The schematic view of that is shown in the Figure 3.3

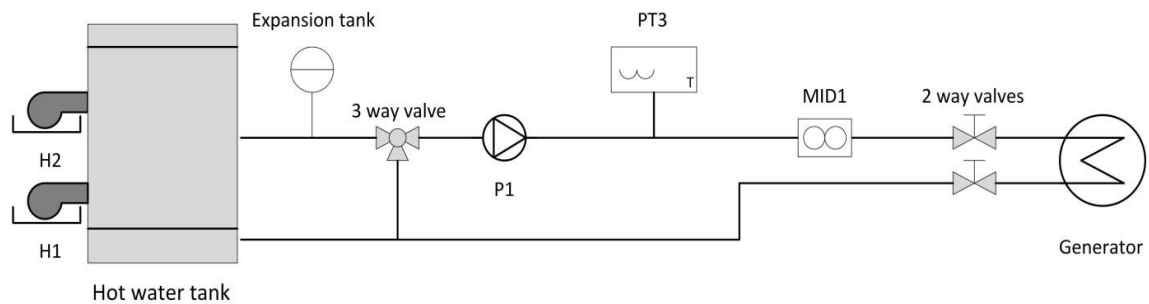


Figure 3.3. A schematic view of the heating loop, from the tank, where the water is heated up and stored, up to the generator, where the heat is delivered to the facility.

As it is shown in the above picture, the hot water comes from a tank, where the fluid is stored and heat up by 2 electric heaters.

The loop is equipped with:

- *Expansion tank*. Where the water can expand when the temperature is high, preventing damages to the circuit.
- *Automatic three-way valve*. This device is useful to regulate the temperature at the inlet of the generator, fixed by the computer and measured by the PT3.
- *PT3*: temperature sensor at the inlet of the generator.
- *MID1*: flow meter at the inlet of the generator.
- *Two-way ball valves*. They have the possibility to isolate the generator from the remaining part of the loop. They were useful especially during the construction and test of the facility (red valves shown in the Figure 3.6).
- *H1, H2*: the 2 electrical resistance heaters, with an overall power of 15 KW.
- *P1*: hot water loop centrifugal pump.
- *500 liters capacity tank*.
- *Rubber and copper pipes*. The copper pipes are organized from the tank up to the two-way valves. On the contrary the rubber pipes are present between the generator and the 2 way valves.

Cold loop

The cold loop is connected with the evaporator of the facility and it has the same structure of the heat loop. A schematic view of it is presented in the Figure 3.4.

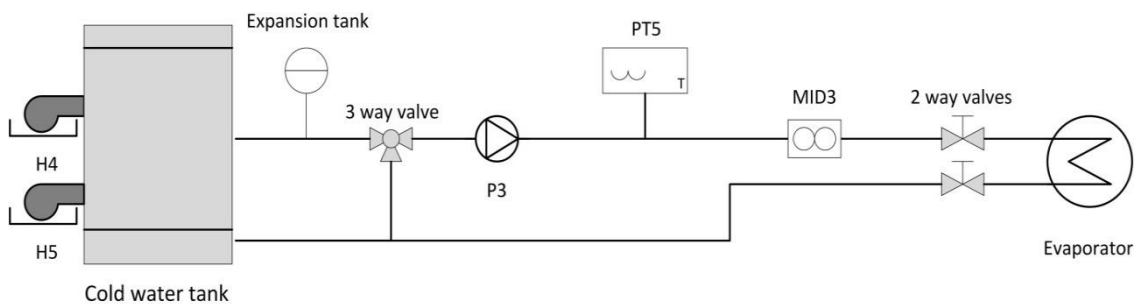


Figure 3.4. A schematic view of the cold loop, from the tank, where the water is kept at a certain temperature, up to the evaporator.

The cold water tank is equipped, like the heat water one, with 2 heaters. They are necessary to keep the water, at the inlet of the evaporator, equal to the value fixed through the computer.

The devices present in that loop are:

- *Expansion tank*. Where the water can expand when the temperature is high, preventing damages to the circuit.
- *Automatic three-way valve*. This valve has the same function of that in the heat loop.
- *PT5*: temperature sensor at the inlet of the evaporator.
- *MID3*: flow meter at the inlet of the evaporator.
- *Two-way ball valves*. They have the possibility to isolate the evaporator from the remaining part of the loop: they were useful especially during the construction and test of the facility (red valves shown in the Figure 3.6).
- *H4, H5*: the 2 electrical resistance heaters, with an electrical power of 16 KW.
- *P3*: hot water loop centrifugal pump.
- *500 liters capacity tank*.
- *Rubber and copper pipes*. The pipes are organized as in the heating loop.

Cooling loop

The cooling water loop purpose is to cool down both the absorber (at first) and the condenser of the absorption cycle.

This circuit is in contact with the building water network through a counter flow plate heat exchanger, to release the heat exported from the facility.

A schematic view of the loop is presented in the Figure 3.5.

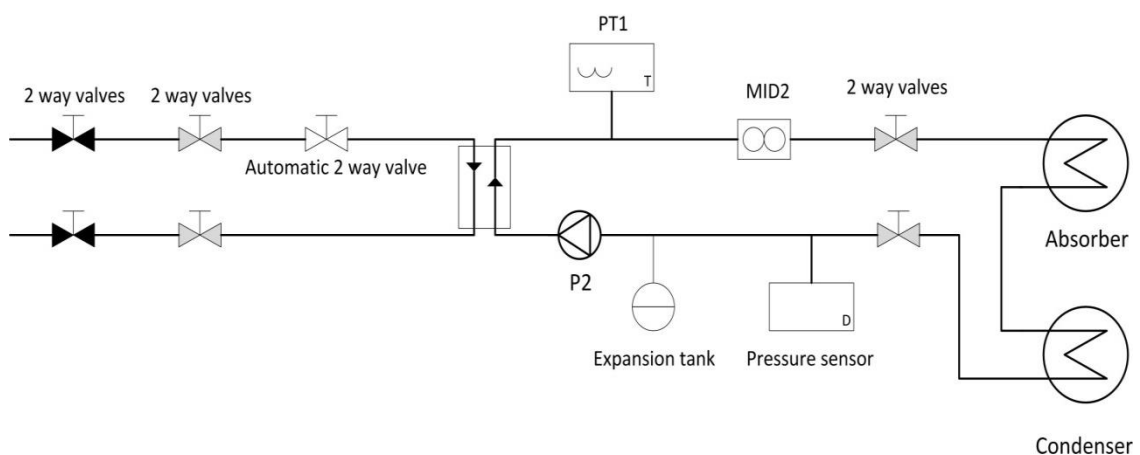


Figure 3.5. The two circuits are shown: respectively the building water network on the left and the facility one on the right, connected through the plate heat exchanger.

The left loop is equipped with:

- *4 two-way ball valves*. The two-way valves on the left, highlighted in black on the Figure 3.5, represent a security device for the laboratory: during the stop time of the facility they are closed to prevent that the water of the building water network flows down on the machine pipes, causing flood possible problems (black valve on the Figure 3.6).
- The two-way valves on the right have the possibility to isolate the plate heat exchanger from the remaining part of building network (red valves shown in the Figure 3.6).
- *Automatic two-way valve*. This device is useful to regulate the temperature at the inlet of the absorber, fixed by the computer and measured by the PT1.
- *Rubber and copper pipes*. The copper pipes are organized from the grey two-way valves (in accordance with the Figure 3.5) up to the plate heat exchanger. On the contrary the rubber pipes are present between the 4 two-way valves of the loop (Figure 3.6).

The right loop is equipped with:

- *PT1*: temperature sensor at the inlet of the absorber.
- *MID2*: flow meter at the inlet of the absorber.
- *Two-way ball valves*. They have the possibility to isolate the absorber and condenser from the remaining part of the loop. They were useful especially during the construction and test of the facility (red valves shown in the Figure 3.6).
- *Pressure sensor*. It is a security device for the circuit, which activates the security valve installed with it.
- *P2*: cooling water loop centrifugal pump.
- *Expansion tank*. Where the water can expand when the temperature is high, preventing damages to the circuit.
- *Rubber and copper pipes*. The copper pipes are organized from the plate heat exchanger up to the two-way valves. On the contrary the rubber pipes are present between the facility heat exchangers and the above mentioned two-way valves.



Figure 3.6. Two-way valves of the facility secondary circuits. From the left to the right the

The flexible plastic black tubes are verified for a working pressure of 15 bar. The valves represent the connection between the rubber and copper tubes of the secondary fluid loop.

red valves are: the two valves which isolate the evaporator from the remaining cold loop, the two valves which isolate both the absorber and the condenser from the remaining cooling loop, the two valves which isolate the building cooling water network from the facility and finally the two valves which separate the generator from the remaining hot loop.

In the background the two black valves mentioned in the Figure 3.5 description can be seen as well.

3.1.3 The control and measurement systems

The working parameters of facility are controlled through the computer and a control electric panel as well. The latest is shown is the Figure 3.7.

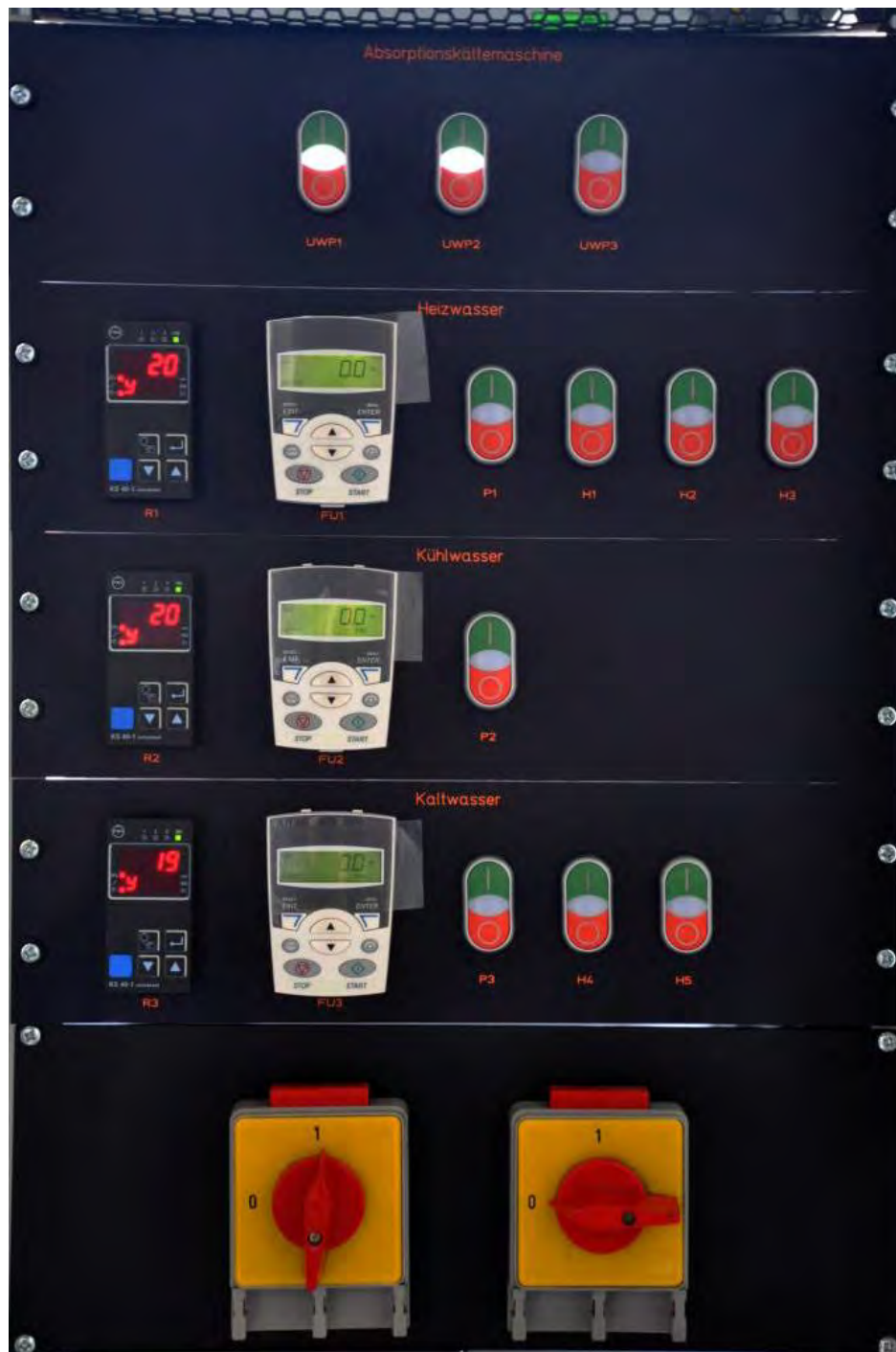


Figure 3.7. The electric control panel.

Only the valves V1, V2, V3 and V4 are controlled by manual control (Figure 3.1).

The two control knobs (Figure 3.7 and in particular 3.10) serve the purpose to supply the electricity to the facility devices and the computer.

The buttons H1...H5 are used to switch on the heaters and the P1...P3 to supply the electricity to the secondary fluids loops pumps.

The control instruments FU1, FU2 and FU3 turn on the power and regulate the above mentioned pumps.

The instruments on the left side R1...R3 control the three-way mixing valves of the secondary loops.

The above mentioned symbols are related to the Figure 3.7.

These valves can be regulated by hand or through the automatic mode and the temperatures affected by their actions are shown in the displays of the panel.

In the control panel is specified to which loops are referred the controls too.



Figure 3.8. Automatic mode button, present on the R1...R3 control valve instruments.



Figure 3.9. When the automatic mode is off, the two arrow buttons on the R1...R3 controls allow the manual regulation of the valves.

The UWP1, UWP2 and UWP3 buttons have the function to switch on the respective pumps.

The temperatures which is affected by the mixing of the valves are fixed by the computer, especially through the LabVIEW software.

Through the sensors system connected to the computer is possible to check the temperatures, the pressure and the volume flow rates which characterize the absorption chiller.

All these data are stored inside the computer in the form of Excel file, with a frequency fixed by the software.

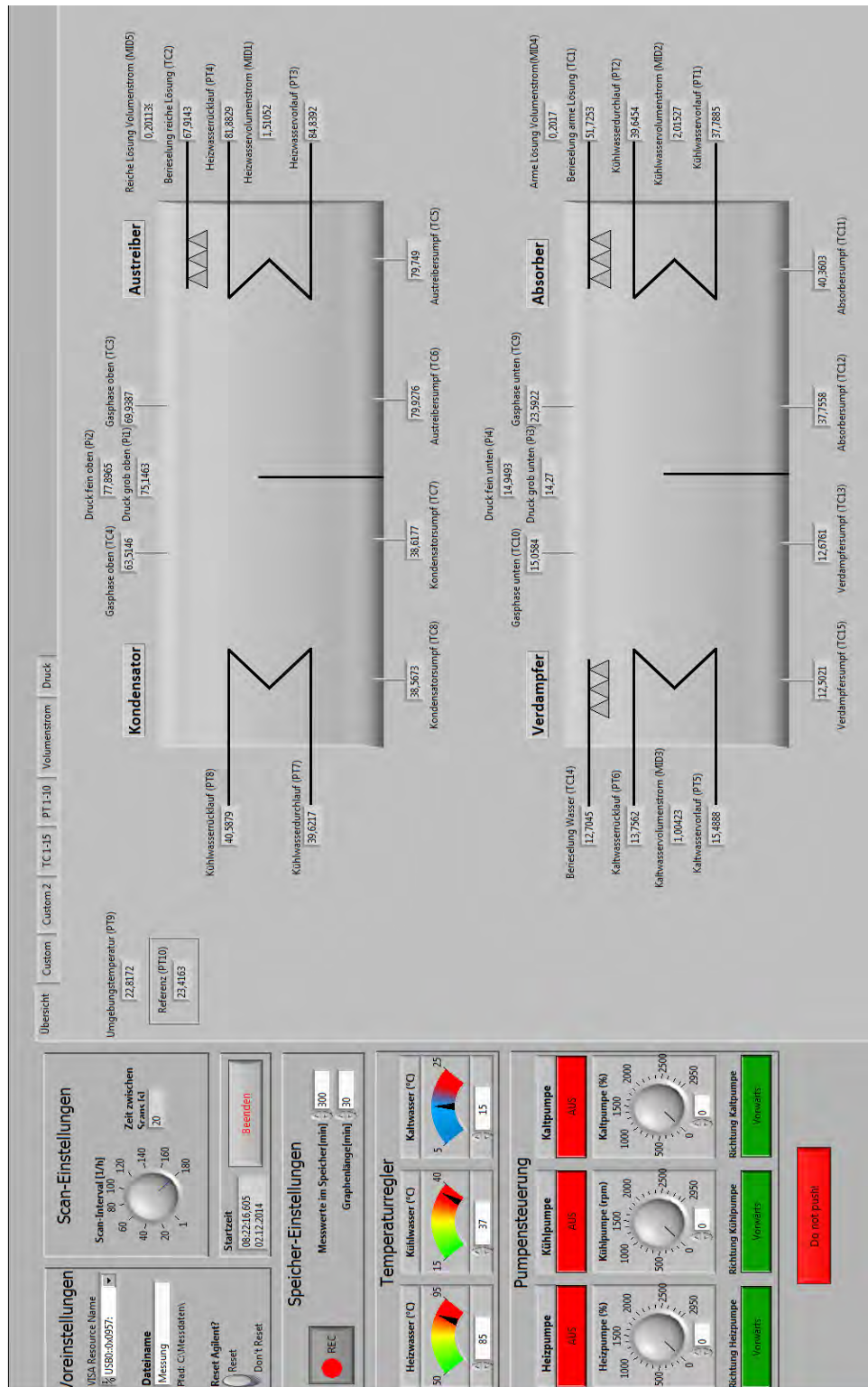


Figure 3.10. LabVIEW overall frame.

The system parameters are measured by:

- 4 pressure sensors ($Pi1 \dots Pi4$);
- 15 thermocouples ($TC1 \dots TC15$);
- 10 PT100 (A class.): platinum resistance thermometers ($PT1 \dots PT10$);
- 5 magnetic inductive flow sensors ($MID1 \dots MID5$).

They are applied to measure respectively the temperatures, the pressures and the volume flow rates of the absorption chiller. More details are shown in the Table 3.2.

	Symbol	Scope	Unit of measurement
Pressure	$Pi1$	Above tank pressure (> 120 mbar)	mbar
	$Pi2$	Above tank pressure (< 120 mbar)	mbar
	$Pi3$	Down tank pressure (> 120 mbar)	mbar
	$Pi4$	Down tank pressure (< 120 mbar)	mbar
Temperature	$TC1$	Poor solution temperature (Absorber inlet)	$^{\circ}\text{C}$
	$TC2$	Rich solution temperature (Generator inlet)	$^{\circ}\text{C}$
	$TC3$	Gas temperature (Generator)	$^{\circ}\text{C}$
	$TC4$	Gas temperature (Condenser)	$^{\circ}\text{C}$
	$TC5$	Generator liquid solution temperature (near the vessel side border)	$^{\circ}\text{C}$
	$TC6$	Generator liquid solution temperature (near the condenser partition)	$^{\circ}\text{C}$
	$TC7$	Condenser liquid solution temperature (near the generator partition)	$^{\circ}\text{C}$
	$TC8$	Condenser liquid solution temperature (near the vessel side border)	$^{\circ}\text{C}$
	$TC9$	Gas temperature (Absorber)	$^{\circ}\text{C}$
	$TC10$	Gas temperature (Evaporator)	$^{\circ}\text{C}$
	$TC11$	Absorber liquid solution temperature (near the vessel side border)	$^{\circ}\text{C}$
	$TC12$	Absorber liquid solution temperature (near the evaporator partition)	$^{\circ}\text{C}$

	<i>TC13</i>	Evaporator liquid solution temperature (near the absorber partition)	°C
	<i>TC14</i>	Recirculating liquid refrigerant temperature (Evaporator inlet)	°C
	<i>TC15</i>	Evaporator liquid solution temperature (near the vessel side border)	°C
	<i>PT1</i>	Cooling water temperature (Absorber inlet)	°C
	<i>PT2</i>	Cooling water temperature (Absorber outlet)	°C
	<i>PT3</i>	Heat water temperature (Generator inlet)	°C
	<i>PT4</i>	Heat water temperature (Generator outlet)	°C
	<i>PT5</i>	Cold water temperature (Evaporator inlet)	°C
	<i>PT6</i>	Cold water temperature (Evaporator outlet)	°C
	<i>PT7</i>	Cooling water temperature (Condenser inlet)	°C
	<i>PT8</i>	Cooling water temperature (Condenser outlet)	°C
	<i>PT9</i>	Ambient temperature	°C
	<i>PT10</i>	Reference	°C
<i>Volume flow rate</i>	<i>MID1</i>	Hot water volume flow rate	m ³ /h
	<i>MID2</i>	Cooling water volume flow rate	m ³ /h
	<i>MID3</i>	Cold water volume flow rate	m ³ /h
	<i>MID4</i>	Poor solution volume flow rate	m ³ /h
	<i>MID5</i>	Rich solution volume flow rate	m ³ /h

Table 3.2. Symbol, position and type of each sensor placed on the facility. The positions are shown in the Figure 3.1.



Figure 3.11. The heat and cold water tanks with the relative secondary fluid loop equipment.

3.2 Experimental setup

3.2.1 Heat source preparation

The first step of the experiment setup is the preparation of the heat source.

It consists in the heating of the water, which, during the experiments, will be sent inside the pipes of the absorption cycle generator.

First of all the electricity has to be supplied with the two control knobs (Figure 3.12). In this way the electric circuits, both of the machine and of the computer are activated.



Figure 3.12. The two control knobs to supply the plan electricity.

Afterwards the heaters of the hot water tank (H1, H2) and the heaters of the cold water tank (H4, H5) have to be turned on at 110°C (maximum capacity), until the pressure inside the heat water tank grows up to a value between 2 and 2.4 bar. Raising the pressure is a precaution to avoid a possible evaporation of the water, which could damage the machine.

After that, the heat loop pump (P1) is switched on and the three way valve is opened to allow the recirculation of the water along the entire heat circuit.

The two red valves on the wall have to be opened as well, to allow the water to flow inside the pipes of the absorption machine.

This work situation is kept as long as the hot water temperature reaches a constant value (close to 110 °C), meaning that there is no more stratification inside the tank.

This procedure is carried out on the first work day after the weekend, to remedy the heat dissipations that take place during those days.

In this way the machine is ready to work from the day after.

3.2.2 *Experiment preparation*

The procedure for the preparation of the experiments is the following:

- Supplying the electricity;
- Turning on of the heaters H1, H2, H4 and H5 for the conservation of the water temperature;
- Make LabVIEW running. Make sure of the data recording pushing REC button;
- Preparation of liquid nitrogen, which has to be taken from a tank outside the laboratory, where the liquid is stored at the temperature of -196 °C (pressure equal to 1 bar). Because of the very low temperature a security gloves and glasses have to be put on.
- Carrying out of the vacuum inside the two machine cylinders.

During this step it is necessary to use a vacuum pump, which is connected through rubber pipes first to one facility vessel and after to the other one, for about 20 minutes each.

The pump is switched off when the temperatures indicated by the sensors TC8 and TC15 and the pressures inside the vessels are in accord with the water saturation curve values. At this moment it is possible to see that the pressures inside both the vessels begin to assume constant trends



Figure 3.13. The vacuum pump: DUO 016 B type of PFEIFFER (Balzers) manufacturer.

Between the vacuum pump and the cylinder is placed a liquid receiver put inside a bucket full of liquid nitrogen (Figure 3.14).



Figure 3.14. The liquid receiver inside a container full of liquid nitrogen.

The purpose of the liquid nitrogen is the freezing, inside the liquid receiver, of the little amount of liquid that could flow from the machine to the vacuum pump, causing possible damages to the latter.

A complete freezing of the liquid receiver must be avoided, or the connection between the pump and the vessel could be interrupted. That requires regular inspections [7].

Actually the two machine vessels do not represent real vacuum chambers, but inside them a rarefied gas is present at a pressure lower than the atmosphere one.

The pressures of both the vessels are included in this range:

$$100 > P > 1 \text{ mbar}$$

Because of that it is said that the machine works with a *low vacuum* level.¹

- Switching on of the UWP3 pump and opening of the V3 valve of 300° manually.



Figure 3.15. The V3 manual valve is open of 300° in the counterclockwise way.

- Switching on of the UWP1 pump and opening of the valve V1. After few minutes the same steps have to be applied to the UWP2 pump and valve V2, trying to keep a constant level of liquid inside both the generator and the absorber. This condition has to be kept as long as the machine works, to ensure a steady state work condition.

A certain amount of liquid has to be ensured in the suction lines of UWP1 and UWP2 pumps to avoid cavitation problems. A good way to operate is keeping the same levels of liquid inside the generator and the absorber.

¹Low vacuum level: $1000 > P > 10^{-2} \text{ mbar}$ [2].

- Setting of the temperatures through the computer and the automatic mode for the mixing valve in the R1, R2 and R3 controllers.
- Pushing the indicator light P1, P2 and P3, respectively for the heat loop pump, cooling loop pump and cold loop pump.
- Activation of the three above-mentioned pumps through the displays FU1, FU2 and FU3 pressing the button ENTER two times and after the button START.

First has to be switched on the cold loop pump, second the cooling loop pump and finally the heat loop pump. This order has to be followed because the evaporator and the absorber have to be activated before the generator. That is to ensure a certain amount of absorption of the solution, which otherwise would have a too low concentration causing crystallization problem.

- Opening of the two-way black valves (Figure 3.6) and of the two-way red valves (Figure 3.6) placed on the heating loop, after the activations respectively of the cooling loop pump and of the heat loop pump.

After this procedure the facility is ready for the measurements.

3.2.3 *Switching off of the plant*

During the facility switching off procedure, which takes around 45 minutes, the most important issue to manage is the crystallization.

This problem can be avoided diluting the solution concentration and so decreasing the temperature in the critical part of the facility: the solution heat exchanger, especially in the poor solution side [7].

First of all the automatic three-way valve of the hot water loop has to be set up in manual mode, in order to close it to stop the hot water flow up to the generator.

These conditions have to be kept until the temperatures indicated by the two sensor TC5 and TC6 go below 45 °C. This is a criteria suggested by the experience to overcome the crystallization problem.

During the decreasing of those temperatures, all the pumps and especially UWP1, UWP2 and UWP3 are active, to accelerate the solution dilution.

When the above mentioned temperatures reach the suitable values, the V1 valve and immediately after the UWP1 are shut down.

When the display of the poor solution pipe indicates that the volume flow rate is close to 0, the V2 valve and the UWP2 pump have to be closed immediately too. The closing of the valve is carried out just a little before that the relative volume flow rate is null, in order to ensure that some liquid is still inside the poor solution pipe, before the valve. That step is made to keep the pressure difference between the two vessels.

Afterwards all the pumps have to be turned off through the FU1, FU2, FU3 displays, pushing the *stop* buttons and after setting up the manual mode in the remaining automatic valves, through the controllers R2 and R3.

For precaution the black valves, which represent the connection with the building cooling water network, have to be closed (see 3.1.2. paragraph, cooling loop description).

The step after is the switching off of all the secondary loop pumps (P1...P3) and all the heaters (H1...H5). After that the V3 valve has to be closed too.

At this point the V4 valve can be closed, in the same way of the V2: ensuring that some liquid is still inside the pipe above the valve, in order to keep the pressure difference.

Finally the recording and the computer can be turn off.

3.3 Experimental procedure

The measurements carried out through the facility aim to investigate various characteristics of it, which can be recapitulated through the Table 3.3.

Work scope	Varying parameter	T hot [°C]	T cool [°C]	T cold [°C]	Hot flow rate [m³/h]	Cool flow rate [m³/h]	Cold flow rate [m³/h]	Solution flow rate [m³/h]
COP and cooling capacity curves	T hot	var	27	10	1.5	2	1	0.15
Dynamic behavior	T hot	var	27	15	1.5	2	1	0.15
Dynamic behavior	T hot	var	27	15	1.5	2	1	0.15

Absorber heat transfer	Solution flow rate	85	27	15	1.5	2	1	var
Absorber heat transfer	Solution flow rate	85	27	15	1.5	2	1	var
Absorber heat transfer	Solution flow rate	85	32	15	1.5	2	1	var
Absorber heat transfer	Solution flow rate	85	32	15	1.5	2	1	var
Absorber heat transfer	Solution flow rate	85	32	15	1.5	2	1	var
Absorber heat transfer	Solution flow rate	85	37	15	1.5	2	1	var
Absorber heat transfer	Solution flow rate	85	37	15	1.5	2	1	var
Absorber heat transfer	Solution flow rate	85	37	15	1.5	2	1	var

Table 3.3. In the table the various investigations are shown. Especially the research purpose, constant parameters and varying parameters are indicated. 'T hot' represents the hot water temperature at the inlet of the generator, 'T cool' the cooling water temperature at the inlet of the absorber and 'T cold' the cold water temperature at the inlet of the absorber. The solution flow rate values are related especially to the poor solution flow rate, regulated by the V2 valve.

3.3.1 COP curve

The first facility analyzed features are the Coefficient of Performance – COP and the cooling capacity at the evaporator – \dot{Q}_v , in function of the hot water temperature at the inlet of the generator.

All of these parameters are evaluated when the machine is in steady state condition. In other words when all the boundary conditions are fixed and kept

stable, by the automatic and manual controls, until the temperatures and the pressures inside both the vessels are constant for 30 minutes at least. The pressures and temperatures trends can be checked out through the LabVIEW frame: an example of is shown in the Figure 3.16.

The data to carry out the calculations are extracted from the Excel datasheet recorded through the computer, where both the time and the measuring sensor for each parameter are indicated. An example of datasheet is posted in the Attachment C.

The LabVIEW program records the value through the sensors each 20 seconds, because of that to carry out the calculations the average values of the last 10 minutes in steady state conditions are used.

To calculate the cooling capacity and COP the following formulas are applied:

$$\dot{Q}_v = \dot{M}_v \cdot c_{p,v} \cdot (T_{ein,v} - T_{aus,v}) \quad 3.2$$

where:

- The cold water mass flow rate \dot{M}_v is calculated from the knowing of both the volumetric flow rate, that is fixed by the valve, and the water density at 10 °C.
- $T_{ein,v}$ is measured by the PT5 temperature sensor.
- $T_{aus,v}$ is measured by the PT6 temperature sensor.
- $c_{p,v}$ is the specific heat of the water at 10 °C.

$$COP = \frac{\dot{Q}_v}{\dot{Q}_g} = \frac{\dot{M}_v \cdot c_{p,v} \cdot (T_{ein,v} - T_{aus,v})}{\dot{M}_g \cdot c_{p,g} \cdot (T_{ein,g} - T_{aus,g})} \quad 3.3$$

where:

- The mass flow rate \dot{M}_g is calculated from the knowing of both the volumetric flow rate, that is fixed by manual hand, and the water density at a temperature equal to $T_{ein,g}$ (T hot on the Table 3.3);
- $T_{ein,g}$ is measured by the PT3 temperature sensor;

- $T_{aus,g}$ is measured by the PT4 temperature sensor;
- $c_{p,g}$ is the specific heat of the water at a temperature equal to $T_{ein,g}$;
- \dot{Q}_v is calculated from the formula 3.2.

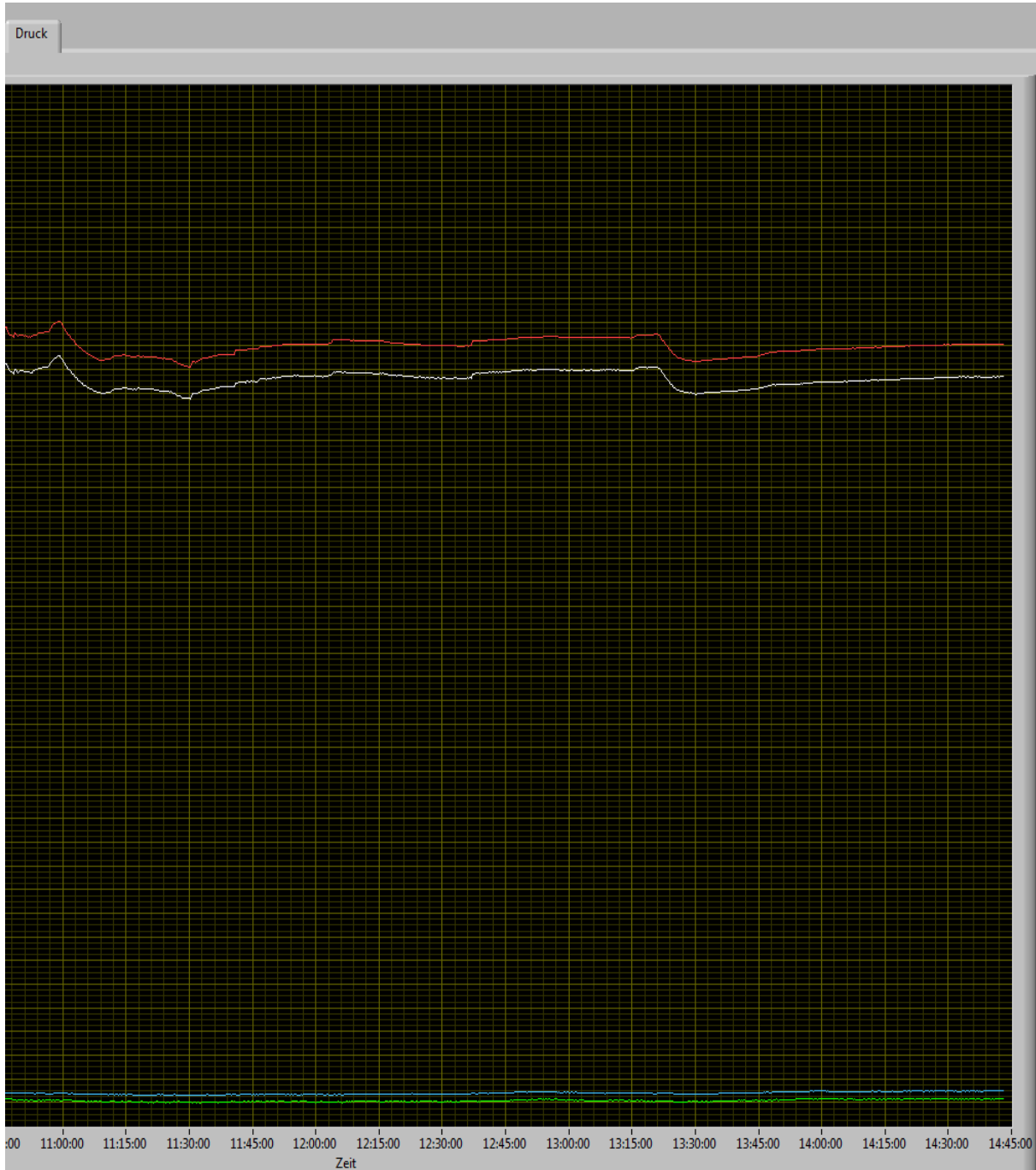


Figure 3.16. The pressure has been being constant for at 30 minutes. If the other pressure and temperature values present the same trend, it is possible to carry out the measurement.

Both the cooling capacity and the COP are calculated for different hot water temperature at the inlet of the generator: from 85 °C to 65 °C, with a variation of 5 °C for each step.

The other significant boundary conditions of the facility are shown in the Table 3.3.

These experimental results, taken for a cold water temperature of 10°C, are going to be compared with the simulations carried out with EES software (see the chapter n. 4).

To widen the results comparison, just for the *COP curve* section, another one referential experimental data collection is taken. This data collection is relative to the same facility and it involves measurements for different cold water temperature at the inlet of the evaporator (10 °C, 15 °C, 20 °C and 25 °C). Moreover, this data are collected when the facility was just built and so the heat exchangers were new, especially the generator, where the corrosion due to the Lithium Bromide is not a negligible aspect. The source where the data collection is taken is [7].

They are posted in the Attachment D.

3.3.2 *Dynamic behavior*

Another important and interesting aspect investigated is the dynamic behavior of the machine. After the facility reaches the steady state conditions, the hot water temperature is changed through the computer control: the purpose is to check the facility variable trends during the step response of the absorption chiller.

The step response is the period which the facility needs to reach a new steady state condition, after the varying of one or more parameter.

The parameters which are evaluated during that time are:

- Cooling capacity \dot{Q}_v ;
- The cold water temperature at the outlet of the evaporator $T_{aus,v}$;
- The cooling water temperature at the outlet of the absorber $T_{aus,ab}$;
- The cooling water temperature at the outlet of the condenser $T_{aus,k}$;
- The hot water temperature at the outlet of the generator $T_{aus,g}$;
- The hot water temperature at the inlet of the generator $T_{ein,g}$: it represents the varying parameter.

The hot water steps are shown in the Table 3.4 and the values of the other boundary conditions are indicated in the Table 3.3.

Hot temperature variation		Step
75 °C	—————→ 70 °C	5 °C
70 °C	—————→ 75 °C	5 °C
75 °C	—————→ 65 °C	10 °C
65 °C	—————→ 75 °C	10 °C
75 °C	—————→ 80 °C	5 °C
80 °C	—————→ 75 °C	5 °C
75 °C	—————→ 85 °C	10 °C
85 °C	—————→ 75 °C	10 °C

Table 3.4. In the table the variation of the hot water temperature, at the inlet of the generator are exhibited. The arrows indicate the directions of the temperature variations.

Each parameter is analyzed as function of the time.

During the measurements the time when the machine reaches a new steady state conditions is written down, in order to calculate the required parameters in the right period: when the step response takes place.

All the machine values are recorded by the LabVIEW software in an Excel file, where is also specified the time when that parameter is recorded. An example of that file is posted in the Attachment C.

The sensors which record the significant temperatures are:

Temperature	Sensor
$T_{\text{aus,v}}$	PT6
$T_{\text{aus,ab}}$	PT2
$T_{\text{aus,k}}$	PT8
$T_{\text{aus,g}}$	PT4
$T_{\text{ein,g}}$	PT3

Table 3.5. Each temperature is recorded by a dedicated sensor.

After the step response time is individuated, all the temperature variations can be written down and plotted as a function of the time.

The cooling capacity at the evaporator is calculated by the following formula at each 20 seconds (time set up by LabVIEW recording):

$$\dot{Q}_v = \rho \cdot \dot{V}_v \cdot c_{pv} \cdot (T_{ein,v} - T_{aus,v}) \quad 3.4$$

where:

- \dot{V}_v is the cold water mass flow rate (MID3 flow meter);
- c_{pv} is the cold water specific heat;
- $T_{ein,v}$ is the cold water inlet temperature at the evaporator (PT5 sensor);
- ρ is the cold water density.

The density and the specific heat are calculated through a little subroutine written by EES, taking the average temperatures between $T_{ein,v}$ and $T_{aus,v}$ values to calculate them. The internal library of that software is used.

3.3.3 Absorber heat transfer

In this section the investigations of the absorber heat transfer coefficients are carried out, in function of the poor solution volume flow rate. In particular it is focused on the heat transfer coefficient α of the film outside the pipes and on the overall heat transfer coefficient K of the absorber.

These coefficients will represent the suggested input values for the mathematical simulations, which will be carried out through Engineering Equations Solver – EES. This section is debated in the chapter 4: *Mathematical model*.

The software adopts an iterative procedure to find the solutions, in particular the Newton - Raphson method.

The work conditions wherein the coefficients are investigated are shown in the Table 3.3.

The measurements are done for various poor solution flow rates and for the three different cooling water inlet temperatures at the absorber.

<i>T cooling [°C]</i>	<i>Poor solution volume flow rate [m³/h]</i>
27	0,35 → 0,30 → 0,25 → 0,20 → 0,15 → 0,10
32	0,35 → 0,30 → 0,25 → 0,20 → 0,15 → 0,10
37	0,35 → 0,30 → 0,25 → 0,20 → 0,15 → 0,10

Table 3.6. In the table all the poor solution volume flow rate values taken in the measurements are shown. The same variation steps are carried out for different cooling water temperatures (inlet of the absorber).

3.3.3.1 Data reduction

The coefficient calculations are performed solving an equation system, which describe the thermodynamics characteristics of the facility, especially of the absorber.

To figure the equation system out, the Engineering Equation Solver – EES software² is used.

As it is above mentioned, the software uses the Newton – Raphson iterative method.

The program script, with example values, is posted in the Attachment D.

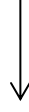
The calculations procedure is summarized by the following flow chart and the procedure has to be carried out for each cooling temperature and each poor solution flow rate.

This section is related to the research of Tomforde [11].

²Engineering Equation Solver was used Professional v 9,472. The material data are integrated into the software as libraries.

$$T_{ein,ab}; \quad T_{aus,ab}; \quad \dot{V}_k; \quad P_u; \quad \dot{V}_{al}; \quad P_{ls}; \quad T_{ls,ein}; \quad T_{ls,aus}$$

$$\rho_{ls,ein,probe}; \quad \rho_{ls,aus,probe}; \quad \text{absorber geometry}$$



$$\eta_k = \eta_{water}((T_{ein,ab} + T_{aus,ab})/2; P_u) \quad 3.5$$

$$\rho_k = \rho_{water}((T_{ein,ab} + T_{aus,ab})/2; P_u) \quad 3.6$$

$$c_{pk} = c_{p,water}((T_{ein,ab} + T_{aus,ab})/2; P_u) \quad 3.7$$

$$\lambda_k = \lambda_{water}((T_{ein,ab} + T_{aus,ab})/2; P_u) \quad 3.8$$

$$\lambda_{Cu} = \lambda_{Cu}((T_{ein,ab} + T_{aus,ab})/2); \quad 3.9$$

$$Pr_k = Pr_{water}((T_{ein,ab} + T_{aus,ab})/2; P_u) \quad 3.10$$

$$w_{ein} = w_{LiBr}(T = 293; \rho_{ls,ein,probe}) \quad 3.11$$

$$w_{aus} = w_{LiBr}(T = 293; \rho_{ls,aus,probe}) \quad 3.12$$



$$\rho_{ls,ein} = \rho_{LiBr}(T_{ls,ein}, w_{ein}) \quad 3.13$$

$$\rho_{ls,aus} = \rho_{LiBr}(T_{ls,aus}, w_{aus}) \quad 3.14$$

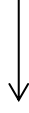
$$\lambda_{ls} = \lambda_{LiBr}(T_{ls,ein}, w_{ein}); \quad 3.15$$

$$\eta_{ls} = \eta_{LiBr}(T_{ls,ein}, w_{ein}) \quad 3.16$$

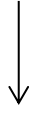
$$T_{ls,gg,ein} = T_{LiBr}(P_{ls}, w_{ein}) \quad 3.17$$

$$T_{ls,gg,aus} = T_{LiBr}(P_{ls}, w_{aus}) \quad 3.18$$

$$\dot{Q} = \dot{V}_k \cdot c_{pk} \cdot \rho_k \cdot (T_{aus,ab} - T_{ein,ab}) \quad 3.19$$



$$\delta_{T,Lm} = \frac{(T_{ls,gg,ein} - T_{aus,ab}) - (T_{ls,gg,aus} - T_{ein,ab})}{\ln \frac{(T_{ls,gg,ein} - T_{aus,ab})}{(T_{ls,gg,aus} - T_{ein,ab})}} \quad 3.20$$



$$\dot{m}_k = \frac{\dot{V}_k \cdot \rho_k}{n_{RR}} \quad 3.21$$



$$u_{kw} = \frac{\dot{m}_k}{\rho_k \cdot \pi \cdot ((d_e - 2s)^2)/4} \quad 3.22$$



$$Re_{kw} = \frac{u_{kw} \cdot \rho_k \cdot (d_e - 2s)}{\eta_k} \quad 3.23$$



$$x_i = (0,782 \cdot \ln Re_{kw} - 1,51)^{-2} \quad 3.24$$



$$Nu_{kw} = \frac{\frac{x_i}{8} \cdot (Re_{kw} - 1000) \cdot Pr_k}{1 + 12,7 \cdot \sqrt{x_i/8} \cdot (Pr_k^{\frac{2}{3}} - 1)} \cdot \left[1 + \left(\frac{d_i}{l}\right)^{\frac{2}{3}}\right] \quad 3.25$$



$$\alpha_{kw} = \frac{Nu_{kw} \cdot \lambda_k}{d_i} \quad 3.26$$



$$k = \frac{\dot{V}_k \cdot c_{pk} \cdot \rho_k \cdot (T_{aus,ab} - T_{ein,ab})}{A_{abs} \cdot \delta_{T,Lm}} \quad 3.27$$



$$\frac{1}{\alpha_{film}} = \frac{1}{k} - \frac{d_e}{d_i \cdot \alpha_{kw}} - \frac{d_e}{2 \cdot \lambda_{Cu}} \cdot \ln \frac{d_e}{d_i} \quad 3.28$$

Where:

- $T_{ein,ab}$ = cooling water temperature at the absorber inlet; K
- $T_{aus,ab}$ = cooling water temperature at the absorber outlet; K
- \dot{V}_k = cooling water volume flow rate; m³/s
- P_u = pressure inside the cooling water pipes; Pa
- \dot{V}_{al} = poor solution volume flow rate; m³/s
- P_{ls} = pressure inside the absorber; Pa
- $T_{ls,ein}$ = poor solution temperature – absorber inlet; K
- $T_{ls,aus}$ = rich solution temperature – absorber outlet; K
- $\rho_{ls,ein,probe}$ = Poor solution density sample at 20°C; kg/m³
- $\rho_{ls,aus,probe}$ = Rich solution density sample at 20°C; kg/m³
- η_k = Cooling water dynamics viscosity Pa · s
- ρ_k = Cooling water density; kg/m³
- c_{pk} = Cooling water specific heat; J/(kg · K)

• λ_k = Cooling water thermal conductivity;	W/(m · K)
• A_{ab} = Absorber area;	m ²
• λ_{Cu} = Copper thermal conductivity;	W/(m · K)
• Pr_k = Cooling water Prandtl number,	
• w_{ein} = Poor solution concentration at 20°C;	
• w_{aus} = Rich solution concentration at 20°C;	
• $\rho_{ls,ein}$ = Poor solution sample density at $T_{ls,ein}$;	kg/m ³
• $\rho_{ls,aus}$ = Poor solution sample density at $T_{ls,aus}$;	kg/m ³
• λ_{ls} = Poor solution thermal conductivity at the inlet of the absorber;	W/(m · K)
• η_{ls} = Poor solution viscosity at the inlet of the absorber;	Pa · s
• $T_{ls,gg,ein}$ = Solution saturation temperature at the absorber inlet;	K
• $T_{ls,gg,aus}$ = Solution saturation temperature at the absorber outlet;	K
• \dot{Q} = Cooling heat exported from the absorber;	W
• u_{kw} = Mean velocity of the cooling water;	m/s
• Re_{kw} = Cooling water Reynolds number;	
• x_i = Friction factor from Colebrook Source: "Process Heat Transfer"- Principles of Application" Eq. 2:39 [12].	
• Nu_{kw}^3 = Cooling water Nusselt number;	
• α_{kw} = Cooling water convection heat transfer coefficient;	W/(m ² · K)
• $\delta_{T,Lm}$ = Logarithmic mean temperature difference - Absorber,	K
• d_e = Pipe external diameter;	m
• d_i = Pipe internal diameter;	m
• k = Overall heat transfer coefficient – Absorber;	W/(m ² · K)
• α_{film} = Film convective heat transfer coefficient;	W/(m ² · K)
• n_{RR} = Number of column;	
• \dot{m}_k = cooling water mass flow rate;	kg/s

³ The Nusselt number of the cooling water is calculated through Gnielinski correlation for turbulent flow and flow in the transition region (allowed for $2100 < Re < 10^6$, $0,6 < Pr < 2000$). See in particular the Attachment C. Source: "Process Heat Transfer"- Principles of Application" Eq. 2:38 [12].

In this case $T_{ls, \text{ein}}$ and $T_{ls, \text{aus}}$ are close to the solution saturation temperatures at the respective concentrations w_{ein} and w_{aus} . It is allowed, therefore, to use the solution saturation temperatures to calculate the logarithmic mean temperature difference $\delta_{T, Lm}$ of the absorber, instead of the solution inlet and outlet temperatures above mentioned.

This method is useful to consider how, in the absorber, the mass transfer affects the sensible heating [11].

The input data for the EES program are posted in the Attachment E and the results in the following paragraph.

As it can be seen in the Figure 7.5 present in the Attachment E, all the input parameters are measured by the sensors system, except the density values, which are obtained by experimental measurements.

In particular, the LabVIEW program records the value through the sensors each 20 seconds, because of that to carry out the calculations of the input data, the average values of the last 10 minutes before the measure are used.

The experimental procedure to obtain the density values is described in the next paragraph.

3.3.3.2 *Density measurements*

The measurement parameters are specified in the Table 3.3 and in the Table 3.6.

All these experiments are performed keeping the machine in steady state conditions, in the same way explained in the paragraph 3.3.1.

The density is measured from solution samples extracted directly from the facility, in particular from the pipe that goes from the absorber up to the generator (rich solution sample density) and from the pipe that goes from the generator to the absorber (poor solution sample density).

Both the rich and poor solution samples are taken from the initial part of solution path, just at the outlet of the two heat exchangers, respectively the absorber and the generator.

The measurements are carried out two times, with the second one 10 minutes after the first.

Unless some error happens, the second measurement values are used for the calculations, because, with 10 minutes more, the facility parameters can be considered more stable.

The driving force to carry out the sample extractions is the pressure difference between the inside and the machine outside. For this purpose a vacuum pump is used (Figure 3.13).

The pump is connected at the machine through rubber pipes and two apparatus for the solution samples storing (Figure 3.17). Between the machine and the pump is also put a liquid receiver inside a vessel containing liquid nitrogen, to prevent that some solution reach the pump.

These two apparatus are composed by a part fixed to the facility and a movable part, where the solution is stored. To prevent permanent corrosion problems, caused by the contact with the Lithium Bromide, both of them are made of inox steel⁴.

The extracting apparatus is furnished with 3 two – way valves for each branch (I, II, III), as it can be seen in the Figure 3.17.

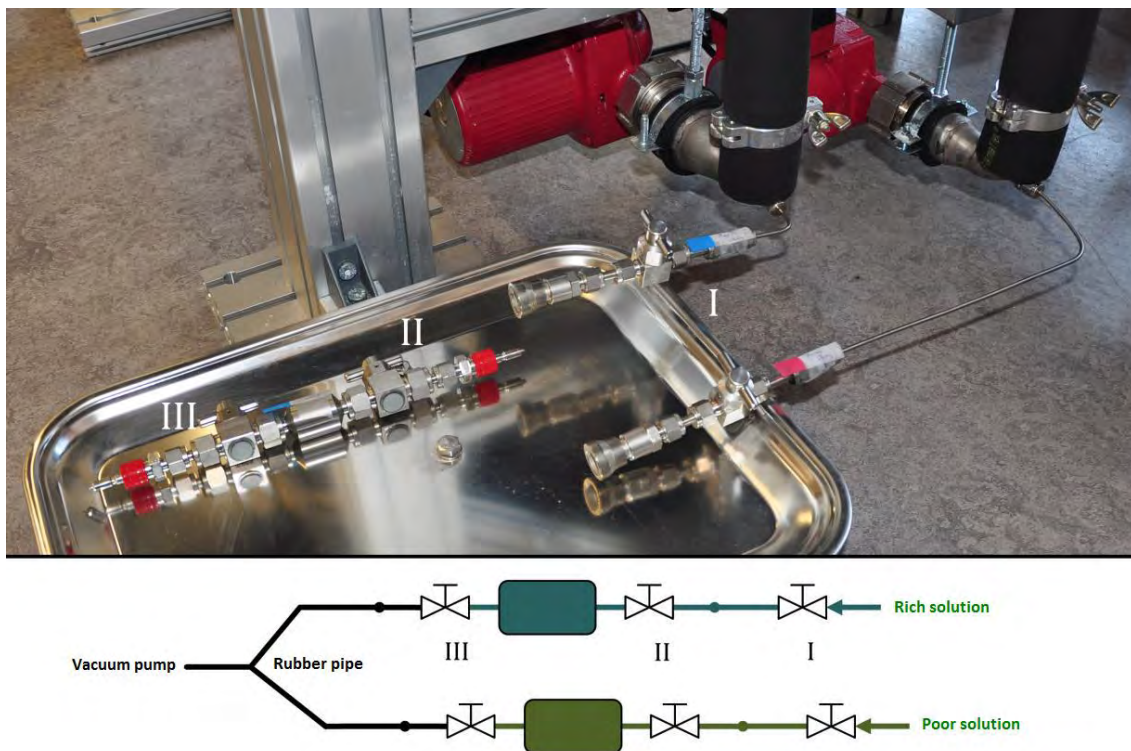


Figure 3.17. The two apparatus for the solution samples storing, one for the poor sample and the second for the rich one.

⁴The Lithium Bromide has corrosive properties, avoiding the contact between it and the skin or clothes is very important. Protective gloves and glasses are recommended to handle it, and the metals have to be immediately cleaned after the use [7].

When the facility reaches the suitable conditions to measure, the vacuum pump is switched on to decrease the pressure inside the pipes connected to the machine, especially inside the two apparatus to store the solution. This procedure takes around 5 minutes, time deduced from the experience, and the valves *I* are the only closed during this period, to avoid the flowing out of the solution.

Afterwards the valves *III* are closed, the pumps is switched off and the valves *I* are opened for about 5 minutes, to leave the solution flows inside the storage tools.

Later the valves *II* and *I* are closed and the solution samples are stored inside the two extracting apparatus.

At the end, the stored solutions are put inside two different test tubes (one for the rich solution and one for the poor solution) and the density measurements can be finally performed. The latest procedure is done by a dedicated machine, which is shown in the Figure 3.18.



Figure 3.18. Mettler TOLEDO DM40 density measurer. The machine gets in contact with the liquid solution through a spike, put directly inside the test tube.

The density measurer returns the solution density values at the temperature of 20 °C and the symbols used to represent them both in the program and in the above flow chart are:

- $\rho_{ls,ein,probe}$ [kg/m³]
- $\rho_{ls,aus,probe}$ [kg/m³]

The all density values measured, in every investigation vase, are shown in the Table 3.7 and they are sorted by the cooling water temperature at the inlet of the absorber $T_{ein,ab}$.



<i>Solution volume flow rate</i> <i>[m³/h]</i>	0,35	0,3	0,25	0,2	0,15	0,1
<i>$T_{ein,ab} = 27^{\circ}C$</i>						
Rich solution density [kg/m ³]	1683,9	1678,5	1680,3	1681,8	1675,5	1668,4
Poor solution density [kg/m ³]	1700,2	1697,3	1702,3	1712,9	1715,4	1721,5
<i>$T_{ein,ab} = 32^{\circ}C$</i>						
Rich solution density [kg/m ³]	1665,8	1670,3	1669,1	1676	1673,7	1660,8
Poor solution density [kg/m ³]	1677,3	1683,6	1684,3	1695	1701	1700,5
<i>$T_{ein,ab} = 37^{\circ}C$</i>						
Rich solution density [kg/m ³]	1657,1	1655,6	1657,1	1661,8	1671,8	1671
Poor solution density [kg/m ³]	1663,5	1663,8	1666,2	1673,1	1686,1	1691,5

Table 3.7. Density solution values, for different volume flow rate and cooling water temperature.

It can be seen that the solution density values generally decrease with the increasing of the cooling water temperature and poor solution ones are in each case superior than the rich ones, as it is expected.

3.3.3.3 Measurements and program results

The Attachment D shows the script of the EES program. The results are obtained through with the following steps:

- Checking the equations :  this function verifies that the numbers of equations and variables are the same, in order to solve the system.
- Solve the equations system  .

The results are shown in a dedicate window and an example of that is exhibited it the Figure 3.19. The interesting parameters returned by the program are highlighted in grey and they are:

- α_{film} : absorber film convective heat transfer coefficient;
- K : absorber overall heat transfer coefficient.

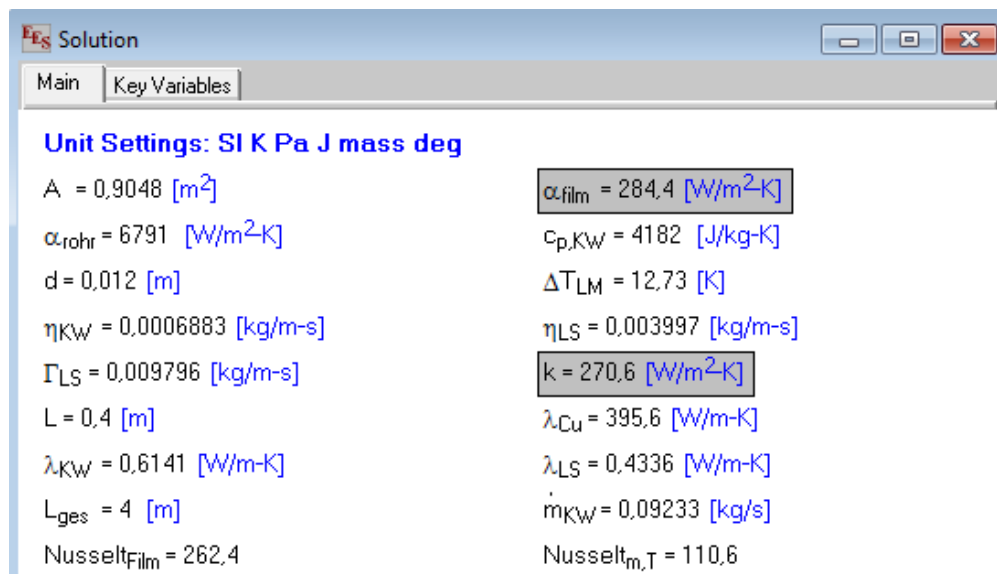


Figure 3.19. EES result window. The program calculates the solution mass flow rate for pipe length as well (Γ_{ls}). The coefficients are plotted in function of that parameter, which is proportional to the solution flow rate (chapter 5).

4. Mathematical model

4.1 Model introduction

The mathematical model of the facility is written through the software Engineering Equation Solver – EES and it describes all the thermodynamic characteristics of the absorber refrigerator by equations systems.

The entire system is composed by 167 equations, which involves the definitions of the fluid properties, the thermodynamics relations, the overall balances of the all heat exchangers, as well as the overall balance of the whole system. It is developed from a basic model realized by the Universität Kassel, Institut für Thermische Energietechnik [13].

The purpose of that model is the calculation of the absorber performance, especially focusing on the cooling capacity and the COP (Figure 4.1.).

The boundary conditions of the model are represented by the inlet temperatures and volume flow rates of the secondary loops, as well as the overall exchange coefficients and the exchange areas of the heat exchangers. All the input data are described in the paragraph 4.2.

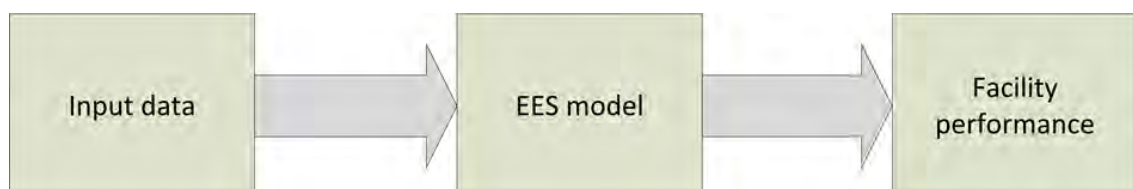


Figure 4.1. The mathematical model aim is to find the facility performance, especially the COP and cooling capacity. The input data are described in the paragraph 4.2.

In addition to the basic heat exchangers, in the model the solution heat exchanger is introduced as well. It is present in the program with fixed area and overall exchange coefficient too. Moreover, in this section, the solution heat exchanger efficiency and the solution concentration calculations are carried out.

An important aspect to underline is that the small temperature differences at each heat exchanger (δ_v , δ_k , δ_{ab} and δ_g) are output data calculated by the program and not fixed boundary conditions.

These parameters represent the small temperature differences respectively at the evaporator, condenser, absorber and generator, as specified in the Figure 4.2.

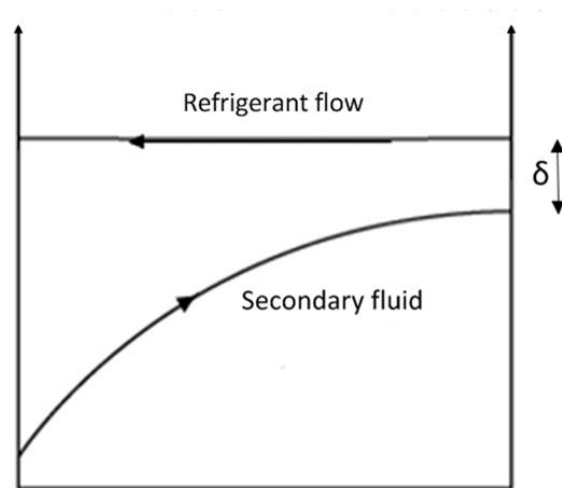


Figure 4.2. In the mathematical model the small temperature differences δ are calculated as output. The figure represent the case of the condenser.

It is interesting to highlight that the solution concentrations do not represent the saturation ones, as in the ideal case (Figure 2.3), but they are calculated trying to consider the real performance of the heat exchangers. Precisely, the concentrations of the rich and poor solution are weighted on the ($K \cdot A$) products of both the absorber and generator. The relative procedure and formulas are described in the paragraph 4.3.

At the end, the model results are compared with the values of the real measurements (Attachment C), especially focusing on the cooling capacity and COP. The output are plotted as function of the inlet hot water temperature at the generator and for different inlet cold water temperature at the evaporator.

4.2 Input data

The program input data are the following and they are the same adopted during the measurements with the real facility, in order to compare the results.

All the volume flow rates of the secondary fluids are kept constant and the (poor) solution volume flow rate as well. Their values are shown in Table 4.1.

Volumetric flow rate		
Symbol	Value	Unit of measurement
\dot{V}_g	1,5	m ³ /h
\dot{V}_k	2	m ³ /h
\dot{V}_v	1	m ³ /h
\dot{V}_{al}	0,15	m ³ /h

Table 4.1. The volume flow rates of the secondary fluids are fixed input data (regulated by the computer) and the solution volume flow rate too (regulated manually by the V2 valve).

Legend:

- \dot{V}_g = Hot water volume flow rate;
- \dot{V}_k = Cooling water volume flow rate;
- \dot{V}_v = Cold water volume flow rate;
- \dot{V}_{al} = Poor solution volume flow rate.

The heat exchanger areas are input data too, as it is mentioned in the previous paragraph.

The geometries of the condenser, evaporator, generator and absorber are described in the Attachment B. The values are related to the heat exchanger external areas.

Heat exchanger area		
Symbol	Value	Unit of measurement
A_g	1,215	m ²
A_k	0,729	m ²
A_{ab}	0,912	m ²
A_v	0,729	m ²
A_{shx}	0,272	m ²

Table 4.2. The areas of all the facility heat exchangers are input data for the model.

Legend:

- A_g = Generator exchange area;
- A_k = Condenser exchange area;
- A_{ab} = Absorber exchange area;
- A_v = Evaporator exchange area;
- A_{shx} = Solution heat exchanger exchange area.

The overall heat transfer coefficients of the condenser, evaporator and solution heat exchanger are evaluated through empirical correlations owned by [13], whereas those of generator and absorber are evaluated from experimental data.

The absorber coefficient is evaluated through the procedure described in the paragraph 3.3.2., for different solution volume flow rates and cooling water temperatures at the inlet of it. The other measured coefficients were already evaluated and are given from the Universität Kassel Institut für Thermische Energietechnik database [13].

Because of the expected differences between the reality and a mathematical model results (see the paragraph 4.3), it is not considered significance to change the absorber heat transfer coefficient value when the cooling water temperature is

shifted; for this reason, for the simulation, the average value of the experimental coefficients is taken ($\dot{V}_{al} = 0,15 \text{ m}^3/\text{h}$).

Overall heat transfer coefficient		
Symbol	Value	Unit of measurement
K_g	1000	$\frac{\text{W}}{\text{m}^2\text{K}}$
K_k	2000	$\frac{\text{W}}{\text{m}^2\text{K}}$
K_{ab}	415	$\frac{\text{W}}{\text{m}^2\text{K}}$
K_v	2000	$\frac{\text{W}}{\text{m}^2\text{K}}$
K_{shx}	2000	$\frac{\text{W}}{\text{m}^2\text{K}}$

Table 4.3. The overall heat transfer coefficients of all the facility heat exchanger are fixed input data.

Legend:

- K_g = Generator overall heat transfer coefficient;
- K_k = Condenser overall heat transfer coefficient;
- K_{ab} = Absorber overall heat transfer coefficient;
- K_v = Evaporator overall heat transfer coefficient;
- K_{shx} = Solution heat exchanger overall heat transfer coefficient.

The temperatures of the secondary loop water, at the inlet of the facility, represent fixed boundary conditions.

As it is shown in the Table 4.4, the simulations are performed for different hot water and cold water temperatures, but keeping the cooling water temperature constant equal to 27 °C.

Secondary loop inlet temperatures		
<i>Symbol</i>	<i>Value</i>	<i>Unit of measurement</i>
T_g	65; 75; 70; 75; 80; 85	°C
T_k	27	°C
T_v	10; 15; 20; 25	°C

Table 4.4. The simulations through the program are carried out changing just the hot and cold water temperatures.

The pressure P_u inside the hot, cooling and cold water pipes is assumed at the same value:

$$P_u = 3 \text{ bar} \quad 4.1$$

4.3 Model description

The mathematical model script, written by EES – Engineering Equation Solver, is posted in the Attachment F.

As it is mentioned in the paragraph 3.1.1, all the apparatus considered in the model are of counter flow type.

The main assumptions considered in the model construction are the following [14], [15]:

1. The simulations performed considering the system under steady state conditions, as in the real measurements (see the chapter 3.3). It means that the refrigerant mass flow rate produced in the generator is equal to the one absorbed one in the absorber.
2. The heat losses between the facility and the surroundings are negligible.
3. The pressure drops in the pipes and in the vessels are negligible.

4. Water as pure refrigerant.

The simulations are carried out fixing the boundary conditions shown in the previous paragraph, varying just the temperature of the heat source, represented by the hot water at the generator inlet, and the temperature of the cold water (evaporator inlet).

The mathematical model is represented by a linear system composed by 167 equations, which are subdivided in 18 independent blocks.

In particular, the program is structured in more sections, which are different because they represent different components of the absorption cycle.

These parts are the following:

- Evaporator;
- Condenser;
- Expansion valve;
- Absorber;
- Generator;
- Solution heat exchanger,
- Poor and rich solution.

Each of them is not independent, but to find the results they have to be linked together in the same script.

The parameters present in the program script are 167 and they included both the fixed variables (input data) and the unknown ones (results).

Each of them represent a specific thermodynamic characteristic of the relative working point or component: in the Figure 4.3 the main symbols are indicated.

In that framework the working points, placed during the refrigerant and solution paths, are specified with the enthalpy symbols, whereas the ones of the secondary loops with the temperatures. In the picture the mass flow rate symbols used in the program are specified as well.

The mass flow rates typed in the program are:

<i>Symbol</i>	<i>Type</i>
\dot{M}_{ref}	<i>Refrigerant mass flow rate</i>
\dot{M}_v	<i>Cold water mass flow rate</i>
\dot{M}_k	<i>Cooling water mass flow rate</i>
\dot{M}_g	<i>Hot water mass flow rate</i>

\dot{M}_{rl}	Rich solution mass flow rate
\dot{M}_{al}	Poor solution mass flow rate
\dot{M}_{av}	Average solution mass flow rate

Table 4.5. Mass flow rate symbols present in the mathematical model.

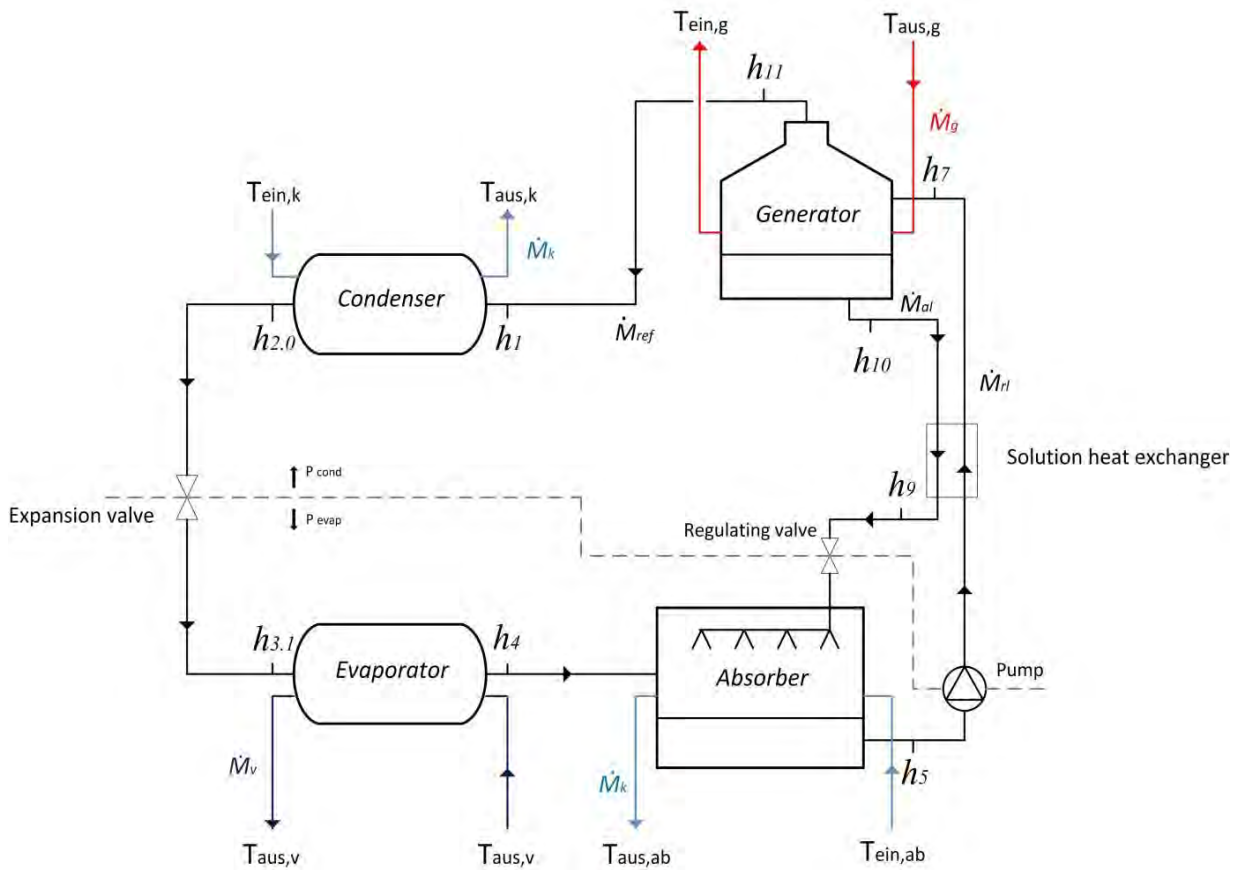


Figure 4.3. The model working points are shown in the picture.

The positions of every other parameters in the program, is fixed by the subscripts exhibited in the Figure 4.3.

After the compilation of the equations, the program is made running (the procedure steps are described in the paragraph 3.3.3.3) and therefore it tries to solve the equations system using the Newton – Raphson iterative method.

The 250 iterations ordered to the software are considered sufficient to understand if the solutions can be found or not and so if the system guess values have to be defined with more accuracy or not (see the paragraph 4.3.1).

The equations of each section are written two times, because the program carried out 2 iterations. The first to find a first value of the refrigerant mass flow rate from the vaporization latent heat and the second one to correct it with the introduction of the quality at the evaporator inlet.

It means that all the parameters are calculated two times: those with the subscript 1 belong to the first iteration and those without subscript at the second one.

The second value of the refrigerant mass flow rate is used to find all the heat amounts exchanged by the various apparatus, especially the cooling capacity at the evaporator.

The descriptions of the program sections are presented below.

They show the main characteristics of the various parts, focusing on the functions which each section has.

More details can be found in the Attachment F, where all the command lines are described.

Evaporator

In this section are written the equations connected both to the evaporator and the cold water line.

First of all, the definitions of the input data are posted (see the paragraph 4.2), attended by the fluid properties calculations.

After that, the heat transfer equations are written:

Heat transfer equation:

$$\dot{Q}_v = K_v \cdot A_v \cdot \delta_{T,v,Lm} \quad 4.2$$

First thermodynamics law, cold water side:

$$\dot{Q}_v = \dot{M}_v \cdot c_{p,v} \cdot (T_{ein,v} - T_{aus,v}) \quad 4.3$$

First thermodynamics law, refrigerant side:

$$\dot{Q}_{v,1} = \dot{M}_{ref,1} \cdot \Delta h_{vap,1} \quad 4.4$$

The subscript 1 means that the equation 4.4 is present just in the first iteration, where the refrigerant mass flow rate is still an unknown parameter. At the beginning of the second iteration, it is possible to carry out the quality calculation from the first iteration result, with which the final refrigerant mass flow rate value can be found:

$$\dot{M}_{ref} = (1 + x_{ein,v}) \cdot \dot{M}_{ref,1} \quad 4.5$$

The mass of refrigerant is corrected through the quality value to consider the steam generated through the expansion valve. The introduction of a known parameter more makes the equation 4.4 not necessary anymore during the second iteration. The cooling capacity is inserted in the heat transfer equations of this part, but it does not represent an output data of the own section. It will be found from the system overall balance. On the contrary, the evaporation pressure can be calculated from just this block of equations.

Condenser

This section presents the equations related both to the condenser and the cooling pipeline. It has a similar structure to the evaporator one.

The following are the heat transfer equations:

Heat transfer equation:

$$\dot{Q}_k = K_k \cdot A_k \cdot \delta_{T,k,Lm} \quad 4.6$$

First thermodynamics law, cooling water side:

$$\dot{Q}_k = \dot{M}_k \cdot c_{p,k} \cdot (T_{aus,k} - T_{ein,k}) \quad 4.7$$

The cooling pipeline crosses first the absorber and after the condenser:

$$T_{aus,ab} = T_{ein,k} \quad 4.8$$

First thermodynamics law, refrigerant side:

$$\dot{Q}_k = \dot{M}_{ref} \cdot \Delta h_{kond} \quad 4.9$$

During just the first iteration, both the sub cooling and superheating are counted and they are multiplied by a reduction factors. These multipliers are introduced to find the solutions in a proper range of expected values (close to the experimental data), when the model is using the first attempt of refrigerant mass flow rate value. Because of that, in the second iteration the sub cooling is not considered anymore and just the superheating is introduced in the calculations:

Superheating calculation:

$$Sh_k = \dot{M}_{ref} \cdot (h_{11} - h_1) \quad 4.10$$

To simplify the model, the superheating is not counted in the first thermodynamics law applied to the cooling water at the condenser. It is a negligible amount in respect to the latent condensation heat, therefore this assumption does not weight on the results.

Expansion valve

The expansion valve section ensures the isenthalpic process:

$$h_{3.1} = h_{2.0} \quad 4.11$$

Absorber

In this subdivision, after the writing of the input data related to the cooling pipeline and the absorber, the heat transfer equations are applied, similarly to the evaporator and condenser sections:

Heat transfer equation:

$$\dot{Q}_{ab} = K_{ab} \cdot A_{ab} \cdot \delta_{T,ab,Lm} \quad 4.12$$

First thermodynamics law, cooling water side:

$$\dot{Q}_{ab} = \dot{M}_k \cdot c_{p,k} \cdot (T_{aus,ab} - T_{ein,ab}) \quad 4.13$$

Energy balance, absorber:

$$\dot{M}_{rl} \cdot h_5 - \dot{M}_{al} \cdot h_9 - \dot{M}_{ref} \cdot h_4 + \dot{Q}_{ab} = 0 \quad 4.14$$

Generator

The section includes the input data of both generator and hot water line. The structure is completely identical to the absorber one.

The following are the heat transfer equations used:

Heat transfer equation:

$$\dot{Q}_g = K_g \cdot A_g \cdot \delta_{T,g,Lm} \quad 4.15$$

First thermodynamics law, hot water side:

$$\dot{Q}_g = \dot{M}_g \cdot c_{p,g} \cdot (T_{ein,g} - T_{aus,g}) \quad 4.16$$

Energy balance, generator:

$$\dot{M}_{ref} \cdot h_{11} + \dot{M}_{al} \cdot h_{10} - \dot{M}_{rl} \cdot h_7 - \dot{Q}_g = 0 \quad 4.17$$

Solution heat exchanger

In this part both the area and the overall heat transfer coefficient of the heat exchanger are specified as input data, as for all the others heat exchanger sections.

The heat transfer equations are the following:

First thermodynamics law, rich solution side:

$$\dot{Q}_{rl} = \dot{M}_{rl} \cdot c_{p,rl} \cdot (T_7 - T_5) \quad 4.18$$

First thermodynamics law, poor solution side:

$$\dot{Q}_{al} = \dot{M}_{al} \cdot c_{p,al} \cdot (T_9 - T_{10}) \quad 4.19$$

Energy balance equivalence:

$$\dot{Q}_{rl} = -\dot{Q}_{al} \quad 4.20$$

Heat transfer equation:

$$\dot{Q}_{rl} = K_{shx} \cdot A_{shx} \cdot \delta_{T,shx,Lm} \quad 4.21$$

It is possible to calculate the solution heat exchanger efficiency as well:

$$\varepsilon = \frac{\dot{Q}_{rl}}{\dot{Q}_{max}} \quad 4.22$$

where \dot{Q}_{max} which represents the maximum heat transferable through the heat exchanger.

Poor and rich solution

This is the sub section dedicated to the rich and poor solution properties calculations. First of all the software calculates the solution ideal concentrations, through its internal library functions. The density calculations are performed through the internal library functions too.

Rich solution saturation concentration:

$$x_{rl,id} = f(T_5, P_{v,sat}) \quad 4.23$$

Poor solution saturation concentration:

$$x_{al,id} = f(T_{10}, P_{k,sat}) \quad 4.24$$

Afterwards, an average value of the concentrations is found. It is weighted on the product $(K \cdot A)$ of both the absorber and generator. This solution is found in agreement with the supervisor Michael Olbricht.

Average weighted value of the solution concentrations:

$$x_{av} = \frac{(K \cdot A)_{ab}}{(K \cdot A)_{ab} + (K \cdot A)_g} \cdot x_{rl,sat} + \frac{(K \cdot A)_g}{(K \cdot A)_{ab} + (K \cdot A)_g} \cdot x_{al,sat} \quad 4.25$$

The average concentration is related to an average mass flow rate, between the rich solution one and the poor solution one. The equations 4.26 fixed the mass balances in the absorber and generator.

Absorber and generator mass balances:

$$\dot{M}_{rl} = \dot{M}_{av} + 0,5 \cdot \dot{M}_{ref} \quad 4.26$$

$$\dot{M}_{al} = \dot{M}_{av} - 0,5 \cdot \dot{M}_{ref} \quad 4.27$$

The refrigerant mass balance allows the calculations of new values of the poor and rich solution concentrations:

Absorber and generator refrigerant mass balances:

$$\dot{M}_{rl} \cdot x_{rl,real} = \dot{M}_{av} \cdot x_{av} + 0,5 \cdot \dot{M}_{ref} \quad 4.28$$

$$\dot{M}_{al} \cdot x_{al,real} = \dot{M}_{av} \cdot x_{av} - 0,5 \cdot \dot{M}_{ref} \quad 4.29$$

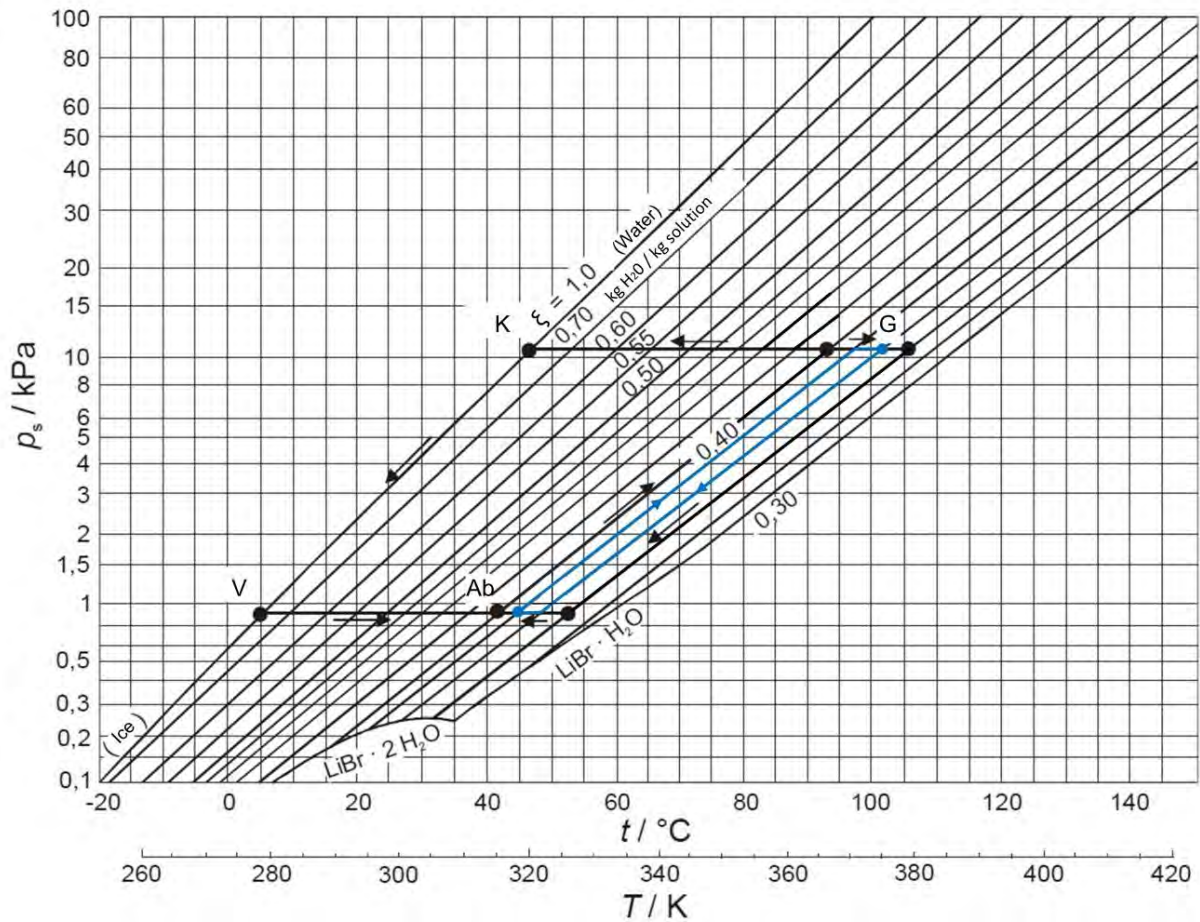


Figure 4.4. The difference of the real concentrations (blue) is smaller than the ideal one (black). Legend: G – Generator; K – Condenser; V – Evaporator; Ab – Absorber.

Their calculations represent significant attempts to represent the reality, where both in the generator and in the absorber the saturation conditions are not reached.

The new values of the poor and rich solution concentrations are closer to each other than the ideal ones, as it can be seen in Figure 4.4 (blue line). It is important to specify that the scale exhibited in the axis is not valid for the two blue curves, because they do not represent saturation condition. The picture is just a representation to show how the concentrations could change from the ideal to the real case. In every case, the difference between the two concentration (rich and poor) decreases when the solution flow rate increase.

COP and cooling capacity

The last sub division of the program includes the COP and overall energy balance equations. The second one allows finding the final value of the cooling capacity.

Coefficient of performance:

$$COP = \frac{\dot{Q}_v}{\dot{Q}_g} \quad 4.30$$

Energy balance of the whole system:

$$\dot{Q}_v + \dot{Q}_g - \dot{Q}_{ab} - \dot{Q}_k - Sh_k = 0 \quad 4.31$$

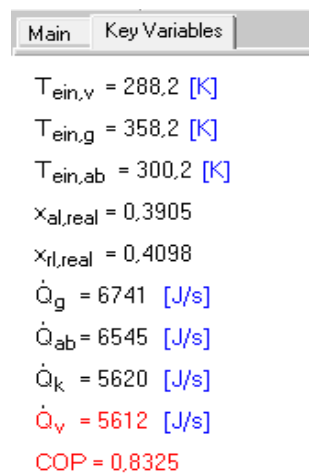
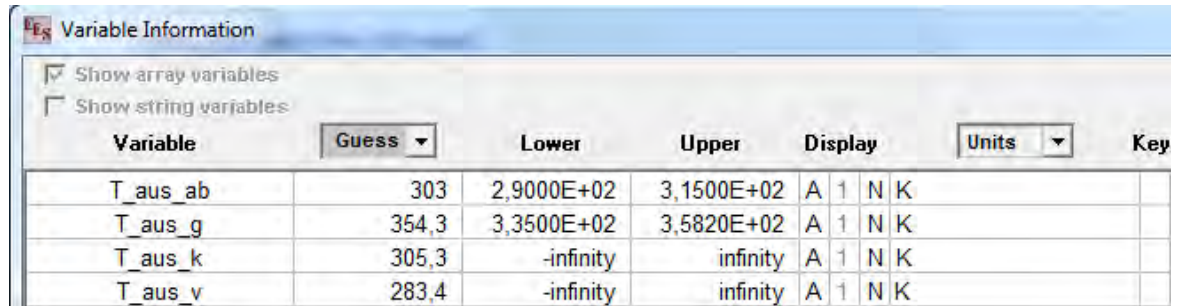


Figure 4.5. The main outcomes highlighted in the result window.

4.3.1 Guess values

In order to allow the program to find the results, the working ranges of all the parameters have to be defined, as it is shown in the Figure 4.6. Because of that, a rough calculation of the absorption cycle variables has to be carried out preliminarily.



Variable	Guess	Lower	Upper	Display	Units	Key
T_aus_ab	303	2,9000E+02	3,1500E+02	A 1 N K		
T_aus_g	354,3	3,3500E+02	3,5820E+02	A 1 N K		
T_aus_k	305,3	-infinity	infinity	A 1 N K		
T_aus_v	283,4	-infinity	infinity	A 1 N K		

Figure 4.6. The working ranges and the guess values of the program parameters can be defined preliminarily. The more the defined parameter ranges are, the better it is, to allow the program to find a solution quickly.

To simplify the calculation, each heat exchanger has been treated alone in a smaller program apart, which will be connected with the others in a successive step.

All the data which the subprogram needs from the others have to be supposed preliminarily, in order to keep the number of equations always equal to the parameter one and to so solve the system. In this way those supposed data become input, which will be taken out after the union with the other subprograms. The experimental results are useful to suppose these temporary input data. For example the cooling capacity is one of those, which in the program can be calculated just when the all heat exchanger subroutines are together.

When all the subprograms are able to operate alone, they can be connected together in a combined program and all the results of the smaller ones, become guess values for the combined ones.

In the Figure 4.7 the steps which have been performed to build the entire model are shown.

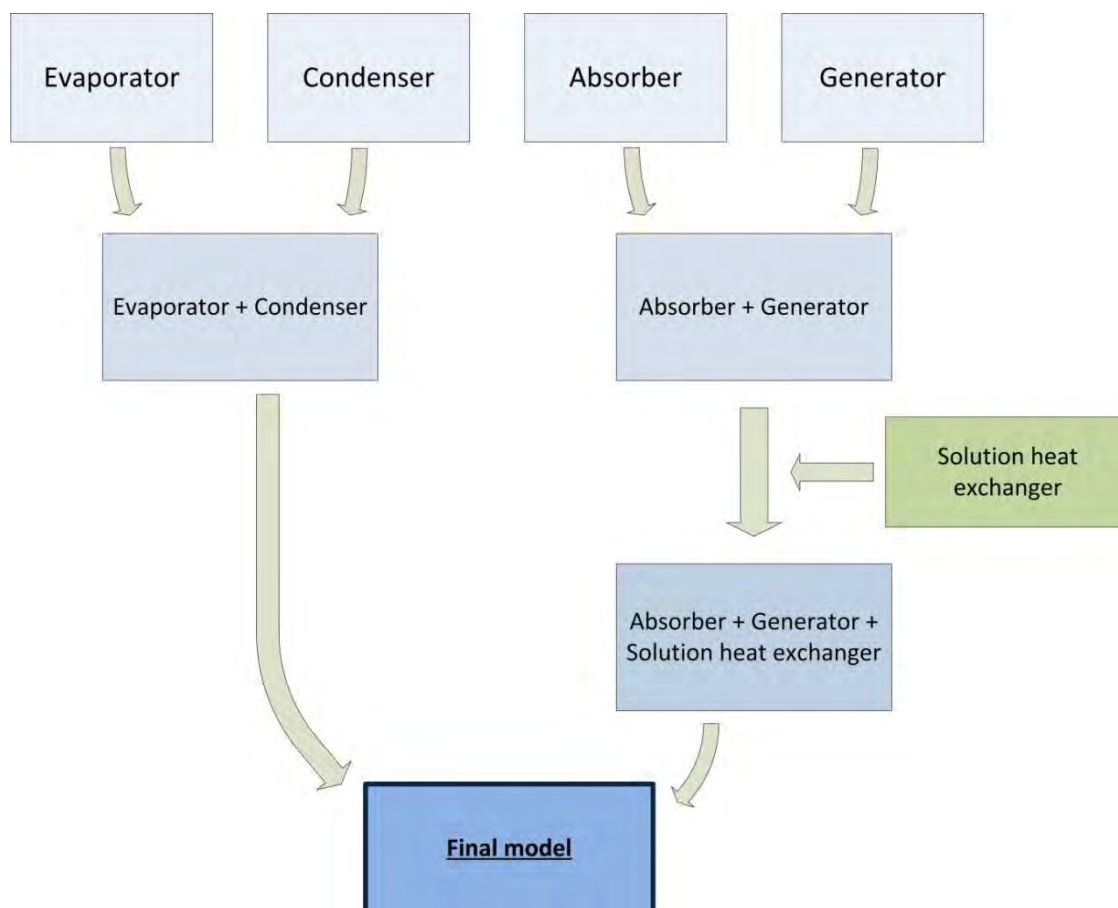


Figure 4.7. The steps to assemble the final program with proper guess values.

5. Results

5.1 Experimental investigation

5.1.1 Dynamic behavior

- $75\text{ }^{\circ}\text{C} \longrightarrow 70\text{ }^{\circ}\text{C}$
 $75\text{ }^{\circ}\text{C} \longleftarrow 70\text{ }^{\circ}\text{C}$

The first investigation has been performed changing the hot water temperature from $75\text{ }^{\circ}\text{C}$ to $70\text{ }^{\circ}\text{C}$ and vice versa, from $70\text{ }^{\circ}\text{C}$ to $75\text{ }^{\circ}\text{C}$.

The other boundary conditions are kept constant and their values are shown in the Table 3.3 (paragraph 3.3).

The cooling capacity and the temperatures analyzed, during the step responses, show the trends exhibited in the graphics below.

The first two graphics are related to the first step ($75\text{ }^{\circ}\text{C} \longrightarrow 70\text{ }^{\circ}\text{C}$), whereas the following two are related to the opposite one ($70\text{ }^{\circ}\text{C} \longrightarrow 75\text{ }^{\circ}\text{C}$).

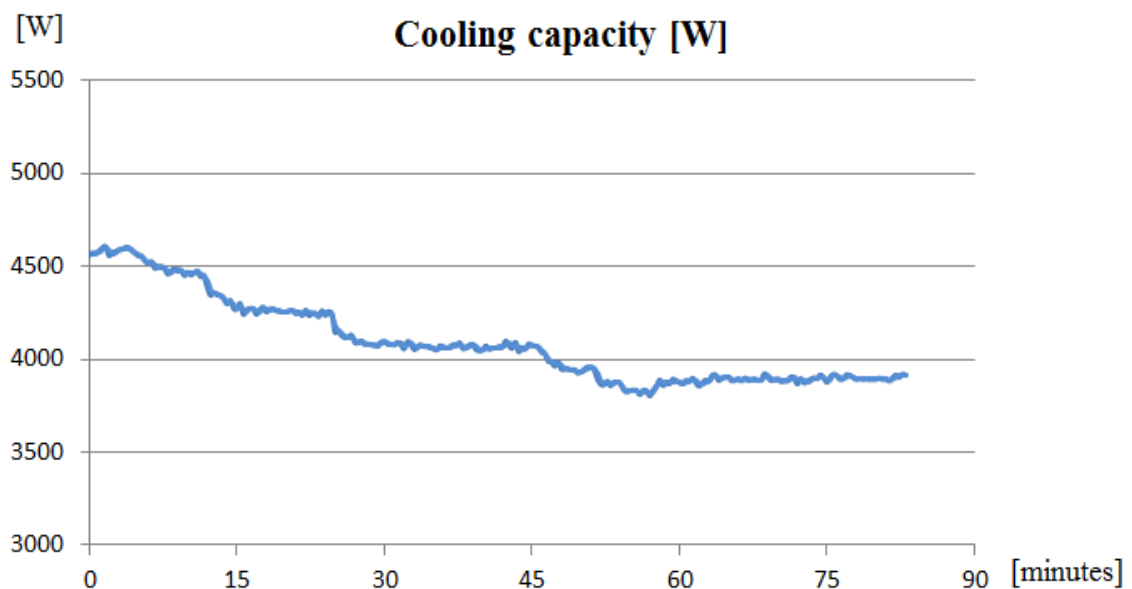


Figure 5.1. Cooling capacity trend after the changing of the hot water inlet temperature (from $75\text{ }^{\circ}\text{C}$ to $70\text{ }^{\circ}\text{C}$).

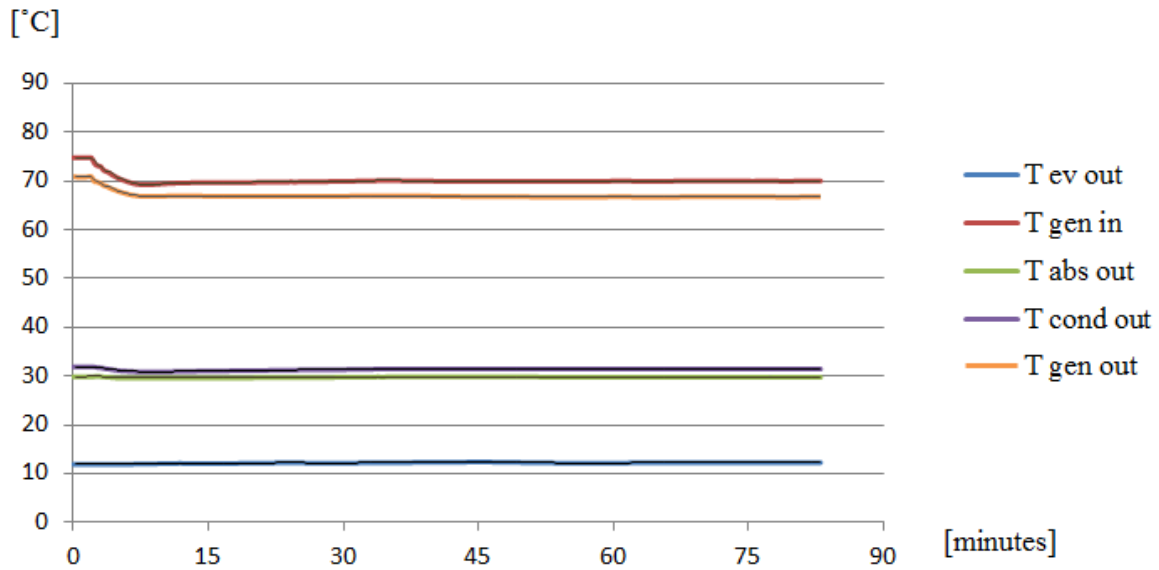


Figure 5.2. Temperature trends after the changing of the hot water inlet temperature (from 75 °C to 70 °C). Legend: $T_{ev\ out}$ = cold water temperature at the evaporator outlet; $T_{gen\ in}$ = hot water temperature at the generator inlet; $T_{abs\ out}$ = cooling water temperature at the absorber outlet; $T_{cond\ out}$ = cooling water temperature at the condenser outlet; $T_{gen\ out}$ = hot water temperature at the generator inlet.

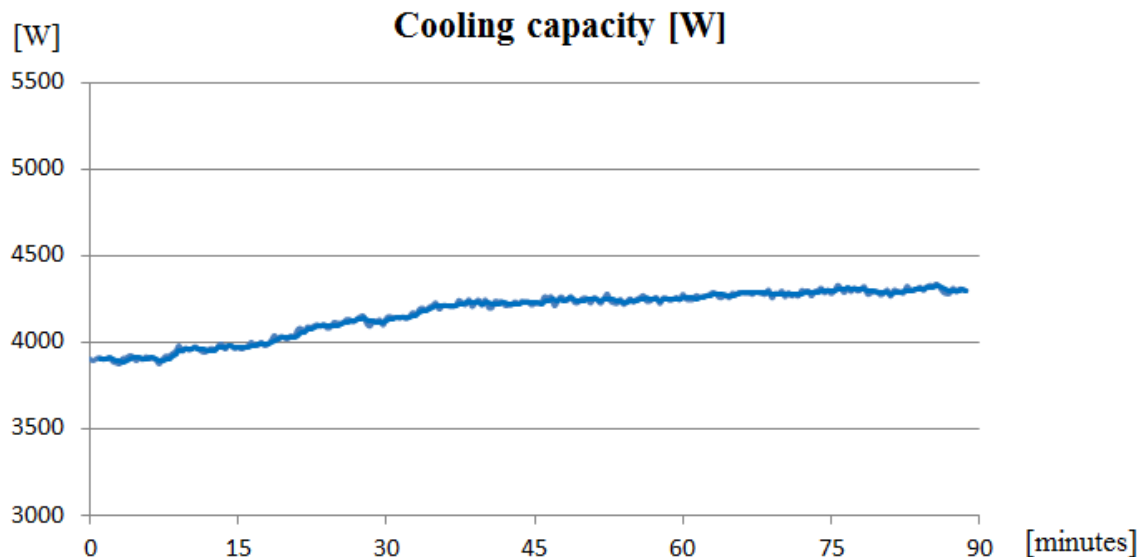


Figure 5.3. Cooling capacity trend after the changing of the hot water inlet temperature (from 70 °C to 75 °C).

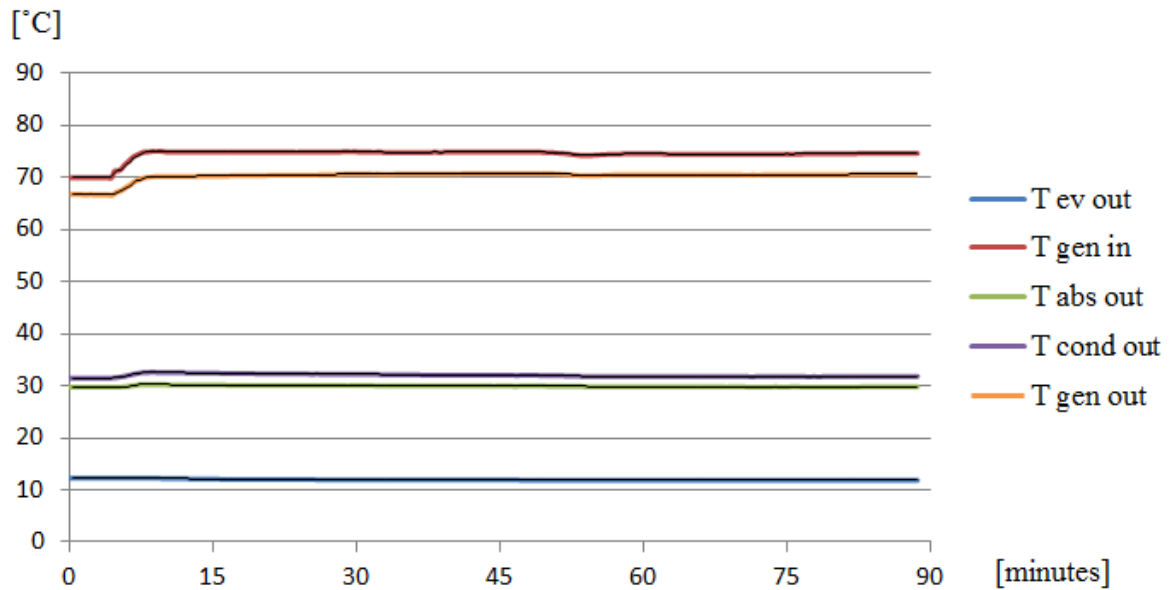


Figure 5.4. Temperature trends after the changing of the hot water inlet temperature (from 70 °C to 75 °C). Legend: $T_{ev\ out}$ = cold water temperature at the evaporator outlet; $T_{gen\ in}$ = hot water temperature at the generator inlet; $T_{abs\ out}$ = cooling water temperature at the absorber outlet; $T_{cond\ out}$ = cooling water temperature at the condenser outlet; $T_{gen\ out}$ = hot water temperature at the generator inlet.

In both the steps the variation of the cooling capacity is about 500 W and it takes around one hour to get a new constant value. The last 30 minutes of measurements, indicated in the graphics, represent the waiting time which ensures that the facility has reached a new steady state condition.

The temperatures at the generator change after few minutes because of the mixing valve. Their influence on the cooling water temperatures (absorber and condenser outlets) is immediate. The cooling water temperatures change just in the first minutes of the step response and after they keep a constant trend.

The evaporator outlet temperature, even if its variation is small, presents a constant trend after about one hour, just when the cooling capacity is becoming stable. It means that the most influencing parameter on the cooling capacity, among the temperatures shown in the graphic, is the evaporator outlet temperature.

- **75 °C \longrightarrow 65 °C**
75 °C \longleftarrow 65 °C

The second investigation has been carried out changing the hot water temperature from 75 °C to 65 °C and vice versa, from 65 °C to 75 °C.

The other boundary conditions are kept constant and their values are shown in the Table 3.3.

The next graphics show the cooling capacity and the temperatures trends during the step response, respectively for the step 75 °C \longrightarrow 70 °C (first two graphics) and for the step 70 °C \longrightarrow 75 °C (following two ones).

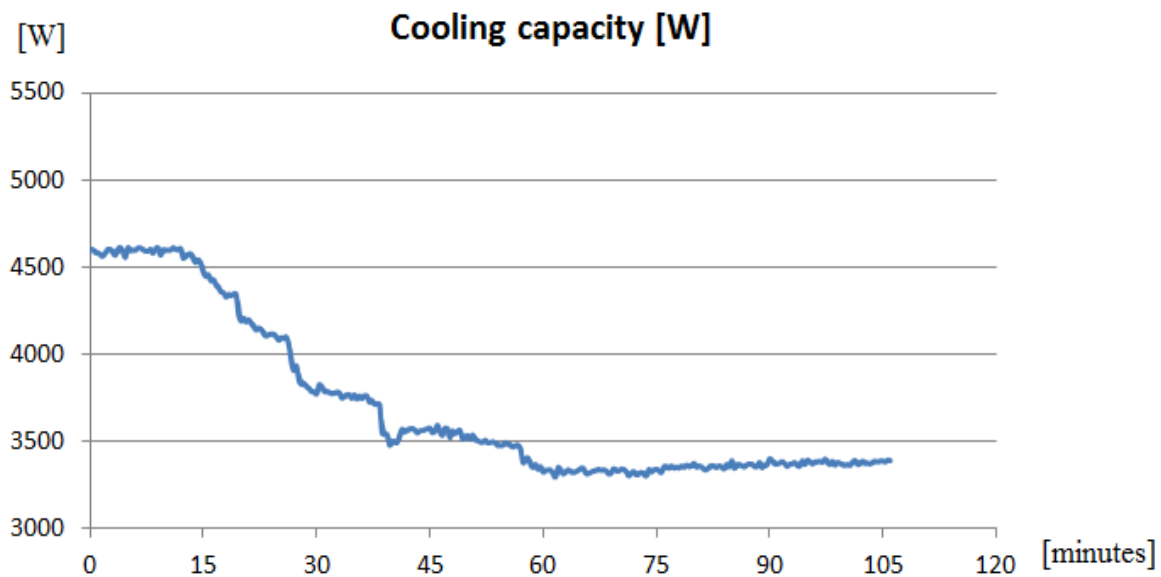


Figure 5.5. Cooling capacity trend after the changing of the hot water inlet temperature (from 75 °C to 65 °C).

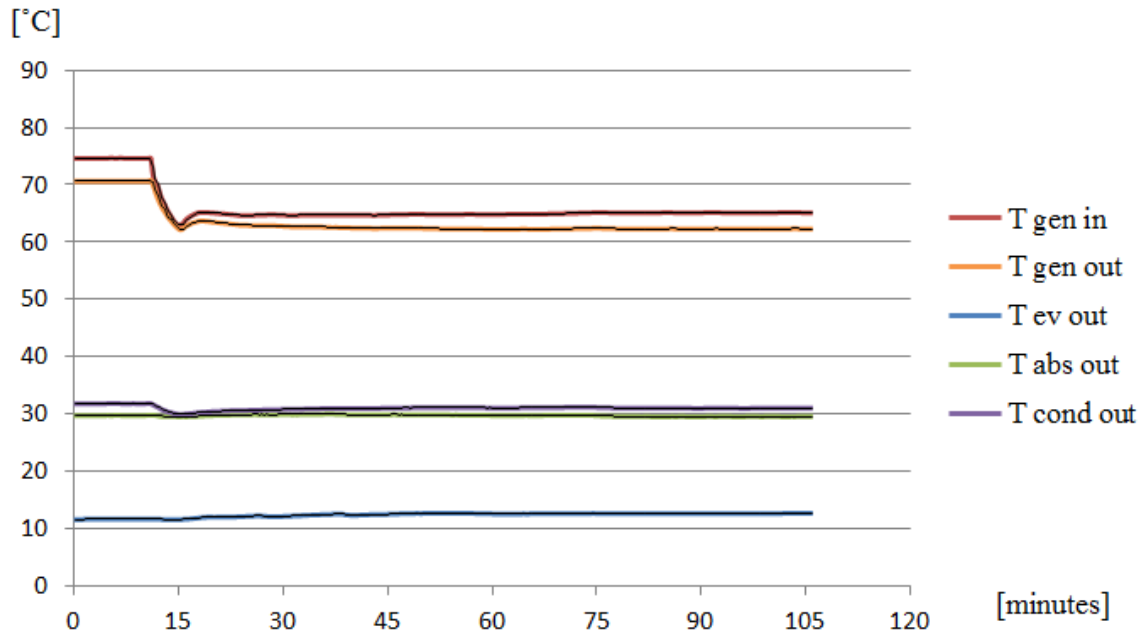


Figure 5.6. Temperature trends after the changing of the hot water inlet temperature (from 75 °C to 65 °C). Legend: $T_{ev\ out}$ = cold water temperature at the evaporator outlet; $T_{gen\ in}$ = hot water temperature at the generator inlet; $T_{abs\ out}$ = cooling water temperature at the absorber outlet; $T_{cond\ out}$ = cooling water temperature at the condenser outlet; $T_{gen\ out}$ = hot water temperature at the generator inlet

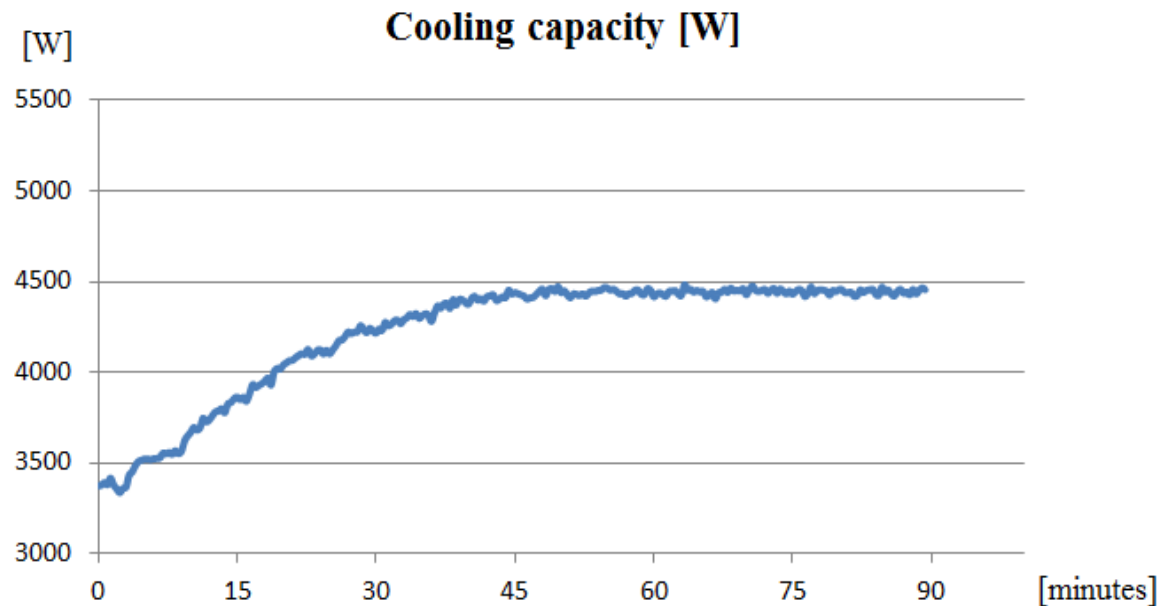


Figure 5.7. Cooling capacity trend after the changing of the hot water inlet temperature (from 65 °C to 75 °C).

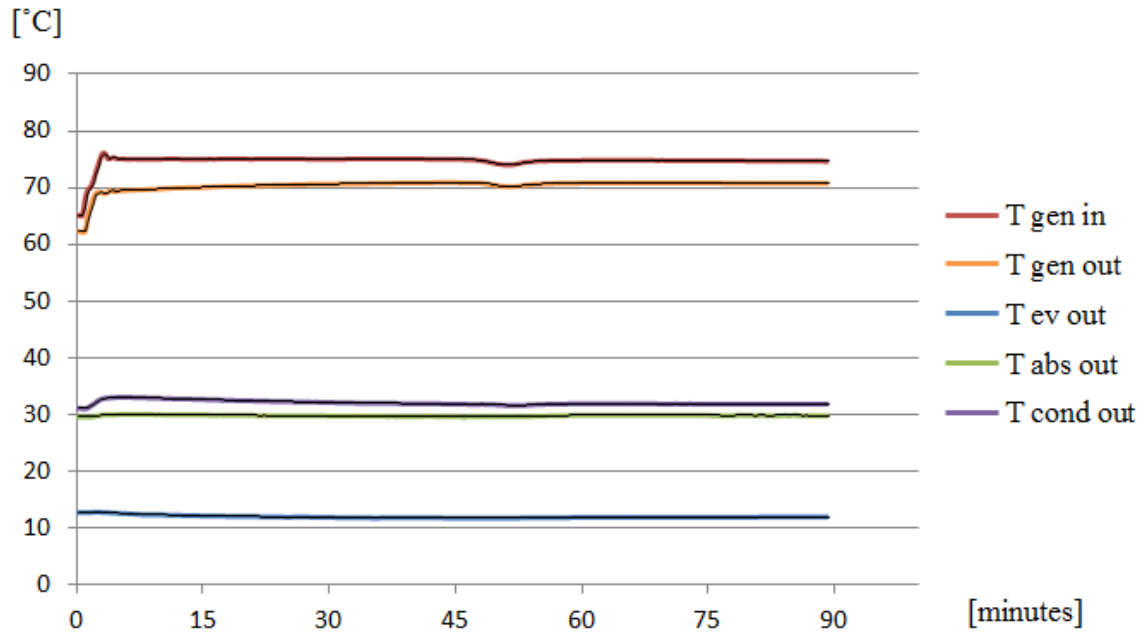


Figure 5.8. Temperature trends after the changing of the hot water inlet temperature (from 65 °C to 75 °C). Legend: $T_{ev\ out}$ = cold water temperature at the evaporator outlet; $T_{gen\ in}$ = hot water temperature at the generator inlet; $T_{abs\ out}$ = cooling water temperature at the absorber outlet; $T_{cond\ out}$ = cooling water temperature at the condenser outlet; $T_{gen\ out}$ = hot water temperature at the generator inlet.

The temperatures and cooling capacity behaviors are the same of which analyzed during the previous step response, but in this case they show more evident changes.

In both the steps the variation of the cooling capacity is about 1000 W and it takes around one hour to get a new constant value, as in the previous investigation.

The temperatures at the generator change after few minutes because of the mixing valve. The cooling water temperature changing happens in the same time, just in the first minutes of the step response.

The evaporator outlet temperature changes just a little, but in a more evident way than for the step 75 °C \longrightarrow 70 °C and vice versa.

It can be seen that the cooling capacity is varying as long as the evaporator outlet temperature is changing. Also in this case the most influence parameter on the cooling capacity, among the temperatures shown in the graphic, is the evaporator outlet temperature

- **75 °C \longrightarrow 80 °C**
75 °C \longleftarrow 80 °C

The third investigation has been performed changing the hot water temperature from 75 °C to 80 °C and vice versa from 80 °C to 75 °C.

The other boundary conditions are kept constant and their values are shown in the Table 3.3.

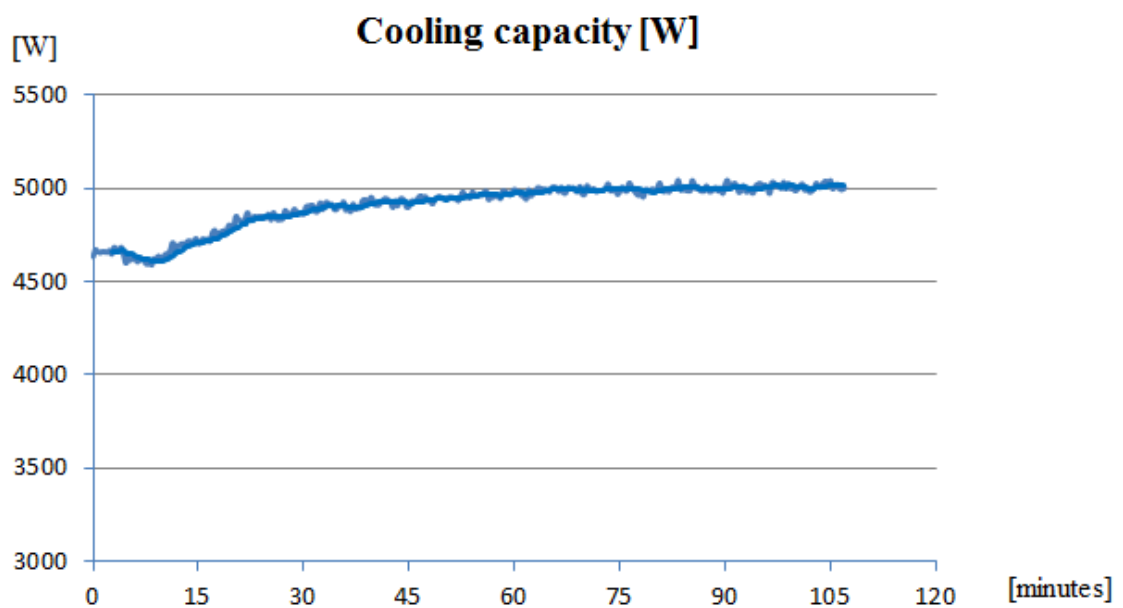


Figure 5.9. Cooling capacity trend after the changing of the hot water inlet temperature (from 75 °C to 80 °C).

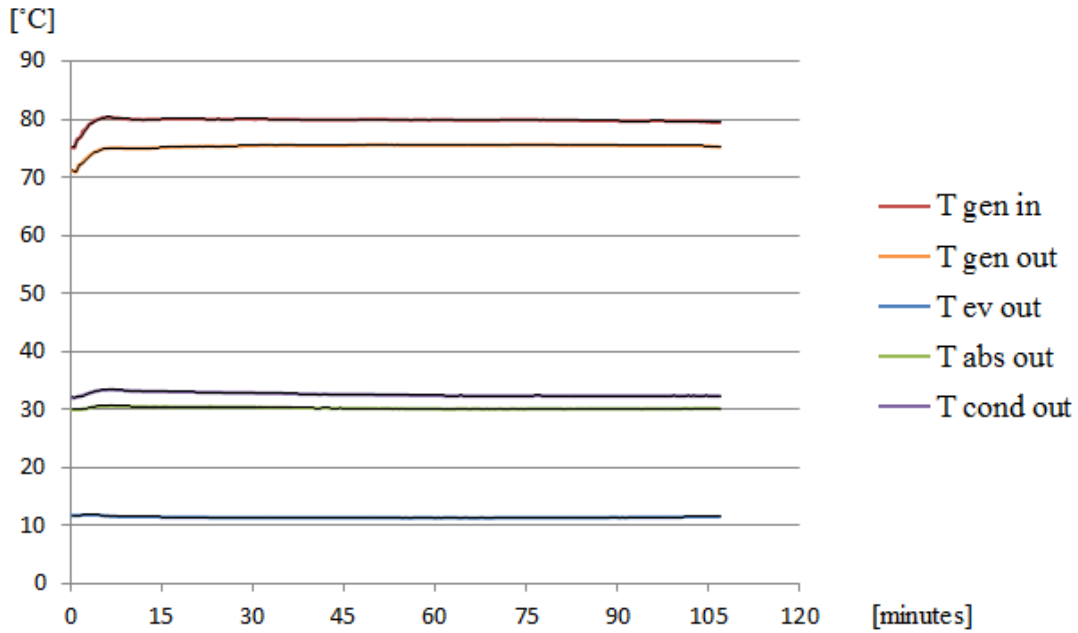


Figure 5.10. Temperature trends after the changing of the hot water inlet temperature (from 75 °C to 80 °C). Legend: $T_{ev\ out}$ = cold water temperature at the evaporator outlet; $T_{gen\ in}$ = hot water temperature at the generator inlet; $T_{abs\ out}$ = cooling water temperature at the absorber outlet; $T_{cond\ out}$ = cooling water temperature at the condenser outlet; $T_{gen\ out}$ = hot water temperature at the generator inlet.

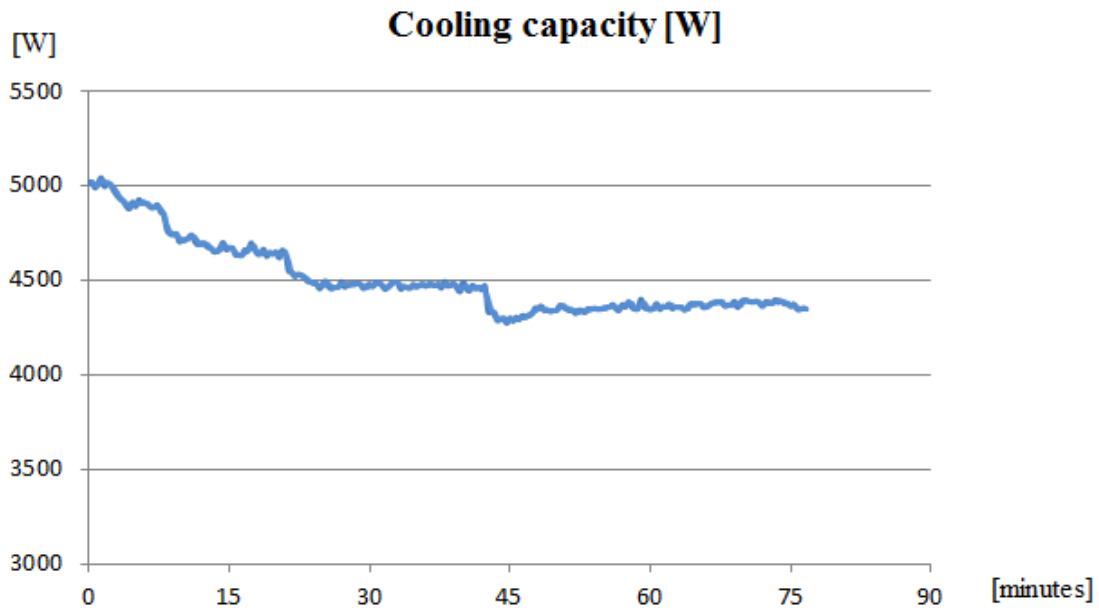


Figure 5.11. Cooling capacity trend after the changing of the hot water inlet temperature (from 80 °C to 75 °C).

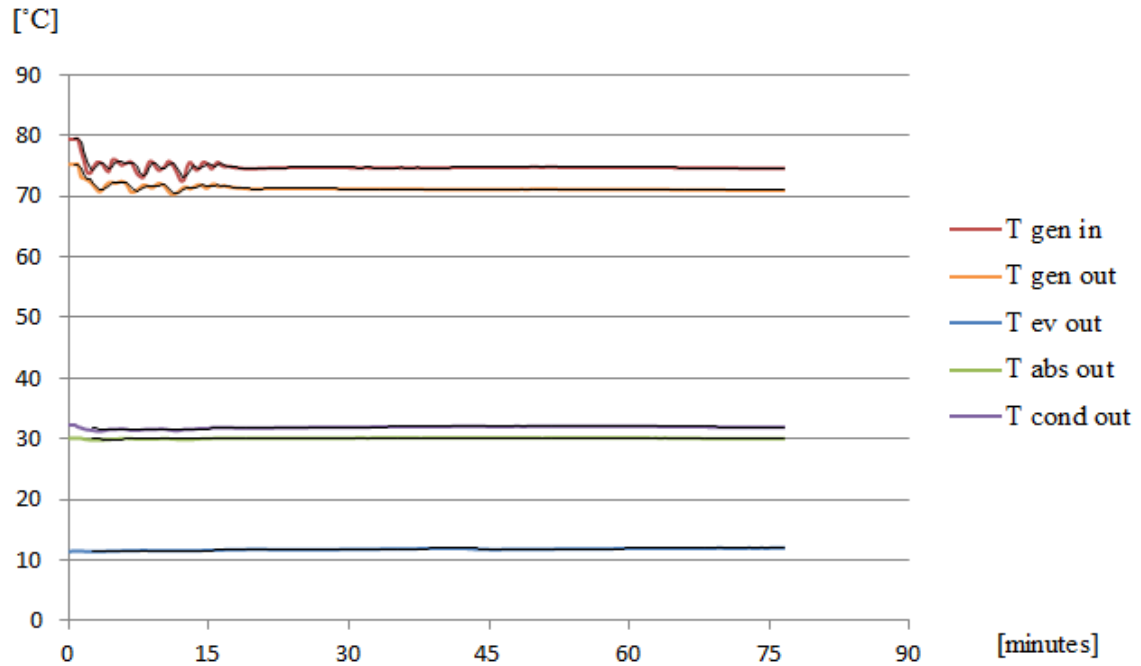


Figure 5.12. Temperature trends after the changing of the hot water inlet temperature (from 80 °C to 75 °C). Legend: $T_{ev\ out}$ = cold water temperature at the evaporator outlet; $T_{gen\ in}$ = hot water temperature at the generator inlet; $T_{abs\ out}$ = cooling water temperature at the absorber outlet; $T_{cond\ out}$ = cooling water temperature at the condenser outlet; $T_{gen\ out}$ = hot water temperature at the generator inlet.

The temperatures and cooling capacity behaviors are the same of which analyzed during the previous step response.

In both the steps the variation of the cooling capacity is about 500 W and it takes around one hour to reach a new constant value.

The temperatures at the generator change after few minutes because of the mixing valve. The fluctuation of the generator temperatures during the first minutes of measurement is due to the automatic control of the mixing valve. When the automatic control system is not able to guarantee a fixed position of the valve for a certain temperature, it has to be regulated by manual control.

- $75\text{ }^{\circ}\text{C} \longrightarrow 85\text{ }^{\circ}\text{C}$
 $75\text{ }^{\circ}\text{C} \longleftarrow 85\text{ }^{\circ}\text{C}$

The last investigation has been carried out changing the hot water temperature from $75\text{ }^{\circ}\text{C}$ to $85\text{ }^{\circ}\text{C}$ and vice versa, from $85\text{ }^{\circ}\text{C}$ to $75\text{ }^{\circ}\text{C}$.

The other boundary conditions are kept constant and their values are shown in the Table 3.3, as in the other cases.

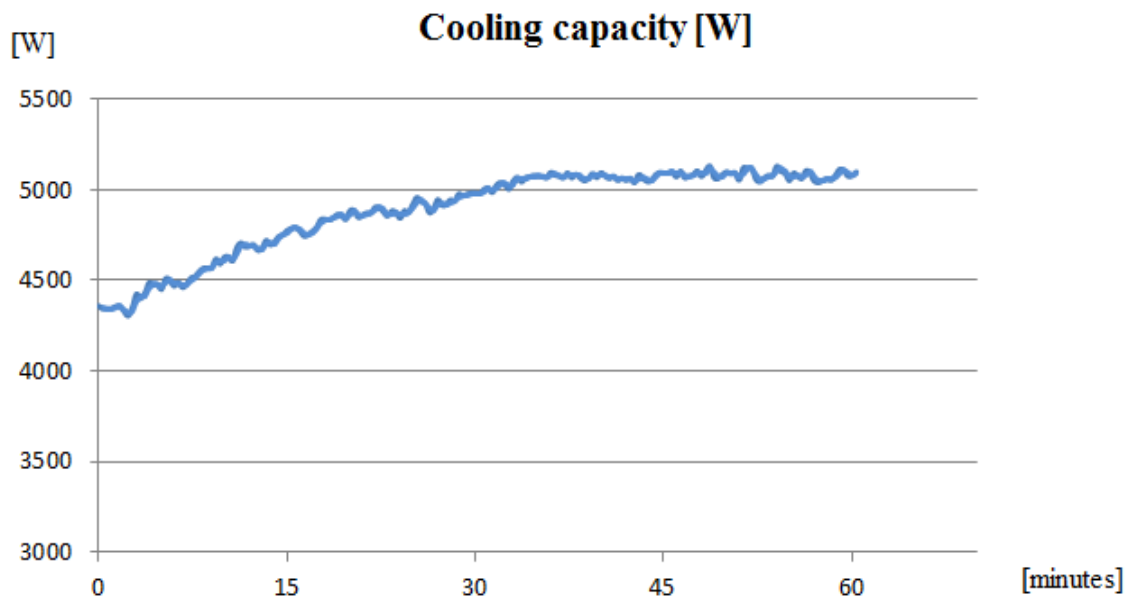


Figure 5.13. Cooling capacity trend after the changing of the hot water inlet temperature (from $75\text{ }^{\circ}\text{C}$ to $85\text{ }^{\circ}\text{C}$).

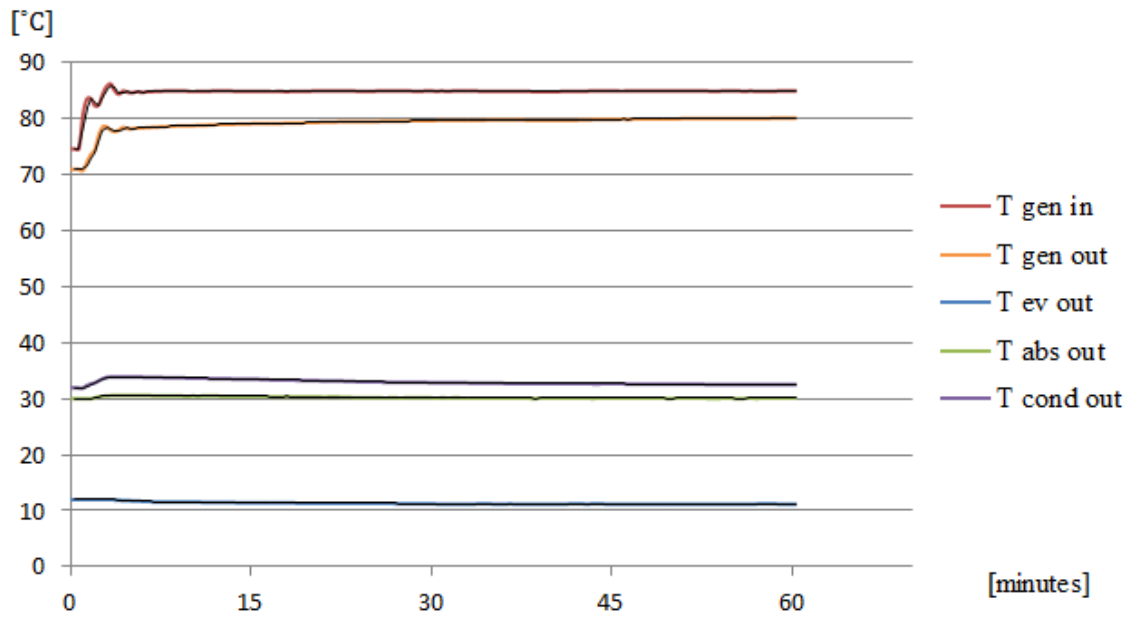


Figure 5.14. Temperature trends after the changing of the hot water inlet temperature (from 75 °C to 85 °C). Legend: $T_{ev\ out}$ = cold water temperature at the evaporator outlet; $T_{gen\ in}$ = hot water temperature at the generator inlet; $T_{abs\ out}$ = cooling water temperature at the absorber outlet; $T_{cond\ out}$ = cooling water temperature at the condenser outlet; $T_{gen\ out}$ = hot water temperature at the generator inlet.

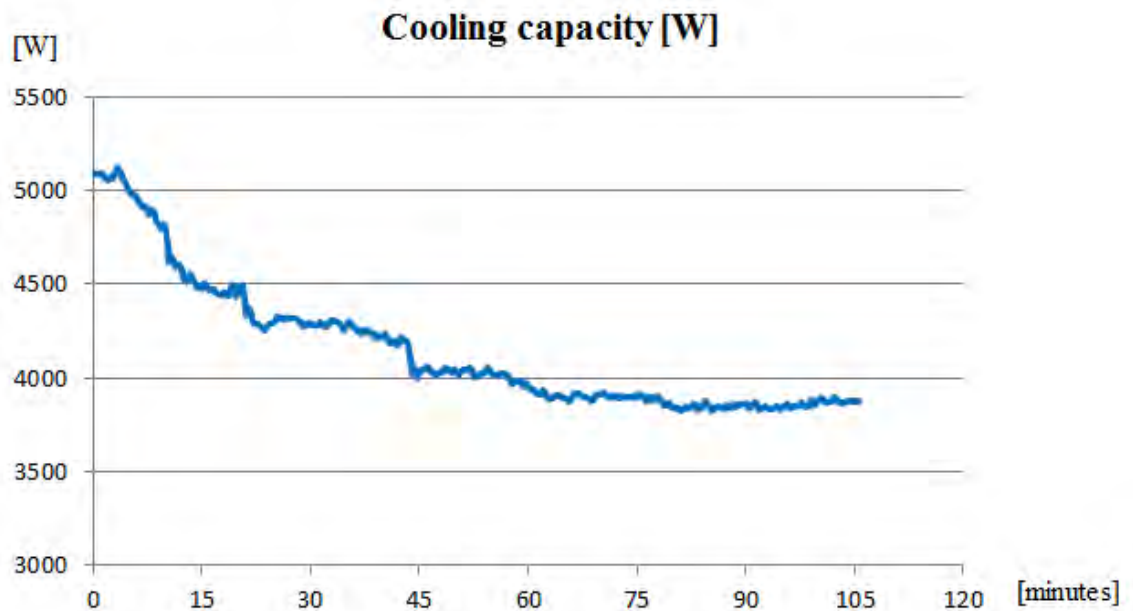


Figure 5.15. Cooling capacity trend after the changing of the hot water inlet temperature (from 85 °C to 75 °C).

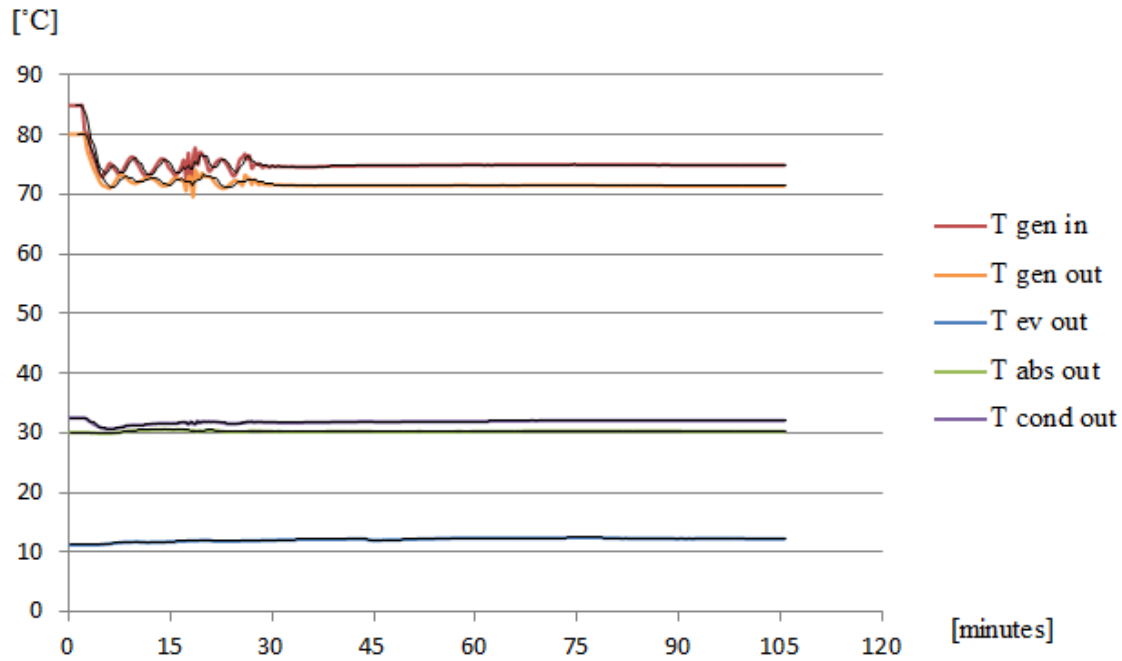


Figure 5.16. Temperature trends after the changing of the hot water inlet temperature (from 85 °C to 75 °C). Legend: $T_{ev\ out}$ = cold water temperature at the evaporator outlet; $T_{gen\ in}$ = hot water temperature at the generator inlet; $T_{abs\ out}$ = cooling water temperature at the absorber outlet; $T_{cond\ out}$ = cooling water temperature at the condenser outlet; $T_{gen\ out}$ = hot water temperature at the generator inlet.

The temperatures and cooling capacity behaviors are the same of which analyzed during the previous steps response.

In both the steps the variation of the cooling capacity is about 1000 W. It takes around 45 minutes to reach a new constant value in the first step, whereas a little more than one hour in the second one.

The generator temperature instabilities present in the first part of the measurement are attributable again to the mixing valve fluctuation.

5.1.2 Absorber heat and mass transfer

The heat transfer coefficients calculated through the EES script are shown in the tables below and they are sorted by the cooling water temperature at the inlet of the absorber.

The coefficients values are exhibited in function of the solution mass flow rate for pipe length, represented by the parameter Γ_{ls} .

The calculation of that one can be performed by the script posted in the Attachment D:

$$\Gamma_{ls} = \frac{\dot{V}_{ls} \cdot \rho_{ls, \text{ein}}}{2 \cdot l \cdot n_{RR}} \quad 5.1$$

where:

- \dot{V}_{ls} is the solution volume flow rate;
- $\rho_{ls, \text{ein}}$ is the solution density at the inlet of the absorber;
- l is the pipe length;
- n_{RR} is the number of pipe column of the absorber.

Except for the cooling water temperature and the solution volume flow rate, all the other boundary conditions are kept constant. Their values are shown in the Table 3.3 in the chapter 3.3.

The coefficient values are exhibited in the tables as function of the experimental average volume flow rate: it is the average among the values recorded in the 10 minutes preceding the measure.

- $T_{\text{ein},ab} = 27\text{ }^{\circ}\text{C}$

Solution volume flow rate	0,35	0,30	0,25	0,20	0,15	0,10	Unit of measurement
α_{film}	704,9	661,7	635,5	550,9	513,8	446,5	$\text{W}/(\text{m}^2 \cdot \text{K})$
K	618,8	584,9	564,1	496,2	465,9	409,9	$\text{W}/(\text{m}^2 \cdot \text{K})$
Experimental solution volume flow rate	0,3483	0,2998	0,2545	0,1996	0,1486	0,0997	$\frac{\text{m}^3}{\text{h}}$

Table 5.1. Overall heat transfer coefficient K and convection coefficient of the solution film on the pipes of the absorber α_{film} .

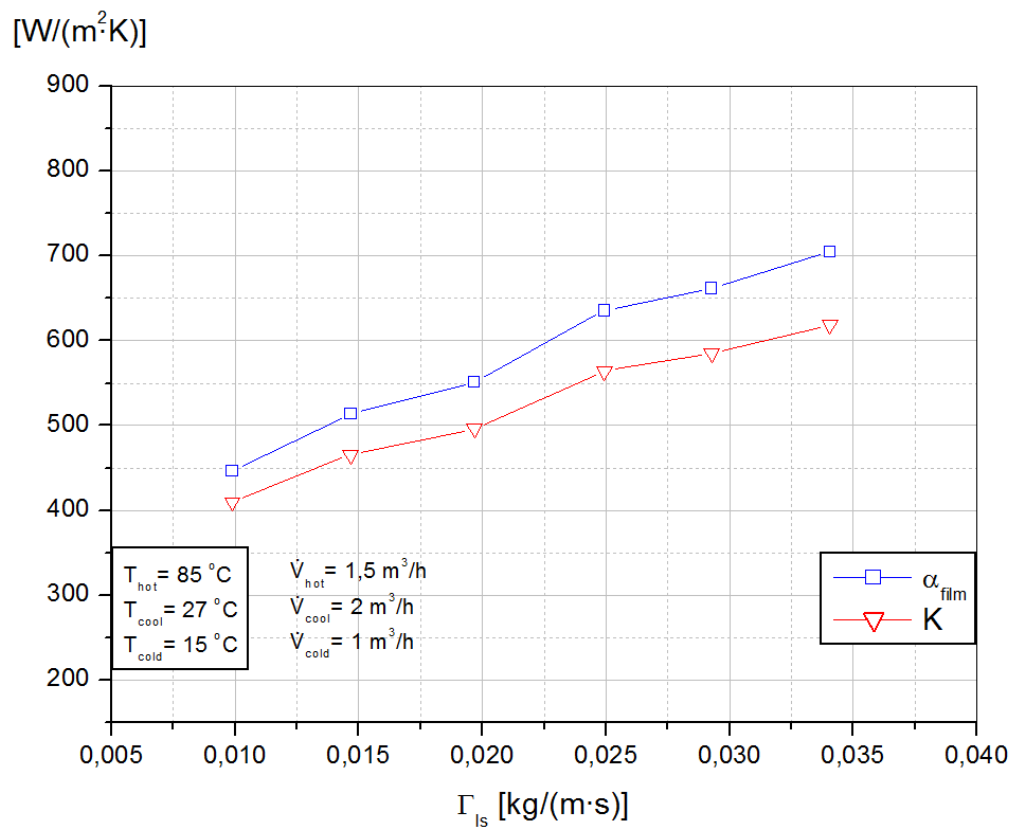


Figure 5.17. K and α_{film} in function of Γ_{ls} .

- $T_{ein,ab} = 32\text{ }^{\circ}\text{C}$

Solution volume flow rate	0,35	0,30	0,25	0,20	0,15	0,10	Unit of measurement
α_{film}	782,1	665,2	627,3	523,2	471,5	408,4	$\text{W}/(\text{m}^2 \cdot \text{K})$
K	681,7	590,8	560,9	476	433	379,2	$\text{W}/(\text{m}^2 \cdot \text{K})$
Experimental solution volume flow rate	0,3520	0,3007	0,2509	0,1976	0,1493	0,0989	$\frac{\text{m}^3}{\text{h}}$

Table 5.2. Overall heat transfer coefficient K and convection coefficient of the solution film on the pipes of the absorber α_{film} .

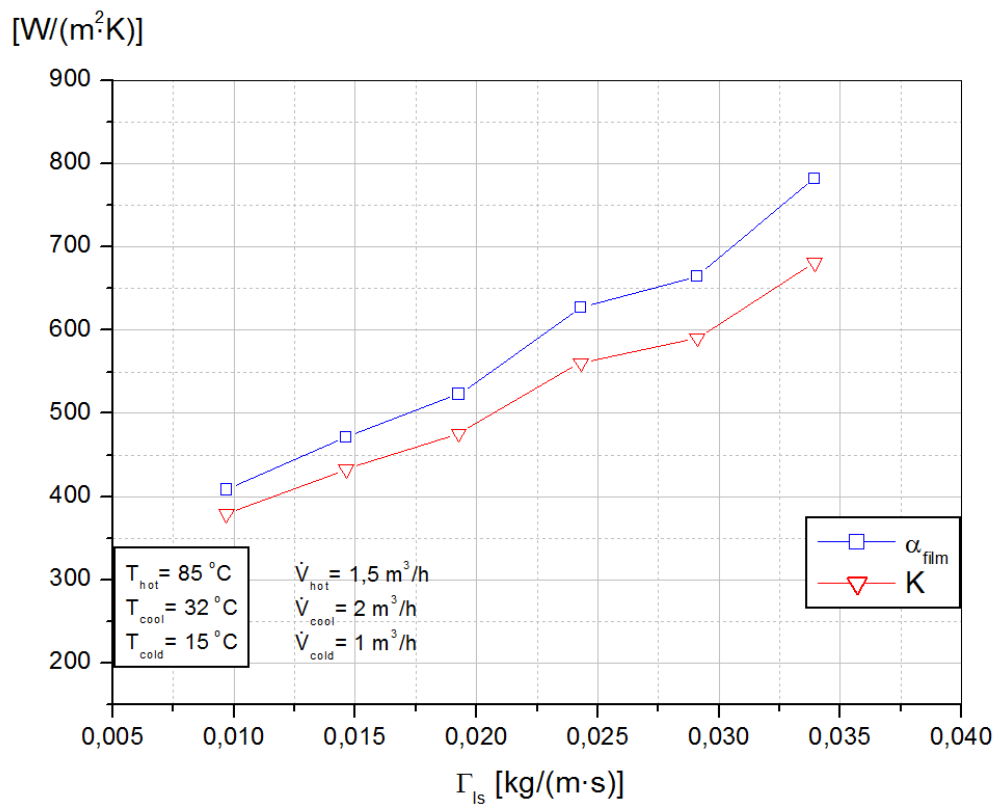


Figure 5.17. K and α_{film} in function of Γ_{ls} .

- $T_{\text{ein},ab} = 37\text{ }^{\circ}\text{C}$

Solution volume flow rate	0,35	0,30	0,25	0,20	0,15	0,10	Unit of measurement
α_{film}	826,1	711,4	628,9	517,5	369	284,4	$\text{W}/(\text{m}^2 \cdot \text{K})$
K	719,5	630,9	565,4	473,7	346,1	270,6	$\text{W}/(\text{m}^2 \cdot \text{K})$
Experimental solution volume flow rate	0,3545	0,2958	0,2460	0,2021	0,1502	0,1006	$\frac{\text{m}^3}{\text{h}}$

Table 5.3. Overall heat transfer coefficient K and convection coefficient of the solution film on the pipes of the absorber α_{film} .

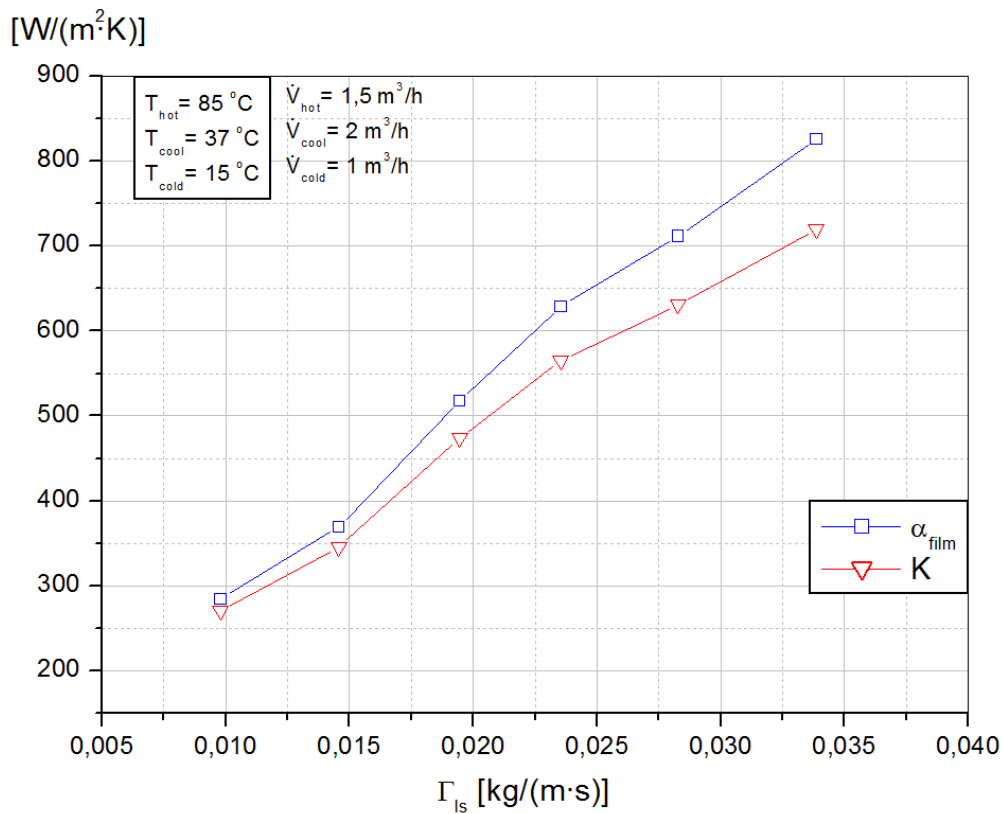


Figure 5.18. K and α_{film} in function of Γ_{ls}

In each case the values of both the coefficients, K and α , are strongly dependent on the Γ_{ls} parameter: when the solution flow rate rises, the coefficients increase.

This growth becomes more intense with high cooling water temperature.

In fact, when the cooling water temperature at the inlet of the absorber is set at 37 °C, the respective coefficients vary from the lowest values to the highest values calculated, for every cooling water temperature.

The trends can be explained focusing on two important aspects: the amount of wetted surface of the heat exchanger and the Reynolds number [10].

Indeed, if the solution volume flow rate is raised up, the amount of wetted surface by the solution increases too and so the effective exchange surface of the absorber is bigger.

The Reynolds number has the same behavior. If the solution flow rate rises, the Reynolds number grows up and the heat transfer characteristics are improved.

On the other hand, if the solution flow rate is too high, after a certain moment the transfer coefficients K and α assume a constant trend, or even it can change the tendency: becoming smaller raising up the volume flow rate of the solution [11].

The reason is that the flow pattern of the falling poor solution, around the absorber pipes, becomes different, because it changes from a falling drops pattern in a falling jets pattern.

In the latest one, the falling solution has a smaller turbulent impact on the pipe film below and, furthermore, it has a bigger thickness around the pipes and so a higher heat transfer resistance. These two the consequences make the heat transfer worse than in the falling drops pattern.

The increasing of cooling water inlet temperature influences the wettability (the viscosity is lower) and the Reynolds number too. Both the aspects bring to the improvement of the heat transfer coefficient K and α . However, as it is mentioned above, when the solution mass flow rate is around the smallest values, these coefficients are lower for high cooling water temperatures (37 °C), rather than for low ones (27 °C). That might be a starting point for new investigations.

The values of the overall heat transfer coefficients K , calculated by the program, represent suggestions for the input data of the mathematical model of the absorption chiller, written by the same software *EES – Engineering Equation Solver*.

5.2 Simulation

The EES model is used to evaluate the COP and the cooling capacity, through a mathematical simulation of the absorber chiller. They are calculated in function of the hot water temperature at the inlet of the generator and for different values of the cold water temperature at the evaporator inlet. The other boundary conditions of the program are the same adopted in the experimental measurements and they are shown in the Table 3.3. The graphics below show the comparison between the results, given by the mathematical model, and the experimental data. Their numerical values are exhibited in the related tables below. The comparisons are sorted by the different cold water temperature at the inlet of the evaporator $T_{ein,v}$.

- $T_{ein,v} = 10\text{ }^{\circ}\text{C}$

The Figure 5.19 and the Figure 5.20 show the comparison between the simulation results and the experimental data, respectively for the cooling capacity and the COP.

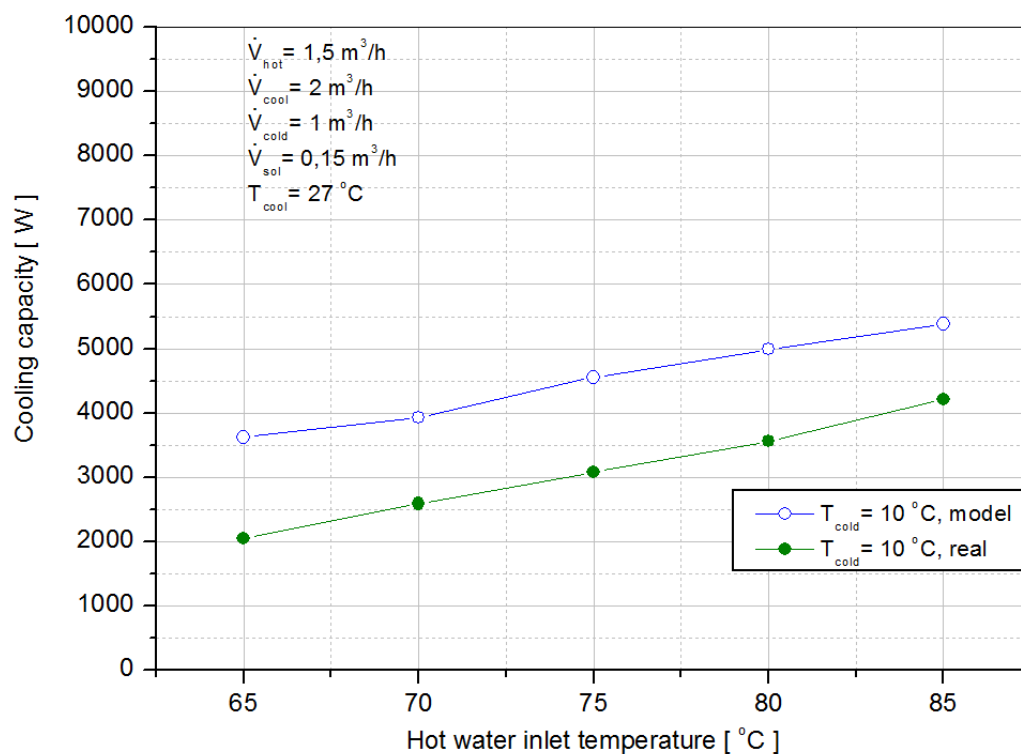


Figure 5.19. Comparison between the simulated cooling capacity (blue) and the real one (green).

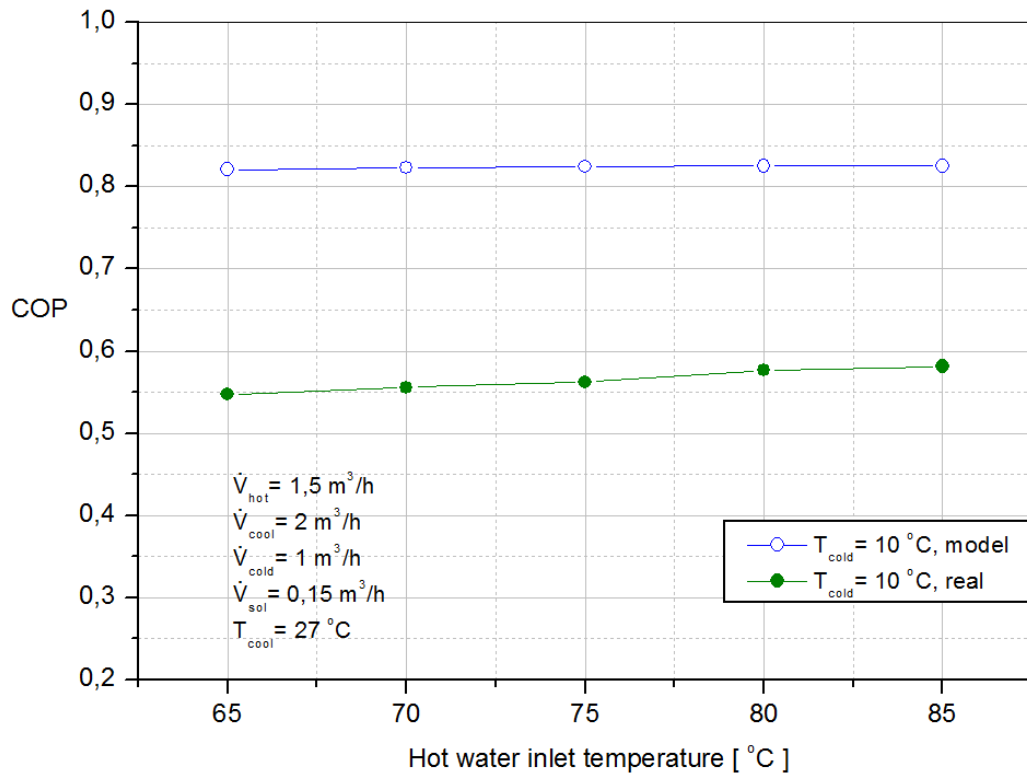


Figure 5.20. Comparison between the simulated COP (blue) and the real one (green).

$T_{ein,v} = 10 \text{ }^\circ\text{C}$	$T_{ein,g}$ [°C]	Cooling capacity, real [W]	Cooling capacity, model [W]	COP, real	COP, model
	65	2.049	3.619	0,5474	0,8209
	70	2.590	3.927	0,5557	0,8228
	75	3.078	4.555	0,5618	0,8242
	80	3.557	4.992	0,5770	0,8251
	85	4.212	5.389	0,5813	0,8253

Table 5.4. Simulated and real values of both the COP and cooling capacity.

The cooling capacity trend, simulated by the mathematical model, is the same of the experimental data one. The COP trends are very similar, except that the

experimental COP rises, with the increasing of the hot water temperature, more than the simulated one.

For an cold water temperature equal to 10°C the values, given by the model, are higher than the experimental data, especially for the COP.

These differences can be attributable to the losses, between the facility and the surroundings, and to the heat transfer coefficients inserted as input data in the model, which can present discrepancy between the real ones.

In particular, the cold water temperature, at the evaporator inlet, is lower than the surroundings temperature (set around 19°C). Because of that the heat, which goes inside the evaporator, evaporates a certain amount of refrigerant, which does not affect the real cooling capacity. For this reason, the real cooling capacity is lower than the simulated one.

- $T_{\text{ein},v} = 15^\circ\text{C}$

The next figure show the comparison between the simulation results and the experiemental data, both for the cooling capacity and the COP.

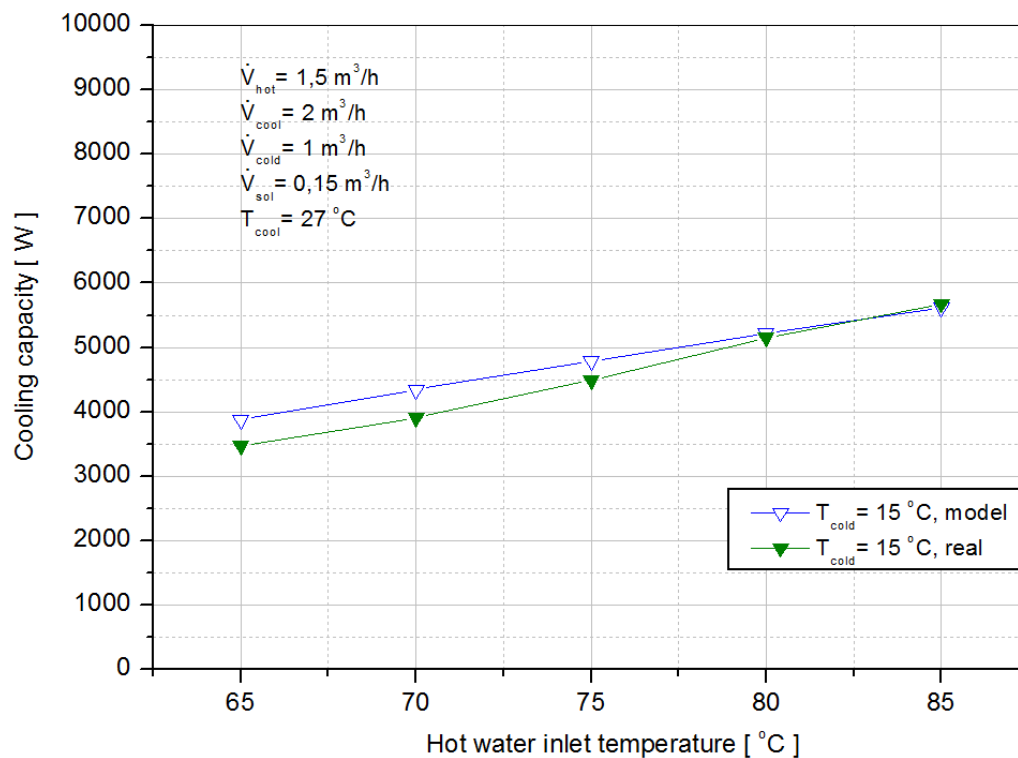


Figure 5.21. Comparison between the simulated cooling capacity (blue) and the real one (green).

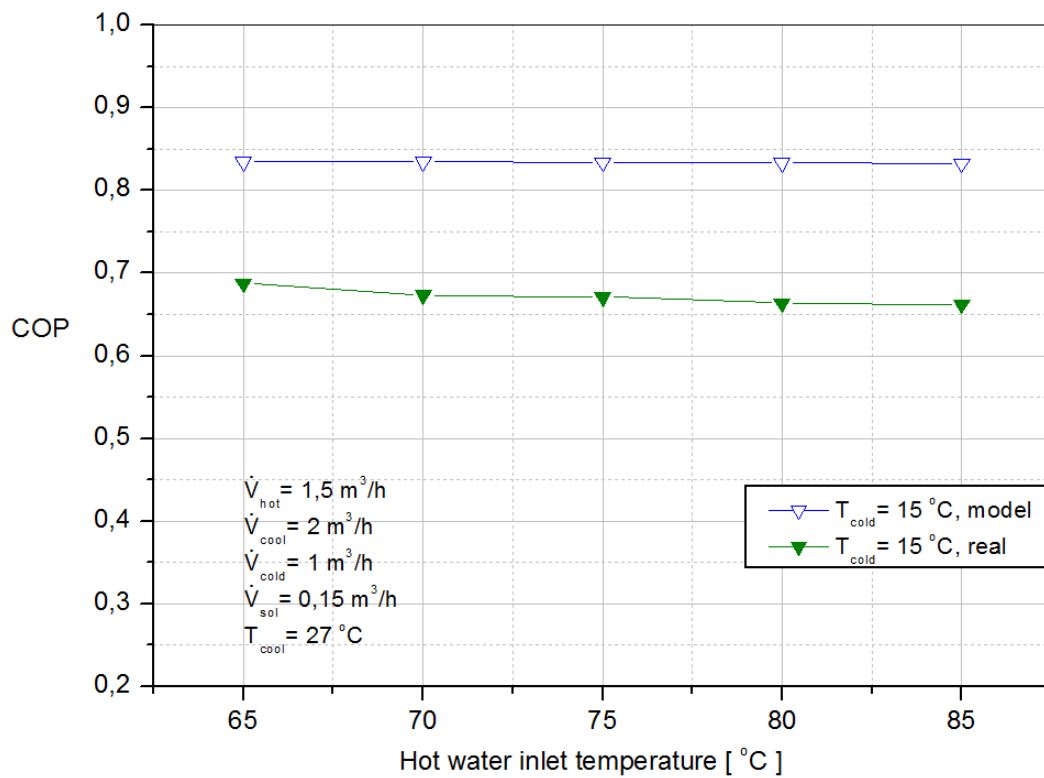


Figure 5.22. Comparison between the simulated COP (blue) and the real one (green).

	$T_{ein,g}$ [°C]	Cooling capacity, real [W]	Cooling capacity, model [W]	COP, real	COP, model
$T_{ein,v} = 15 \text{ }^\circ\text{C}$	65	3.472	3.879	0,6874	0,8346
	70	3.907	4.343	0,6733	0,8342
	75	4.482	4.789	0,6710	0,8338
	80	5.146	5.215	0,6635	0,8333
	85	5.677	5.612	0,6622	0,8325

Table 5.5. Simulated and real values of both the COP and cooling capacity.

The cooling capacity trend simulated by the mathematical model is the same of the experimental data one, in this case as well. The COP trends are very similar,

except that the experimental COP rises, with the increasing of the hot water temperature, more than the simulated one.

In this case the COP given back by the model is higher than the real one, but the simulated cooling capacity is for each hot water temperature very close to the experimental data values. The difference between the two cooling capacity at maximum is 10% of the real one.

These differences can be attributable to the losses between the facility and the surroundings and to the heat transfer coefficients inserted as input data in the model, which can present discrepancy between the real ones.

- $T_{ein,v} = 20\text{ }^{\circ}\text{C}$

The Figure 5.23 and the Figure 5.24 show the comparison between the simulation results and the experimental data, respectively for the cooling capacity and the COP.

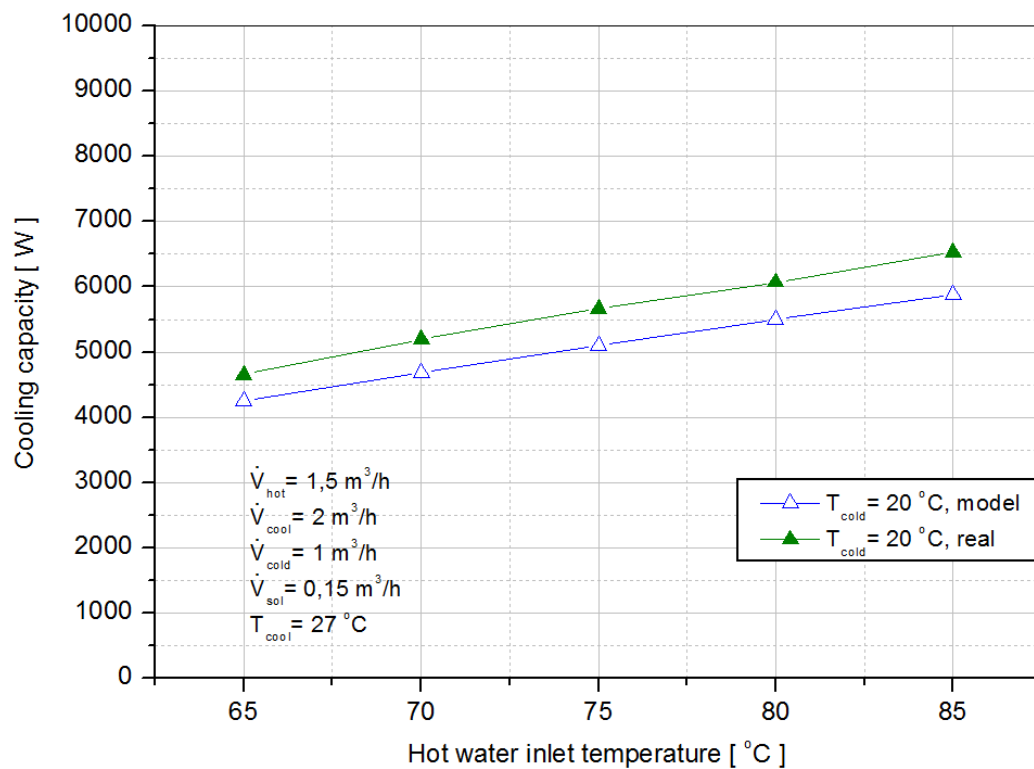


Figure 5.23. Comparison between the simulated cooling capacity (blue) and the real one (green).

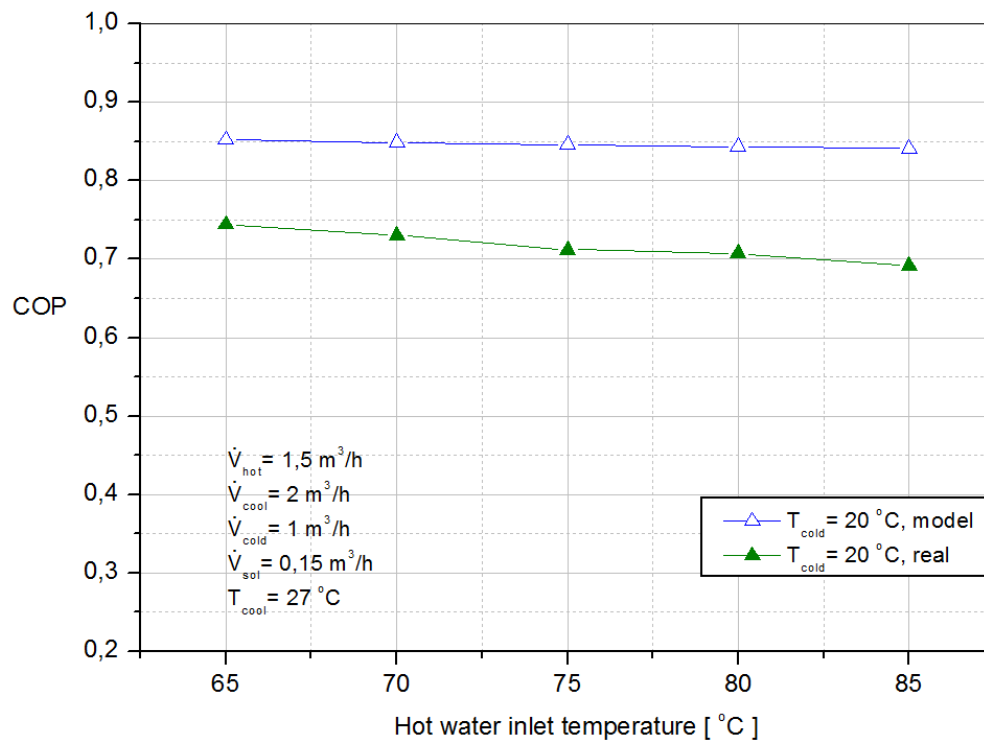


Figure 5.24. Comparison between the simulated COP (blue) and the real one (green).

	$T_{ein,g}$ [°C]	Cooling capacity, real [W]	Cooling capacity, model [W]	COP, real	COP, model
$T_{ein,v} = 20 \text{ }^\circ\text{C}$	65	4.652	4.246	0,7441	0,8520
	70	5.194	4.684	0,7301	0,8486
	75	5.659	5.099	0,7119	0,8455
	80	6.068	5.497	0,7070	0,8430
	85	6.530	5.878	0,6916	0,8408

Table 5.6. Simulated and real values of both the COP and cooling capacity.

The cooling capacity trend, simulated by the mathematical model, is the same of the experimental data one, in this case as well. The real COP and the simulated

one are closer than the cases for lower cold temperature, but the one given by the model is still higher.

The cooling capacity values are closer too, for each hot water temperature value.

The maximum discrepancy between them is about 10% of the real cooling capacity value.

- $T_{\text{ein},v} = 25\text{ }^{\circ}\text{C}$

The next figure show the comparison between the simulation results and the experiemental data, both for the cooling capacity and the COP. The cold water temperature is equal to $25\text{ }^{\circ}\text{C}$.

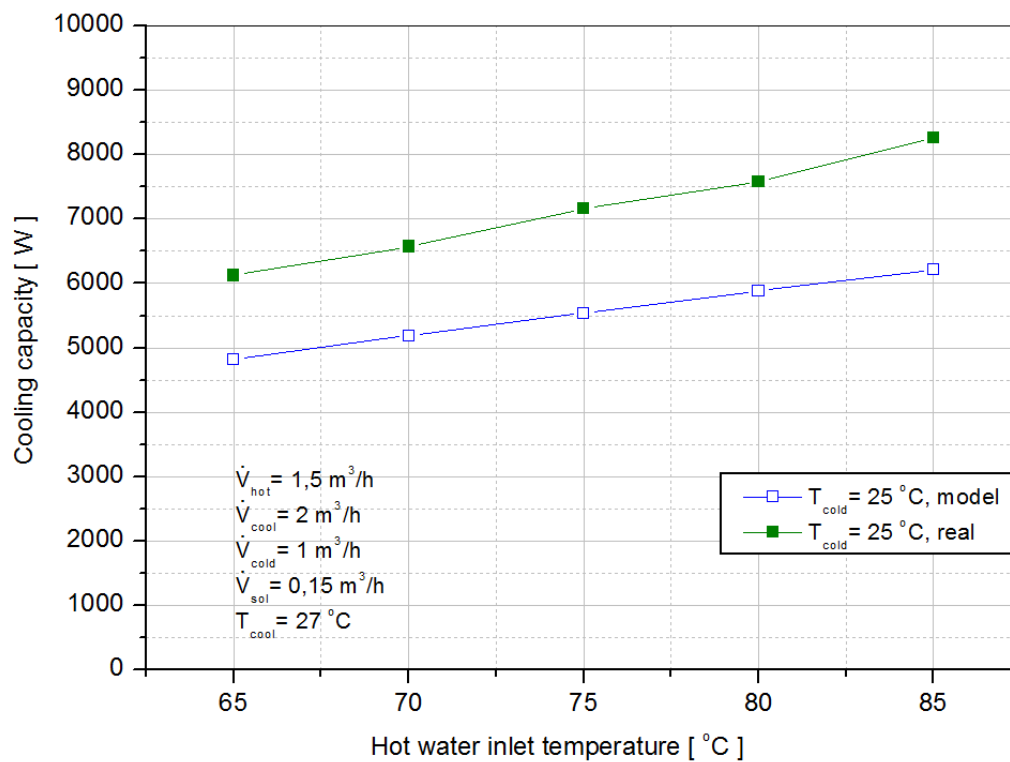


Figure 5.25. Comparison between the simulated cooling capacity (blue) and the real one (green).

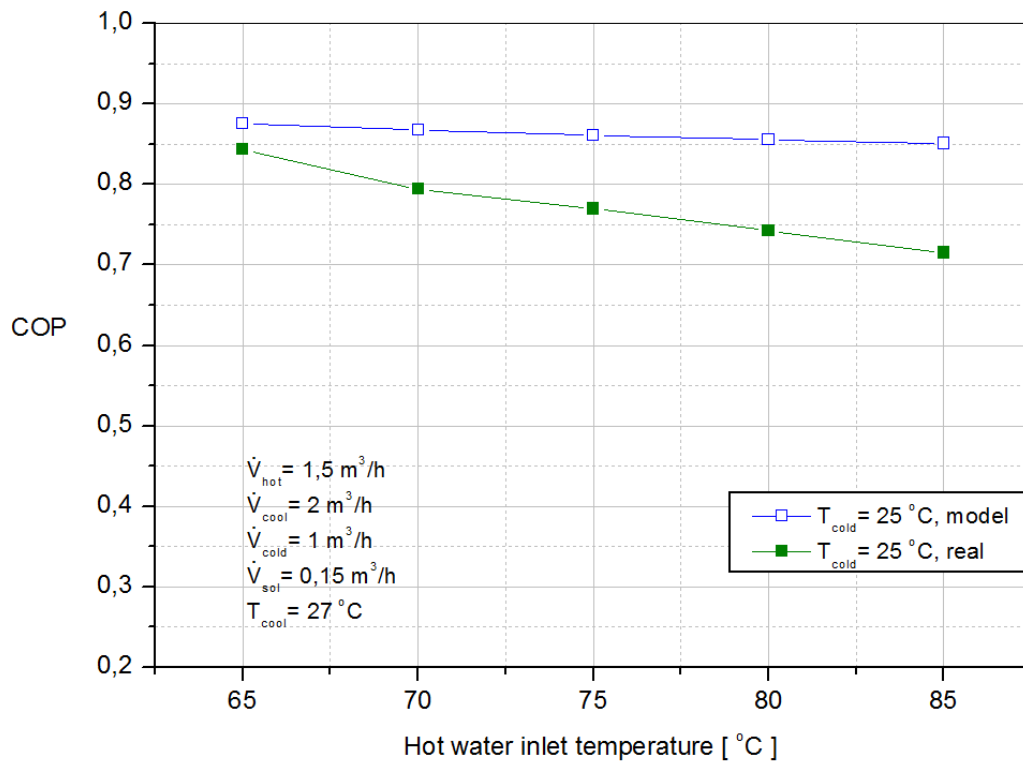


Figure 5.26. Comparison between the simulated COP (blue) and the real one (green).

	$T_{ein,g}$ [°C]	Cooling capacity, real [W]	Cooling capacity, model [W]	COP, real	COP, model
$T_{ein,v} = 25\text{ °C}$	65	6.121	4.817	0,8430	0,8751
	70	6.574	5.189	0,7938	0,8674
	75	7.157	5.538	0,7698	0,8607
	80	7.583	5.878	0,7423	0,8552
	85	8.259	6.213	0,7151	0,8508

Table 5.7. Simulated and real values of both the COP and cooling capacity.

The cooling capacity trend simulated by the mathematical model is very close to the experimental data one, but the real cooling capacity for each hot water temperature value is higher. The COP trend given by the model decreases with the

growth of the cold water temperature, but in a lighter way than the real one, as in all the cases.

The COP simulated values are still higher than the real ones, but it can be noticed that for low hot water temperature (65 °C) they are very close.

The reason is still attributable to the heat exchange between the environment and the facility. In particular, it represents the opposite case to the first one, in which is used a cold water temperature equal to 10°C.

Comparing all the cases, it is noticed how both the cooling capacity and COP increase, with the growth of the temperature of the cold water. The reason is that the temperature difference, between the cold water and the cooling water, which exports the heat (fixed at 27 °C), decreases. It brings to an increase of the cooling capacity and to a reduction of the heat demand at the generator [10].

Moreover, it is shown that the COP assumes different trends, changing the cold water temperature. If the cold water is low (10 °C in the investigation) the COP rises with the going up of the hot water temperature, but if the cold water is fixed at higher values (15...25 °C) the COP shows the opposite tendency.

With the increasing of the hot water temperature, the difference between the cooling water temperature (fixed at 27 °C) and the generator one grows. This temperature difference is proportional to the energy wasted by the system and which has to be supplied by the generator.

Since the cooling capacity increases with the growth of the hot water temperature, this effect seems to balance the previous one and to determine the trend direction change at a certain value of cold water temperature [10].

6. Conclusions

At first, the experimental working session concerned the facility dynamic behavior investigations. After the hot water temperature change, the attention has been paid to the time that the cooling capacity and the water temperatures at the outlet of the heat exchangers took to reach a new steady state condition. The step response of these facility parameters determines the working limits of the mathematical model, which is supposed to function in steady state conditions.

The hot water temperature can be switched through the automatic valve very rapidly and sometimes it presents some fluctuations, as it can be seen in the graphs in chapter 5. This is the typical situation in the district heating [10]. It can be observed that the cooling capacity is not affected immediately by the hot water temperature variation, but its trend depends on the cold water value, which changes very slowly. It means that the facility effectiveness would not be affected by possible fluctuations of the power input of the heating network.

The cold water temperature at the outlet of the evaporator and the cooling capacity took between 45 minutes and one hour to get the new steady state conditions and they needed more time than the other variables. Because of that, only the value measured either at the beginning or at the end of the cooling capacity (or cold water temperature) curve can be inserted into the program. In fact, during the variation of the above mentioned parameters, the model cannot represent the absorption chiller reliably, even if the other analyzed temperatures have already a constant trend.

The measurements and the data reduction to get the overall absorber heat transfer coefficient and the heat transfer convective coefficient of the solution film on the absorber pipes have represented the last part of the experimental session. The trends of the coefficients are shown in chapter 5, in function of the solution mass flow rate for the pipe length, represented by the parameter Γ_{ls} , and for three different values of cooling water temperature at the inlet of the absorber. As it has been expected (see page 80, chapter 5) the coefficients rise with the increase of the solution flow rate and, for high Γ_{ls} values, with the increase of the cooling water temperature as well. However, for low Γ_{ls} values, the coefficients decrease with the growth of the cooling water temperature. That might be a starting point for new investigations.

Comparisons between the model results and the experimental data have been made and they are shown in the graphs in chapter 5. In particular, attention has

been paid to the cooling capacity and COP values, on varying of the hot water temperature at the generator and for different cold water temperatures at the evaporator inlet.

The comparison graphs show that the model can be considered a satisfying instrument to represent the thermodynamic characteristics of the facility, especially for the cooling capacity calculations. In fact, when the inlet cold water temperature is set equal to 15 °C or 20 °C, the cooling capacity values given by the model turn out to be close to the experimental data (error lower than 10%). The reason is that the room temperature (set to 19 °C) is close to the cold water temperature and therefore the heat losses (which the model does not count), between the evaporator and the surroundings, are very low.

When the inlet cold water temperature at the evaporator is set to 10 °C or 25 °C, the simulated cooling capacity values diverge from the experimental ones, especially in the first case. In particular for a temperature equal to 10 °C, the cooling capacity given by the model is higher than the real one, whereas for a cold water temperature equal to 25 °C it is lower, as it is expected (see page 83, chapter 5).

Despite the COP simulations turn out to be higher than the real COP in every working conditions, the results given by the mathematical model can be considered satisfying, since always the experimental trend is reproduced. Because of that, the model might be a useful instrument to investigate the COP trend inversion causes, when the cold water temperature changes. The analysis of the program results, especially focusing on the variations of the cycle temperatures, might be a correct way.

The program might be useful also to identify the limiting apparatus of the entire cycle. Some investigations were carried out, changing the areas of each heat exchanger and focusing on the variations in the cooling capacity and COP. It has been noticed that the most influent exchange area variation is the absorber one. That means that it is the limiting component of the cycle, as it was expected [8].

7. Appendix

7.1 Attachment A: Vessel technical data

This Attachment belongs to the paragraph 3.1.1.

The 2 vessels are identical, they present the following technical file:

Producer: PFEIFFER VACUUM TrinosLine

Product type: Vacuum container

Project number: P21691

Material: AISI 316L (containers), AISI 316Ti (flanges)

Year : 2013

Net mass: 215 kg

Pressure range: 0 mbar to ambient pressure

Volume: $0,36 \text{ m}^3 = 360 \text{ l}$

Temperature range: from -15 °C to 150 °C

Production: Made in Germany
Trinos Vakuum-Systeme GmbH
Anna-Vandenhoeck-Ring 44
37081 Göttingen

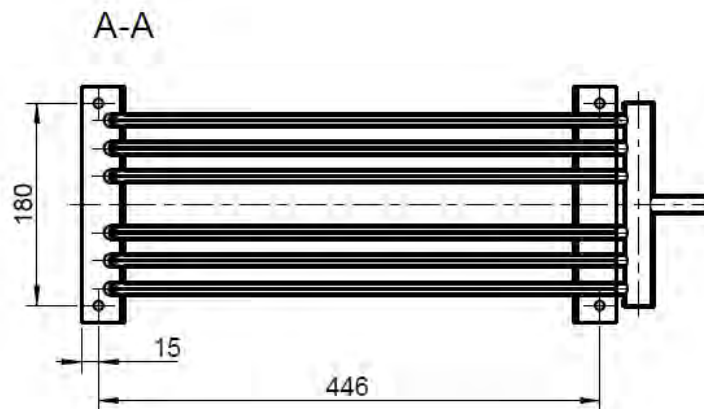
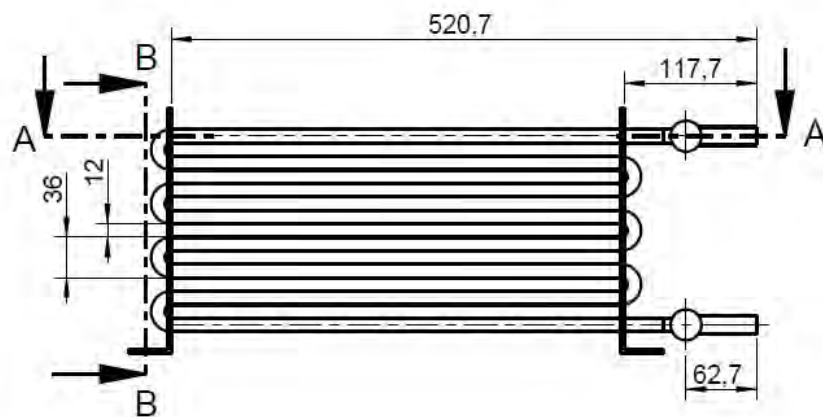
7.2 Attachment B: Shell and tube heat exchanger geometry

This Attachment belongs to the paragraph 3.1.1

In the figures below it can be seen the geometry of the shell and tube heat exchangers. Especially the figures show the evaporator and condenser dimensions.

The generator and the absorber present the same geometry of the above mentioned heat exchangers; the only differences among them are the number of columns and pipes lines, as it is specified in the Table 7.1.

The pipes are made of pure copper.



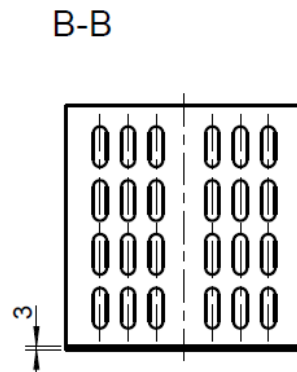


Figure 7.1. The main three views of the evaporator and condenser are shown. All dimensions are in millimeters.

Dimensions:

	Evaporator	Condenser	Absorber	Generator	Unit of measurement
Area	0,729	0,729	0,912	1,215	m ²
Pipe length	0,403	0,403	0,403	0,403	m
Pipe external diameter	0,012	0,012	0,012	0,012	m
Pipe thickness	0,001	0,001	0,001	0,001	m
Columns number	6	6	6	8	/
Lines number	8	8	10	10	/

Table 7.1. Main dimensions of the four main heat exchangers o the facility.

7.3 Attachment C: Recorded facility data

This Attachment belongs to the paragraphs 3.3.1 and 3.3.2

In the Figure 7.2. an example of recorded data by LabVIEW is shown. It can be noticed that both the sensors and the time, related to each parameter, are indicated.

They are written down in an Excel file.

A	B	C	D
PT1	Zeit	PT2	Zeit
22,573692	08:08:36	22,942078	08:08:37
22,383439	08:08:50	22,957818	08:08:51
22,387757	08:09:10	22,958385	08:09:11
22,390044	08:09:30	22,957793	08:09:31
22,387731	08:09:50	22,957818	08:09:51
22,385726	08:10:10	22,956658	08:10:11
22,38863	08:10:30	22,956375	08:10:31
22,387191	08:10:50	22,957509	08:10:51
22,388887	08:11:10	22,958385	08:11:11
22,388039	08:11:30	22,956065	08:11:31
22,388039	08:11:50	22,958695	08:11:51
22,388887	08:12:10	22,958102	08:12:11
22,3866	08:12:30	22,956375	08:12:31
22,384904	08:12:50	22,957793	08:12:51
22,388039	08:13:10	22,956942	08:13:11
22,387165	08:13:30	22,954674	08:13:31
22,390018	08:13:50	22,954648	08:13:51

Figure 7.2. A section of the Excel file where the software LabVIEW records the data.

7.4 Attachment C: COP and cooling capacity results

This Attachment belongs to the paragraph 3.3.1

The following graphics and tables show the trends and the values of both the COP and cooling capacity, evaluated from the experimental measurements. These data collection is taken from [7].

The measure modality and the boundary conditions are exactly the same of those indicated in the paragraph 3.3.1.

The facility parameters fixed are shown in the Table 3.3 of the paragraph 3.3. and they are:

- $\dot{V}_g = 1,5 \text{ m}^3/h$, which is the volume flow rate of the hot water at the generator inlet;
- $\dot{V}_k = 2 \text{ m}^3/h$, which is the volume flow rate of the cooling water across both the absorber and condenser;
- $\dot{V}_v = 1 \text{ m}^3/h$, which is the volume flow rate of the cold water at the evaporator inlet;
- $\dot{V}_{sol} = 0,15 \text{ m}^3/h$, which is the volume flow rate of the solution flowing through the solution heat exchangers;
- $T_{ein,ab} = 27 \text{ }^\circ\text{C}$, which is the cooling water temperature at the inlet of the absorber.

	$T_{in,gen} [^\circ\text{C}]$	Cooling capacity	COP
$T_{ein,v} = 10 \text{ }^\circ\text{C}$	65	2.049,48	0,547430685
	70	2.590,87	0,555703591
	75	3.078,95	0,561888936
	80	3.557,96	0,577034747
	85	4.212,40	0,581358738

Table 7.2. Cop and cooling capacity values, experimental data. The cold water temperature at the evaporator inlet is equal to 10 °C.

	$T_{in,gen} [^{\circ}C]$	Cooling capacity	COP
$T_{ein,v} = 15^{\circ}C$	65	3.472,22	0,687456908
	70	3.907,18	0,673300167
	75	4.482,19	0,671064848
	80	5.146,52	0,663539552
	85	5.677,02	0,662241171

Table 7.3. Cop and cooling capacity values, experimental data. The cold water temperature at the evaporator inlet is equal to 15 °C.

	$T_{in,gen} [^{\circ}C]$	Cooling capacity	COP
$T_{ein,v} = 20^{\circ}C$	65	4.652,15	0,744109503
	70	5.194,37	0,730141058
	75	5.659,55	0,711935812
	80	6.068,58	0,707050049
	85	6.530,90	0,691639219

Table 7.4. Cop and cooling capacity values, experimental data. The cold water temperature at the evaporator inlet is equal to 20 °C.

	$T_{in,gen} [^{\circ}C]$	Cooling capacity	COP
$T_{ein,v} = 25^{\circ}C$	65	6.121,11	0,843076518
	70	6.574,29	0,793886388
	75	7.157,12	0,769851393
	80	7.583,20	0,742391432
	85	8.259,75	0,715134701

Table 7.5. Cop and cooling capacity values, experimental data. The cold water temperature at the evaporator inlet is equal to 25 °C.

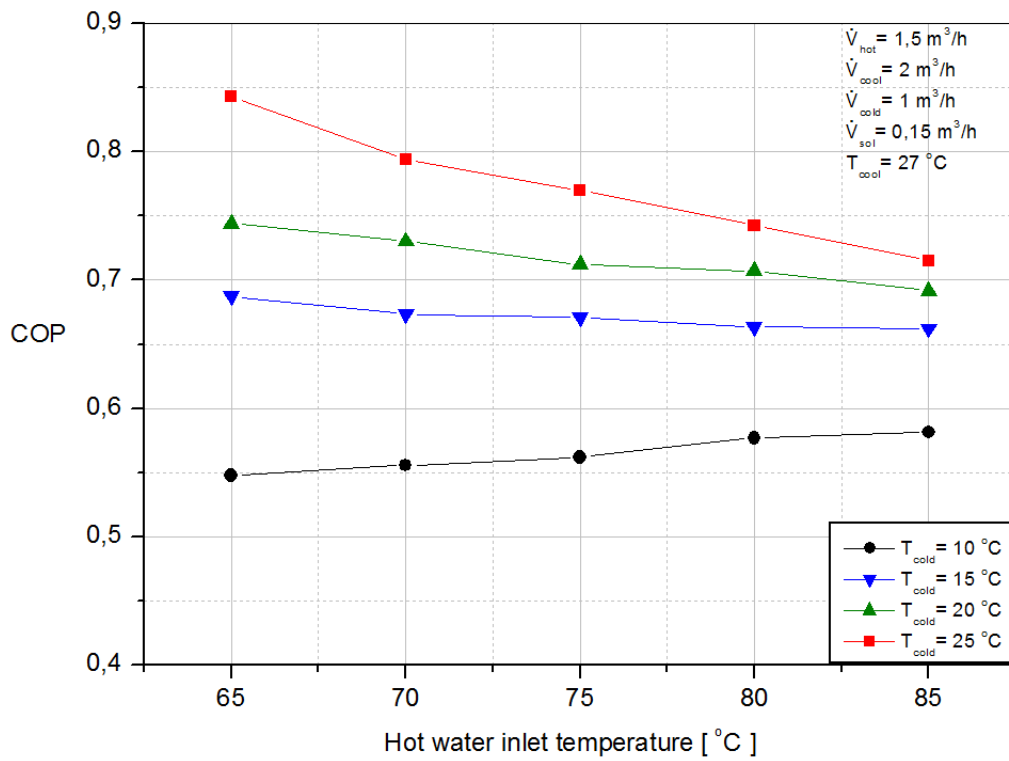


Figure 7.3. Cop trends, experimental data.

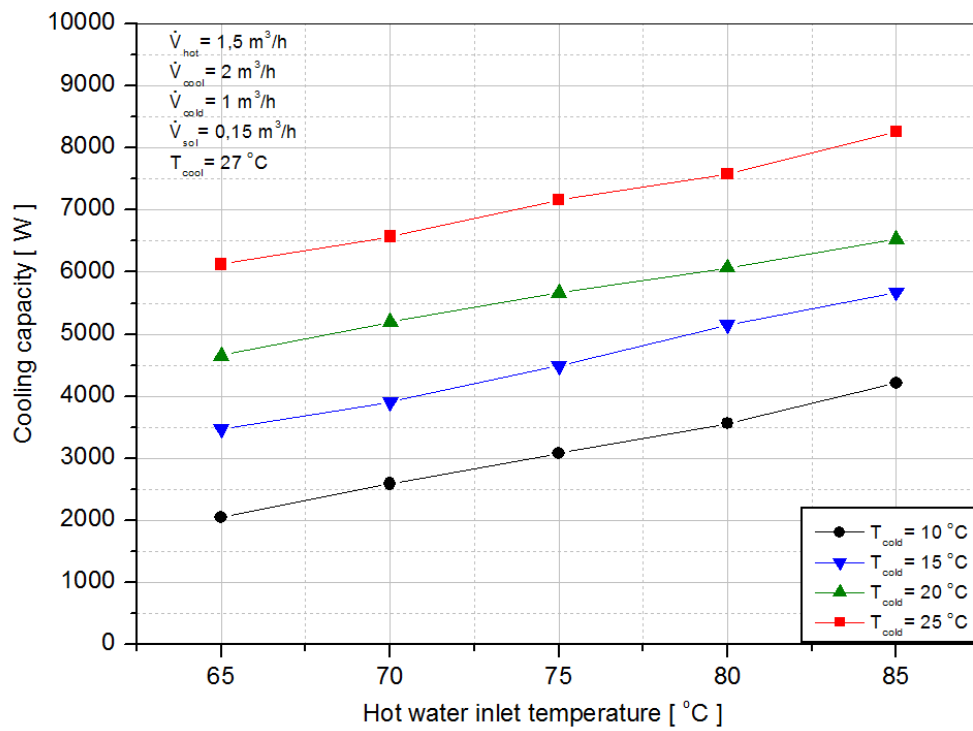


Figure 7.4. Cooling capacity trends, experimental data.

7.5 Attachment D: EES – script, absorber coefficients calculations

This Attachment belongs to the paragraph 3.3.3.

// α film and overall heat transfer coefficient calculations from the absorber measured data

{Input data}

Cooling water data

T_KW_ein = 273,15[K]+37,26460335[K]

{ PT1: Cooling water temperature at the inlet of the absorber }

T_KW_au = 273,15[K]+38,60985735[K]

{ PT2: Cooling water temperature at the outlet of the absorber }

p_KW = 300000[Pa]

{ Pressure inside the cooling water pipe }

V_dot_KW = 0,000557686[m³/s]

{ MID2: Cooling water volume flow rate}

Solution data - Inlet and outlet of the absorber

V_dot_LS=2,79714E-05[m³/s]

{ MID4: Poor solution volume flow rate - Absorber inlet (over the pipes)}

p_LS =1512,103939[Pa]

{ Pi4: Working pressure inside the absorber}

T_LS_ein= 273,15[K]+50,28863932[K]

{ TC1: Solution temperature at the inlet of the absorber (poor solution)}

T_LS_au=273,15[K]+39,0978511[K]

{ TC11: Solution temperature at the outlet of the absorber (rich solution)}

rho_LS_ein_probe =1691,5 [kg/m³]

{ Poor solution sample density at 20°C}

rho_LS_au_probe = 1671[kg/m³]

{ Rich solution sample density at 20°C}

{Input data - end}

Absorber geometry

$$L = 0,4[\text{m}]$$

{ Pipes lenght }

$$d = 0,012[\text{m}]$$

{ Pipes external diameter }

$$s = 0,001[\text{m}]$$

{ Pipes thickness }

$$n_{RR} = 6$$

{ j: Number of column }

$$n_{RPR} = 10$$

{ n: Number of lines }

{ Input data - end }

Properties

Cooling water properties

$$\eta_{KW} = \text{Viscosity}(\text{Water}; T = ((T_{KW_ein} + T_{KW_ein})/2); P = p_{KW})$$

{ Cooling water dynamics viscosity }

$$\rho_{KW} = \text{Density}(\text{Water}; T = ((T_{KW_ein} + T_{KW_ein})/2); P = p_{KW})$$

{ Cooling water density }

$$\lambda_{KW} = \text{Conductivity}(\text{Water}; T = ((T_{KW_ein} + T_{KW_ein})/2); P = p_{KW})$$

{ Cooling water thermal conductivity }

$$c_{p_KW} = \text{Cp}(\text{Water}; T = ((T_{KW_ein} + T_{KW_ein})/2); P = p_{KW})$$

{ Cooling water specific heat }

$$Pr_{KW} = \text{Prandtl}(\text{Water}; T = ((T_{KW_ein} + T_{KW_ein})/2); P = p_{KW})$$

{ Prandtl number of cooling water }

Material properties for the copper pipes

$$\lambda_{Cu} = k_{\text{'Copper'}}; ((T_{KW_ein} + T_{KW_ein})/2)$$

{ Copper thermal conductivity }

Solution properties

$$\rho_{LS_ein_probe} = \rho_{LiBrH_2O}(293[\text{K}]; w_{ein})$$

{Inlet solution concentration calculation (kg_LiBr/kg_solution) from the density of the poor solution sample (sample conditions: T= 20°C und P=1bar)}

$\rho_{LS_aus_probe} = \rho_{LiBrH_2O}(293[K]; w_{aus})$

{Outlet solution concentration calculation (kg_LiBr/kg_solution) from the density of the rich solution sample (sample conditions: T= 20°C und P=1bar)}

$\rho_{LS_ein} = \rho_{LiBrH_2O}(T_{LS_ein}; w_{ein})$

{Poor solution density at the inlet of the absorber}

$\rho_{LS_aus} = \rho_{LiBrH_2O}(T_{LS_aus}; w_{aus})$

{Rich solution density at the outlet of the absorber}

$\lambda_{LS} = \text{Cond}_{LiBrH_2O}(T_{LS_ein}; w_{ein})$

{Poor solution thermal conductivity at the inlet of the absorber}

$\eta_{LS} = \text{Visc}_{LiBrH_2O}(T_{LS_ein}; w_{ein})$

{Poor solution viscosity at the inlet of the absorber}

Thermodynamics characteristics

Equilibrium conditions

$T_{LS_gg_ein} = T_{LiBrH_2O}(p_{LS}; w_{ein})$

{Solution saturation temperature calculated with the inlet solution concentration}

$T_{LS_gg_aus} = T_{LiBrH_2O}(p_{LS}; w_{aus})$

{Solution saturation temperature calculated with the outlet solution concentration}

Absorber geometry

$n_{ges} = n_{RR} \cdot n_{RPR}$

{Total number of the pipes in the absorber}

$A = \pi \cdot d \cdot L_{ges} \cdot n_{RR}$

{Heat exchanger area}

Heat transfer

Heat transfer calculation through the absorber. Calculations of the film heat transfer coefficient and of the overall heat transfer coefficient

$\dot{Q} = \dot{V}_{KW} \cdot \rho_{KW} \cdot c_{p_KW} \cdot (T_{KW_aus} - T_{KW_ein})$

{Heat transfer calculation, secondary fluid side}

$\dot{Q} = k \cdot A \cdot \Delta T_{LM}$

{Overall heat transfer coefficient K calculation}

$k = (1/\alpha_{film} + d/((d-2s) \cdot \alpha_{rohr}) + (d/(2 \cdot \lambda_{Cu})) \cdot (\ln(d/(d-2s))))^{-1}$

{Alpha film calculation}

$$\text{DELTAT_LM} = ((T_{\text{LS_gg_ein}} - T_{\text{KW_aus}}) - (T_{\text{LS_gg_aus}} - T_{\text{KW_ein}})) / \ln((T_{\text{LS_gg_ein}} - T_{\text{KW_aus}}) / (T_{\text{LS_gg_aus}} - T_{\text{KW_ein}}))$$

{Logarithmic mean temperature difference calculation}

$$\text{Nusselt_Film} = \alpha_{\text{film}} * L / \lambda_{\text{LS}}$$

Calculation of heat transfer coefficient value for turbulent pipe flow (cooling water in the tube) through Gnielinski correlation

$$L_{\text{ges}} = n_{\text{RPR}} * L$$

{Lenght of an entire column of pipes}

$$\dot{m}_{\text{KW}} = (V_{\text{dot_KW}} / n_{\text{RR}}) * \rho_{\text{KW}}$$

{Mass flow rate calculation}

$$\dot{m}_{\text{KW}} = u_{\text{KW}} * \rho_{\text{KW}} * \pi * ((d - 2*s)^2) / 4$$

{Calculation of the mean flow velocity of the cooling water}

$$\text{Re_KW} = (u_{\text{KW}} * (d - 2*s) * \rho_{\text{KW}}) / \eta_{\text{KW}}$$

{Reynold number calculation}

$$\xi = (0,782 * \ln(\text{Re_KW}) - 1,51)^{-2}$$

{Friction factor from Colebrook [17].}

$$\text{Nusselt_k_w} = ((\xi/8) * (\text{Re_KW} - 1000) * \text{Pr_KW}) / (1 + 12,7 * \sqrt{\xi/8} * (\text{Pr_KW}^{2/3} - 1)) * (1 + ((d - 2*s) / L_{\text{ges}})^{2/3})$$

{Correlation for the inner tube-side heat transfer by Gnielinski for turbulent flow and flow in the transition region [17]}

$$\text{Nusselt_k_w} = (\alpha_{\text{rohr}} * (d - 2*s)) / \lambda_{\text{KW}}$$

{Alpha secondary fluid calculation}

$$\text{GAMMA_LS} = ((1/n_{\text{RR}}) * V_{\text{dot_LS}}) * \rho_{\text{LS_ein}} / (2*L)$$

{Irrigation density calculation from given measurements}

$$\text{Re_LS} = (4 * \text{GAMMA_LS}) / \eta_{\text{LS}}$$

{Film Reynolds number calculation in the absorber}

7.6 Attachment E: EES input data – heat transfer coefficients calculations

This Attachment belongs to the paragraph 3.3.3.

The input data for the EES program, which calculates the absorber heat transfer coefficients are shown in the Figure 7.5.

The program script is posted in the Attachment D.

These input data are obtained doing the average of the values recorded during the last 10 minutes before the measure.

NAME		SENSOR	VALUE	UNIT OF MEASURE
Cooling water at the absorber inlet		PT1	273,15 + 37,26460335	K
Cooling water at the absorber outlet		PT2	273,15 + 38,60985735	K
Cooling water volume flow rate		MID2	0,00055769	m ³ /s
Pressure inside the cooling water pipes		Fixed	300000	Pa
Poor solution volume flow rate		MID4	2,80E-05	m ³ /s
Pressure inside the absorber		Pi4	1512,10394	Pa
Poor solution temperature - absorber inlet		TC1	273,15+50,28863932	K
Rich solution temperature - absorber outlet		TC11	273,15+39,0978511	K
Poor solution sample density at 20°C;		Experiment	1691,5	kg/m ³
Rich solution sample density at 20°C;		Experiment	1671	kg/m ³
Pipes length			0,403	m
Pipes external diameter			0,012	m
Pipes thickness			0,001	m
Column number			6	
Lines number			10	

Figure 7.5. Input data for the calculation of the absorber heat transfer coefficients.

7.7 Attachment F: EES script – absorption chiller performance

This Attachment belongs to the paragraph 4.3

In this attachment the EES program script is posted. The descriptions are highlighted in grey and they are placed under the respective command line.

The program is subdivided in more sections: the beginning and the end of each section is indicated between curly brackets.

```
{-----EVAPORATOR-----}

{FIRST ITERATION}

{:: Predefined Properties - Beginning}

V_Dot_v = (1/3600) [m^3/s]
{ Cold water volume flow rate }

T_ein_v=288,2[K]
{Cold water temperature at the entrance of the evaporator }

P_u=300000[Pa]
{ Pressure inside the cooling pipeline}

K_v=2000[(J/s)/(K*m^2)]
{Overall heat transfer coefficient of the evaporator}

A_v=0,729 [m^2]
{ Evaporator exchange area}

{:: Predefined Properties - End}

rho_v=Density(Water;T=T_ein_v;P=P_u)
{ Density of the cold water, cold pipeline and cooling pipeline have the same work pressure}

M_Dot_v=rho_v*V_Dot_v
{ Mass flow rate of the cold water}

cp_v=Cp(Water;T=T_ein_v;P=P_u)
{ Cold water specific heat }

Q_dot_v_1=M_dot_v*cp_v*(T_ein_v-T_au_v_1)
{ Cold water first law of thermodynamics}

Delta_T_v_Lm_1= ((T_ein_v-T_v_1)-(T_au_v_1-T_v_1))/Ln(Delta_T_v_ratio_1)
{ Logarithmic mean temperature difference - Evaporator }
```

$\Delta T_{v_ratio_1} = (T_{ein_v} - T_{v_1}) / (T_{aus_v_1} - T_{v_1})$
{Ratio between ΔT_{big} and ΔT_{small} - Evaporator}

$\dot{Q}_{v_1} = K_v \cdot A_v \cdot \Delta T_{v_lm_1}$
{ Evaporator heat balance }

$\Delta T_{v_1} = T_{aus_v_1} - T_{v_1}$
{ ΔT_{klein} - Evaporator}

$P_{v_sat_1} = P_{sat}(\text{Water}; T = T_{v_1})$
{ Evaporation pressure}

$h_{4_1} = \text{Enthalpy}(\text{Water}; T = T_{v_1}; x = 1)$
{ h_{4_1} - Refrigerant enthalpy at the outlet of the evaporator}

$\Delta h_{vap_1} = \text{Enthalpy_vaporization}(\text{Water}; T = T_{v_1})$
{ Refrigerant enthalpy difference through the evaporator }

$\dot{Q}_{v_1} = \dot{M}_{ref_1} \cdot \Delta h_{vap_1}$
{ First law of thermodynamics - refrigerant side}

$h_{3_1} = h_{4_1} - \Delta h_{vap_1}$
{Refrigerant enthalpy value at the outlet of the expansion valve}

{-----EVAPORATOR -end -----}

{-----CONDENSER-----}

{:: Predefined Properties - Beginning}

$\dot{V}_k = (2/3600) \text{ [m}^3\text{/s]}$
{Cooling water volume flow rate }

$K_k = 2000 \text{ [(J/s)/(K} \cdot \text{m}^2\text{)]}$
{ Overall heat transfer coefficient- Condenser}

$K_k = 0,729 \text{ [m}^2\text{]}$
{ Condenser exchange area}

$T_{ein_ab} = 300,2 \text{ [K]}$
{ Cooling water temperature at the inlet of the absorber}

{:: Predefined Properties - End}

$T_{ein_k_1} = T_{aus_ab_1}$
{The cooling pipeline passes first through the absorber and after through the condenser}

$\rho_K = \text{Density}(\text{Water}; T = T_{ein_ab}; P = P_u)$
{ Density of the cooling water}

```

M_Dot_k=rho_k*V_Dot_k
{ Mass flow rate of the cooling water}

cp_k=Cp(Water;T=T_ein_ab;P=P_u)
{ Cooling water specific heat }

DELTAT_k_1=T_k_1-T_aus_k_1
{ Delta T_small - Condenser}

Q_dot_k_1= M_dot_k*cp_k*(T_aus_k_1-T_ein_k_1)
{ Cooling water first law of thermodynamics}

Q_Dot_k_1=M_Dot_ref_1*DELTAh_kond_1
{ First law of thermodynamics - refrigerant side}

DELTAh_kond_1=Enthalpy_vaporization(Water;T=T_k_1)
{ Condensation heat }

Delta_T_k_Lm_1= ((T_k_1-T_ein_k_1)-(T_k_1-T_aus_k_1))/Ln(Delta_T_K_ratio_1)
{ Logarithmic mean temperature difference - Condenser }

Delta_T_K_ratio_1=((T_k_1-T_ein_k_1)/(T_k_1-T_aus_k_1))
{Ratio between Delta_T_big and Delta_T_small - Condenser}

P_k_sat_1=P_sat(Water;T=T_k_1)
{ Condensation pressure }

h_1_1=Enthalpy(Water;T=T_k_1;x=1)
{ h_1 - refrigerant enthalpy at the inlet of the condenser}

Q_dot_k_1=K_k*A_k*Delta_T_k_Lm_1
{ Condenser heat balance }

h_11_1=Enthalpy(Water;T=T_10_1;x=1)
{Refrigerant enthalpy value at the outlet of the generator}

h_2.0_1=Enthalpy(Water;T=T_k_1;x=0)
{Refrigerant enthalpy value at the outlet of the condenser}

Sh_k_1=M_dot_ref_1*(h_11_1-h_1_1)*0,74
{Superheating}

Sc_k_1=M_dot_ref_1*(h_2.0_1-h_2_1)*0,74
{Subcooling}

{-----CONDENSER - end-----}

{EXPANSION VALVE}

h_3_1=h_2_1
{ Isoenthalpic process through the expansion valve}

```

{EXPANSION VALVE END}

{-----ABSORBER-----}

{:: Predefined Properties - Beginning}

$A_{ab}=0,912 \text{ [m}^2\text{]}$
{ Absorber exchange area }

$K_{ab}=415[(\text{J/s})/(\text{K}\cdot\text{m}^2)]$
{ Overall heat transfer coefficient- Absorber}

$V_{dot_al}=(0,15/3600)[\text{m}^3/\text{s}]$
{Volume flow rate of the poor solution}

{:: Predefined Properties - End}

$M_{Dot_al_1}=\rho_{al_1}\cdot V_{dot_al}$
{ Mass flow rate of the poor solution}

$\Delta T_{ab_klein_1}=T_{5_1}-T_{ein_ab}$
{ Small temperature difference - Absorber}

$\Delta T_{ab_gro\ss_1}=T_{9_1}-T_{aus_ab_1}$
{ Big temperature difference - Absorber}

$\Delta T_{ab_ratio_1}=\Delta T_{ab_gro\ss_1}/\Delta T_{ab_klein_1}$
{ Ratio between ΔT_{big} and ΔT_{small} - Absorber}

$\Delta T_{ab_Lm_1}=(\Delta T_{ab_gro\ss_1}-\Delta T_{ab_klein_1})/\ln(\Delta T_{ab_ratio_1})$
{ Logarithmic mean temperature difference - Absorber }

$Q_{dot_ab_1}=K_{ab}\cdot A_{ab}\cdot \Delta T_{ab_Lm_1}$
{ Absorber heat balance }

$Q_{Dot_ab_1}=M_{dot_k}\cdot c_{p_k}\cdot (T_{aus_ab_1}-T_{ein_ab})$
{ Cooling water first law of thermodynamics - Absorber}

$M_{dot_rl_1}\cdot h_{5_1}-M_{dot_al_1}\cdot h_{9_1}-M_{dot_ref_1}\cdot h_{4_1}+Q_{Dot_ab_1}=0$
{ Absorber first law of thermodynamics }

{-----ABSORBER -end -----}

{-----POOR AND RICH SOLUTION-----}

$x_{al_id_1}=1-x_{LiBrH_2O}(T_{10_1};P_{k_sat_1})$
{Ideal poor solution concentration - Generator outlet}

$x_{rl_id_1} = 1 - x_{LiBrH_2O}(T_{5_1}; P_{v_sat_1})$
{Ideal rich solution concentration - Absorber inlet}

$x_{al_LiBr.H_2O_id_1} = 1 - x_{al_id_1}$
{LiBr mass fraction - poor solution}

$x_{rl_LiBr.H_2O_id_1} = 1 - x_{rl_id_1}$
{LiBr mass fraction - rich solution}

$\rho_{al_1} = \rho_{LiBrH_2O}(T_{10_1}; x_{al_LiBr.H_2O_1})$
{Poor solution density}

$\rho_{rl_1} = \rho_{LiBrH_2O}(T_{5_1}; x_{rl_LiBr.H_2O_1})$
{Rich solution density}

$h_{5_1} = h_{LiBrH_2O}(T_{5_1}; x_{rl_LiBr.H_2O_1})$
{ h_5 - Refrigerant enthalpy at the outlet of the absorber - Rich solution}

$h_{10_1} = h_{LiBrH_2O}(T_{10_1}; x_{al_LiBr.H_2O_1})$
{ h_{10} - Refrigerant enthalpy at the outlet of the generator - Poor solution}

$h_{9_1} = h_{LiBrH_2O}(T_{9_1}; x_{al_LiBr.H_2O_1})$
{ h_9 - Refrigerant enthalpy at the inlet of the absorber - Poor solution}

$h_{7_1} = h_{LiBrH_2O}(T_{7_1}; x_{rl_LiBr.H_2O_1})$
{ h_7 - Refrigerant enthalpy at the inlet of the generator - Rich solution}

$Cp_{rl_1} = Cp_{LiBrH_2O}(T_{5_1}; x_{rl_LiBr.H_2O_1})$
{Poor solution specific heat}

$Cp_{al_1} = Cp_{LiBrH_2O}(T_{10_1}; x_{al_LiBr.H_2O_1})$
{Rich solution specific heat}

$x_{av_1} = \frac{K_{ab} \cdot A_{ab} \cdot x_{rl_id_1}}{(K_{ab} \cdot A_{ab} + K_g \cdot A_g)} + \frac{K_g \cdot A_g \cdot x_{al_id_1}}{(K_{ab} \cdot A_{ab} + K_g \cdot A_g)}$
{Average weighted value of the solution concentration}

$\dot{M}_{rl_1} = \dot{M}_{av_1} + 0,5 \cdot \dot{M}_{ref_1}$
{Average mass flow rate between rich and poor solution pipes}

$\dot{M}_{al_1} = \dot{M}_{av_1} - 0,5 \cdot \dot{M}_{ref_1}$
{Average mass flow rate between rich and poor solution pipes}

$x_{al_real_1} = (x_{av_1} \cdot \dot{M}_{av_1} - 0,5 \cdot \dot{M}_{ref_1}) / \dot{M}_{al_1}$
{Ideal poor solution concentration - Absorber inlet - second iteration}

$x_{rl_real_1} = (x_{av_1} \cdot \dot{M}_{av_1} + 0,5 \cdot \dot{M}_{ref_1}) / \dot{M}_{rl_1}$
{Ideal rich solution concentration - Absorber outlet - second iteration}

$x_{al_LiBr.H_2O_1} = 1 - x_{al_real_1}$
{LiBr mass fraction - poor solution - second iteration}

$x_{rl_LiBr.H_2O_1} = 1 - x_{rl_real_1}$
{LiBr mass fraction - rich solution - second iteration}

{-----POOR AND RICH SOLUTION - end-----}

{-----SOLUTION HEAT EXCHANGER-----}

{:: Predefined Properties - Beginning}

A_shx=0,272[m^2]
{ SHX exchange area }

K_shx=2000[(J/s)/(K*m^2)]
{ Overall heat transfer coefficient - SHX }

{:: Predefined Properties - End}

Q_dot_al_1 = M_dot_al_1*Cp_al_1*(T_9_1-T_10_1)
{ Poor solution first law of thermodynamics }

Q_dot_rl_1 = M_dot_rl_1*Cp_rl_1*(T_7_1-T_5_1)
{ Rich solution first law of thermodynamics }

-Q_dot_al_1=Q_dot_rl_1
{ Energy balances equivalence -SHX }

Delta_T_shx_groß_1=T_10_1-T_7_1
{ Small temperature difference - SHX }

Delta_T_shx_klein_1=T_9_1-T_5_1
{ Big temperature difference - SHX }

Delta_T_shx_ratio_1=Delta_T_shx_groß_1/Delta_T_shx_klein_1
{ Ratio between Delta_T_big and Delta_T_small - SHX }

Delta_T_shx_Lm_1 = (Delta_T_shx_groß_1 -
Delta_T_shx_klein_1)/Ln(Delta_T_shx_ratio_1)
{ Logarithmic mean temperature difference - SHX }

Q_dot_rl_1=A_shx*K_shx*Delta_T_shx_Lm_1
{ SHX heat balance }

{ -----SOLUTIONE HEAT EXCHANGER - end ----- }

{-----GENERATOR -----}

{:: Predefined Properties - Beginning}

V_Dot_g = (1,5/3600) [m^3/s]
{ Hot water volume flow rate }

$$K_g=1000[(J/s)/(K*m^2)]$$

{ Overall heat transfer coefficient- Generator}

$$A_g=1,215[m^2]$$

{ Generator exchange area }

$$T_{ein_g}=358,2[K]$$

{Hot water temperature at the inlet of the generator }

{:: Predefined Properties - End}

$$cp_g=Cp(Water;T=T_{ein_g};P=P_u)$$

{Hot water specific heat}

$$\rho_g=Density(Water;T=T_{ein_g};P=P_u)$$

{Hot water density}

$$M_{Dot_g}=\rho_g*V_{Dot_g}$$

{Hot water mass flow rate}

$$Q_{dot_g_1}=M_{dot_g}*cp_g*(T_{ein_g}-T_{aus_g_1})$$

{ Hot water first law of thermodynamics - Generator}

$$\Delta T_{g_klein_1}=T_{ein_g}-T_{10_1}$$

{Small temperature difference - Generator}

$$\Delta T_{g_groß_1}=T_{aus_g_1}-T_{7_1}$$

{Big temperature difference - Generator}

$$\Delta T_{g_ratio_1}=\Delta T_{g_groß_1}/\Delta T_{g_klein_1}$$

{ Ratio between ΔT_{big} and ΔT_{small} - Generator}

$$\Delta T_{g_lm_1}=(\Delta T_{g_groß_1}-\Delta T_{g_klein_1})/\ln(\Delta T_{g_ratio_1})$$

{ Logarithmic mean temperature difference - Generator }

$$Q_{dot_g_1}=K_g*A_g*\Delta T_{g_lm_1}$$

{ Generator heat balance }

$$M_{dot_ref_1}*h_{11_1}-Q_{dot_g_1}-M_{dot_rl_1}*h_{7_1}+M_{dot_al_1}*h_{10_1}=0$$

{ Generator first law of thermodynamics }

{-----GENERATOR - end-----}

$$Q_{dot_v_1}+Q_{dot_g_1}-Q_{dot_ab_1}-Q_{dot_k_1}-Sh_{k_1}-Sc_{k_1}=0$$

{First law of thermodynamics - entire system}

$$COP_1=Q_{dot_v_1}/Q_{dot_g_1}$$

{Coefficient of Performance}

{SECOND ITERATION}

{-----EVAPORATOR -----}

$x_{ein_v} = \text{Quality}(\text{Water}; P = P_{v_sat}; h = h_{3.1})$
{Quality at the evaporator inlet}

$M_{dot_ref} = M_{dot_ref_1} * (1 + x_{ein_v})$
{Refrigerant mass flow rate - second iteration}

$Q_{dot_v} = M_{dot_v} * c_{p_v} * (T_{ein_v} - T_{aus_v})$
{ Cold water first law of thermodynamics}

$\Delta T_{v_Lm} = ((T_{ein_v} - T_v) - (T_{aus_v} - T_v)) / \ln(\Delta T_{v_ratio})$
{ Logarithmic mean temperature difference - Evaporator }

$\Delta T_{v_ratio} = (T_{ein_v} - T_v) / (T_{aus_v} - T_v)$
{Ratio between ΔT_{big} and ΔT_{small} - Evaporator}

$Q_{dot_v} = K_v * A_v * \Delta T_{v_Lm}$
{ Evaporator heat balance }

$\Delta T_{v_klein} = T_{aus_v} - T_v$
{ ΔT_{klein} - Evaporator}

$P_{v_sat} = P_{sat}(\text{Water}; T = T_v)$
{ Evaporation pressure}

$h_4 = \text{Enthalpy}(\text{Water}; T = T_v; x = 1)$
{ h_4 - Refrigerant enthalpy at the outlet of the evaporator}

{-----EVAPORATOR - end-----}

{-----CONDENSER-----}

$T_{ein_k} = T_{aus_ab}$
{The cooling pipeline passes first through the absorber and after through the condenser}

$\Delta T_{k_small} = T_k - T_{aus_k}$
{ ΔT_{small} - Condenser}

$Q_{dot_k} = M_{dot_k} * c_{p_k} * (T_{aus_k} - T_{ein_k})$
{ Cooling water first law of thermodynamics}

$Q_{Dot_k} = M_{Dot_ref} * \Delta h_{kond}$
{ First law of thermodynamics - refrigerant side}

$\Delta h_{kond} = \text{Enthalpy_vaporization}(\text{Water}; T = T_k)$
{ Condensation heat}

$\Delta T_{k_Lm} = ((T_{k_T_ein_k}) - (T_{k_T_aus_k})) / \ln(\Delta T_{K_ratio})$
 { Logarithmic mean temperature difference - Condenser }

$\Delta T_{K_ratio} = ((T_{k_T_ein_k}) / (T_{k_T_aus_k}))$
 { Ratio between ΔT_{big} and ΔT_{small} - Condenser }

$P_{k_sat} = P_{sat}(\text{Water}; T = T_{k_T})$
 { Condensation pressure }

$h_{1_T} = \text{Enthalpy}(\text{Water}; T = T_{k_T}; x = 1)$
 { h_{1_T} - refrigerant enthalpy at the inlet of the condenser }

$\dot{Q}_{k_T} = K_{k_T} \cdot A_{k_T} \cdot \Delta T_{k_Lm}$
 { Condenser heat balance }

$h_{11_T} = \text{Enthalpy}(\text{Water}; T = T_{10_T}; x = 1)$
 { Refrigerant enthalpy value at the outlet of the generator }

$h_{2.0_T} = \text{Enthalpy}(\text{Water}; T = T_{k_T}; x = 0)$
 { Refrigerant enthalpy value at the outlet of the condenser }

$Sh_{k_T} = \dot{M}_{ref} \cdot (h_{11_T} - h_{1_T})$
 { Superheating }

{-----CONDENSER - end-----}

{EXPANSION VALVE}

$h_{3.1_T} = h_{2.0_T}$
 { Isoenthalpic process through the expansion valve }

{EXPANSION VALVE- end}

{-----ABSORBER -----}

$\dot{M}_{Dot_al} = \rho_{al} \cdot \dot{V}_{dot_al}$
 { Mass flow rate of the poor solution }

$\Delta T_{ab_klein} = T_{5_T} - T_{ein_ab}$
 { Small temperature difference - Absorber }

$\Delta T_{ab_gro\beta} = T_{9_T} - T_{aus_ab}$
 { Big temperature difference - Absorber }

$\Delta T_{ab_ratio} = \Delta T_{ab_gro\beta} / \Delta T_{ab_klein}$
 { Ratio between ΔT_{big} and ΔT_{small} - Absorber }

$\Delta T_{ab_Lm} = (\Delta T_{ab_gro\beta} - \Delta T_{ab_klein}) / \ln(\Delta T_{ab_ratio})$
 { Logarithmic mean temperature difference - Absorber }

$\dot{Q}_{dot_ab} = K_{ab} \cdot A_{ab} \cdot \Delta T_{ab_Lm}$
 { Absorber heat balance }

$Q_Dot_ab = M_dot_k * cp_k * (T_aus_ab - T_ein_ab)$
 { Cooling water first law of thermodynamics - Absorber }

$M_dot_rl * h_5 - M_dot_al * h_9 - M_dot_ref * h_4 + Q_Dot_ab = 0$
 { Absorber first law of thermodynamics }

{-----ABSORBER - end -----}

{-----POOR AND RICH SOLUTION-----}

$x_al_id = 1 - x_LiBrH2O(T_10; P_k_sat)$
 {Ideal poor solution concentration - Generator outlet}

$x_rl_id = 1 - x_LiBrH2O(T_5; P_v_sat)$
 {Ideal rich solution concentration - Absorber inlet}

$x_al_LiBr.H2O_id = 1 - x_al_id$
 {LiBr mass fraction - poor solution}

$x_rl_LiBr.H2O_id = 1 - x_rl_id$
 {LiBr mass fraction - rich solution}

$\rho_al = \rho_LiBrH2O(T_10; x_al_LiBr.H2O)$
 {Poor solution density}

$\rho_rl = \rho_LiBrH2O(T_5; x_rl_LiBr.H2O)$
 {Rich solution density}

$h_5 = h_LiBrH2O(T_5; x_rl_LiBr.H2O)$
 { h_5 - Refrigerant enthalpy at the outlet of the absorber - Rich solution }

$h_10 = h_LiBrH2O(T_10; x_al_LiBr.H2O)$
 { h_10 - Refrigerant enthalpy at the outlet of the generator - Poor solution }

$h_9 = h_LiBrH2O(T_9; x_al_LiBr.H2O)$
 { h_9 - Refrigerant enthalpy at the inlet of the absorber - Poor solution }

$h_7 = h_LiBrH2O(T_7; x_rl_LiBr.H2O)$
 { h_7 - Refrigerant enthalpy at the inlet of the generator - Rich solution }

$Cp_rl = Cp_LiBrH2O(T_5; x_rl_LiBr.H2O)$
 {Poor solution specific heat}

$Cp_al = Cp_LiBrH2O(T_10; x_al_LiBr.H2O)$
 {Rich solution specific heat}

$x_av = \frac{K_ab * A_ab * x_rl_id}{(K_ab * A_ab + K_g * A_g)} + \frac{K_g * A_g * x_al_id}{(K_ab * A_ab + K_g * A_g)}$
 {Average weighted value of the solution concentration}

$M_dot_rl = M_dot_av + 0,5 * M_dot_ref$
 {Average mass flow rate between rich and poor solution pipes}

$$M_dot_al = M_dot_av - 0,5 * M_dot_ref$$

{Average mass flow rate between rich and poor solution pipes}

$$x_al_real = (x_av * M_dot_av - 0,5 * M_dot_ref) / M_dot_al$$

{Ideal poor solution concentration - Absorber inlet - second iteration}

$$x_rl_real = (x_av * M_dot_av + 0,5 * M_dot_ref) / M_dot_rl$$

{Rich poor solution concentration - Absorber outlet - second iteration}

$$x_al_LiBr.H2O = 1 - x_al_real$$

{LiBr mass fraction - poor solution - second iteration}

$$x_rl_LiBr.H2O = 1 - x_rl_real$$

{LiBr mass fraction - rich solution - second iteration}

{-----POOR AND RICH SOLUTION - end -----}

{-----SOLUTION HEAT EXCHANGER-----}

$$Q_dot_al = M_dot_al * Cp_al * (T_9 - T_10)$$

{Poor solution first law of thermodynamics}

$$Q_dot_rl = M_dot_rl * Cp_rl * (T_7 - T_5)$$

{Rich solution first law of thermodynamics}

$$-Q_dot_al = Q_dot_rl$$

{Energy balances equivalence }

$$\Delta T_shx_gro\beta = T_10 - T_7$$

{ Small temperature difference - SHX }

$$\Delta T_shx_klein = T_9 - T_5$$

{ Big temperature difference - SHX }

$$\Delta T_shx_ratio = \Delta T_shx_gro\beta / \Delta T_shx_klein$$

{ Ratio between ΔT_big and ΔT_small - SHX }

$$\Delta T_shx_Lm = (\Delta T_shx_gro\beta - \Delta T_shx_klein) / \ln(\Delta T_shx_ratio)$$

{ Logarithmic mean temperature difference - SHX }

$$Q_dot_rl = A_shx * K_shx * \Delta T_shx_Lm$$

{ SHX heat balance }

$$C_dot_al = M_dot_al * Cp_al$$

{Poor solution heat capacity}

$$C_dot_rl = M_dot_rl * Cp_rl$$

{Rich solution heat capacity}

```

Q_dot_max=C_dot_rl*(T_10-T_5)
{ Maximum heat transferable through the solution heat exchanger. Calculation done
using the smaller heat capacity between the fluids }

epsilon=Q_dot_rl/Q_dot_max
{Solution heat exchanger efficiency}

{ -----SOLUTION HEAT EXCHANGER - end-----}

{-----GENERATOR -----}

Q_dot_g=M_dot_g*cp_g*(T_ein_g-T_aus_g)
{ Hot water first law of thermodynamics - Generator}

Delta_T_g_klein=T_ein_g-T_10
{Small temperature difference - Generator}

Delta_T_g_groß=T_aus_g-T_7
{Big temperature difference - Generator}

Delta_T_g_ratio=Delta_T_g_groß/Delta_T_g_klein
{ Ratio between Delta_T_big and Delta_T_small - Generator}

Delta_T_g_lm=(Delta_T_g_groß-Delta_T_g_klein)/Ln(Delta_T_g_ratio)
{ Logarithmic mean temperature difference - Generator }

Q_dot_g=K_g*A_g*Delta_T_g_lm
{ Generator heat balance }

M_dot_ref*h_11-Q_dot_g-M_dot_rl*h_7+M_dot_al*h_10=0
{ Generator first law of thermodynamics }

{-----GENERATOR - end-----}

{-----COP and COOLING CAPACITY calculations - begin -----}

COP= Q_dot_v/Q_dot_g
{Coefficient of Performance}

Q_dot_v+Q_dot_g-Q_dot_ab-Q_dot_k-Sh_k=0
{First law of thermodynamics - entire system}

{-----COP and COOLING CAPACITY calculations - end -----}

{-----PROGRAM -----END -----}

```

8. References

- [1] Bahador Bakhtiari, Louis Fradette, Robert Legros, Jean Paris. *A model for analysis and design of H₂O – LiBr absorption heat pumps*. Energy Conversion and Management 52 (2001) 1439-1448.
- [2] M. I. Karamangil, S. Coskun, O. Kaynakli, N. Yamankaradeniz. *A simulation study of performance evaluation of a single-stage absorption refrigeration system using conventional working fluids and alternatives*. Renewable and Sustainable Energy Reviews 14 (2010) 1969-1978.
- [3] Jean Francois Cap, Benoit Stutz, Fredy Hualylla. *Model of H₂O/LiBr absorption machine using falling films*. ISES Conference Proceedings (2014).
- [4] Riffat SB, Afonso CF, Oliveira AC, Reay DA. *Natural refrigerants for refrigeration and air-conditioning system*. Appl Therm Eng 1997; 17:33-42.
- [5] Riffat SB, James SE, Wong CW. *Experimental analysis of the absorption and desorption rates of HCOOK/H₂O and LiBr/H₂O*. Int J energy Res 1998;22:1099-103.
- [6] Dincer I. *Refrigeration systems and applications*. John Wiley and Sons; 2003.
- [7] Dominic Dederling. *Inbetriebnahme einer neuartig entwickelten Absorptionskältemaschine*. Universität Kassel Masterarbeit.
- [8] Eric Granryd, Ingvar Ekroth, Per Lundqvist, Ake Melinder, Björn Palm, Peter Rohlin. *Refrigerating engineering*. KTH Energy Technology.
- [9] F. L. Lansing. *Computer Modeling of a Single – Stage Lithium Bromide/Water Absorption Refrigeration Unit*. JPL Deep Space Network Progress Report 42-32.
- [10] Michael Olbricht, Andrea Luke. *Betriebserfahrungen mit einer Absorptionskältemaschine mit 5kW Kälteleistung*. DKV-Tagung 2014, Düsseldorf, AA II.1

- [11] Tomforde, Cord; Luke, Andrea: *Experimental investigation on heat and mass transfer on a horizontal tube bundle*. 4th IIR Conference on Thermophysical Properties and Transfer Processes of Refrigerants, Delft, Niederlande (2013).
- [12] R. W. Serth. *Process Heat Transfer, Principles and Applications*. Academic Pr (2007).
- [13] Universität Kassel, Institut für Thermische Energietechnik database.
- [14] Khalid A. Joudi, Ali H. Lafta. *Simulation of a simple absorption refrigeration system*. Energy Conversion and Management 42 (2001) 1575-1605.
- [15] Krzysztof Banasiak, Joachim Koziol. *Mathematical modelling of a LiBr – H₂O absorption chiller including two-dimensional distribution of temperature and concentration fields for heat and mass exchangers*. International Journal of Thermal Sciences 48 (2009) 1755-1764.
- [16] *ASHRAE 2009 HVAC Fundamentals Handbook*. American Society of Heating, Refrigerating and Air-Conditioning Engineers, Inc.
- [17] *VDI Heat Atlas*. Verein Deutscher Ingenieure
VDI-Gesellschaft Verfahrenstechnik und Chemieingenieurwesen (GVC) Editor.

